

AD A 052812

**U.S. ARMY  
MISSILE  
RESEARCH  
AND  
DEVELOPMENT  
COMMAND**

DUPLICATE FILE COPY



Redstone Arsenal, Alabama 35809

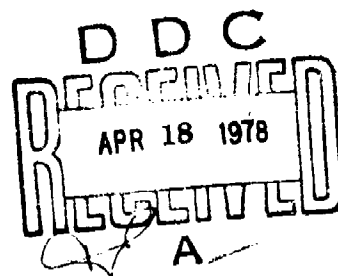
DMI FORM 1000, 1 APR 77

**TECHNICAL REPORT T-78-31**

**AN INVESTIGATION OF THE AERODYNAMIC  
STABILIZING EFFECTIVENESS OF SEVERAL  
SPLIT FLARE AFTERBODY CONFIGURATIONS  
IN THE PRESENCE OF AN UNDEREXPANDED  
JET PLUME AT TRANSONIC MACH NUMBERS**

James R. Burt  
Aeroballistics Directorate  
Technology Laboratory

9 January 1978



Approved for public release; distribution unlimited

#### **DISPOSITION INSTRUCTIONS**

**DESTROY THIS REPORT WHEN IT IS NO LONGER NEEDED. DO NOT  
RETURN IT TO THE ORIGINATOR.**

#### **DISCLAIMER**

**THE FINDINGS IN THIS REPORT ARE NOT TO BE CONSTRUED AS AN  
OFFICIAL DEPARTMENT OF THE ARMY POSITION UNLESS SO DESIGNATED  
BY OTHER AUTHORIZED DOCUMENTS.**

#### **TRADE NAMES**

**USE OF TRADE NAMES OR MANUFACTURERS IN THIS REPORT DOES  
NOT CONSTITUTE AN OFFICIAL INDORSEMENT OR APPROVAL OF  
THE USE OF SUCH COMMERCIAL HARDWARE OR SOFTWARE.**

REPORT DOCUMENTATION PAGE		READ INSTRUCTIONS BEFORE COMPLETING FORM
1. REPORT NUMBER <b>UNCLASSIFIED</b>	2. GOVT ACCESSION NO.	3. REPORT'S CATALOG NUMBER <b>(9)</b>
4. TITLE (and Subtitle) <b>An Investigation of the Aerodynamic Stabilizing Effectiveness of Several Split Flare Afterbody Configurations in the Presence of an Underexpanded Jet Plume at Transonic Mach Numbers.</b>		5. TYPE OF REPORT & PERIOD COVERED <b>Technical Report</b>
6. AUTHOR(s) <b>(10) James R. Burt</b>		7. PERFORMING ORG. REPORT NUMBER <b>(14) RTR-026-2</b>
8. CONTRACT OR GRANT NUMBER(s)		9. PROGRAM ELEMENT, PROJECT, TASK AREA & WORK UNIT NUMBERS <b>(15) DAAK40-77-C-0008</b>
10. PERFORMING ORGANIZATION NAME AND ADDRESS <b>Commander, US Army Missile Research and Development Command ATTN: DRDMI-TD Redstone Arsenal, Alabama 35809</b>		11. REPORT DATE <b>(11) 9 Jan 78</b>
11. CONTROLLING OFFICE NAME AND ADDRESS <b>Commander, US Army Missile Research and Development Command ATTN: DRDMI-TI Redstone Arsenal, Alabama 35809</b>		12. NUMBER OF PAGES <b>87</b>
14. MONITORING AGENCY NAME & ADDRESS (if different from Controlling Office) <b>(12) 83p.</b>		15. SECURITY CLASS. (of this report) <b>Unclassified</b>
16. DISTRIBUTION STATEMENT (of this Report) <b>Approved for public release, distribution unlimited.</b> <b>(18) DRDMI-T</b>		15a. DECLASSIFICATION/DOWNGRADING SCHEDULE
17. DISTRIBUTION STATEMENT (of the abstract entered in Block 20, if different from Report) <b>(19) 78-34</b>		
18. SUPPLEMENTARY NOTES <b>This report was prepared from data plotted by REMTECH, Inc., Huntsville, AL. All data presented are in a data base maintained by REMTECH and are available in tabular or magnetic tape form.</b>		
19. KEY WORDS (Continue on reverse side if necessary and identify by block number) Thrust Effects Longitudinal Stability Plume Effects Base Pressure Plume Boundary Layer Separation		
20. ABSTRACT (Continue on reverse side if necessary and identify by block number) <b>A study of the stabilizing effectiveness of several folding, split flare afterbodies in the presence of an underexpanded jet plume is presented. Mach number was varied from 0.7 to 1.4 and angle of attack from -4° to 6°. It is shown that the split flare afterbody can be an effective stabilizing device for tube launched missiles.</b>  <b>deg</b>		

408564

1/3

## TABLE OF CONTENTS

	Page
I. INTRODUCTION . . . . .	3
II. EXPERIMENTAL PROGRAM . . . . .	3
A. TEST FACILITY . . . . .	3
B. MODEL . . . . .	4
III. TEST PROCEDURE . . . . .	4
IV. DATA . . . . .	5
V. DISCUSSION AND RESULTS . . . . .	5
VI. SUMMARY AND CONCLUSIONS . . . . .	6
NOMENCLATURE . . . . .	7

ACCESSION NO. 44-38861-1000

NY'S	WFO's Section	<input checked="" type="checkbox"/>
CCO	Buff Section	<input checked="" type="checkbox"/>
UN-ANNOUNCED		<input checked="" type="checkbox"/>
ADMINISTRATIVE		

BY \_\_\_\_\_

DATE \_\_\_\_\_

FILE NO. \_\_\_\_\_

100-44-38861-1000

A

## I. INTRODUCTION

A common requirement for tube launched missiles is that the aerodynamic stabilizing surfaces be approximately the same diameter as the missile body when in the tube. Several devices have been designed and tested which satisfy this requirement. Among these are: wraparound fins, folding fin configurations, and trailing ring-tails. All of these devices have disadvantages in certain flight conditions. Wraparound fins generally have large induced roll moments which vary with Mach number. Folding fins usually have a high aspect ratio and, therefore, lose much of their stabilizing effectiveness at high supersonic Mach numbers. The effectiveness of trailing ring-tails is greatly reduced by an underexpanded rocket plume; and therefore, they are not suitable for a high acceleration rocket with a motor burning after tube exit.

An alternate to the above stabilizing devices is a split flare which would be folded into a cylindrical shape while in the launch tube and expanded into a partial or split flare upon tube exit. Intuitively, this configuration would have two advantages over the other stabilizing devices suitable for a tube launched, high acceleration, supersonic rocket. Solid flares are more effective than fins as stabilizing devices at high supersonic Mach numbers; therefore, a split flare may also be more effective. Also, a solid flare is an effective device for inhibiting the onset of the adverse effects of an underexpanded rocket plume on rocket static stability; therefore, a split flare may also be effective as a thrust effects inhibitor.

Wind tunnel data were obtained for seven model configurations consisting of solid flares, split flares, and a cylindrical afterbody in the presence of a normal jet plume simulator.

Mach number was varied from 0.7 to 1.4, and the angle of attack range was  $-4^{\circ}$  to  $6^{\circ}$ . The effect of roll angle on split flare effectiveness was investigated.

## II. EXPERIMENTAL PROGRAM

### A. Test Facility.

The AEDC-PWT Aerodynamic Wind Tunnel (1T) is a continuous flow, nonreturn facility, with Mach number capability from 0.2 to 1.5. The tunnel total pressure is essentially nonvariant at approximately 2850 psfa with  $\pm 5$  percent variation. The total temperature variation can be controlled from 80 to 120 degrees F. The test section is one foot square and 37.5 inches long with 6 percent porosity with all four perforated walls installed.

During the visualization phase the sidewalls were replaced with solid transparent walls.

A more detailed description of the IT facility may be found in the AEDC Test Facility Handbook (reference 1).

#### B. Model

The model was a sting mounted body of revolution having a diameter of 1.1 inches, Figure 1. It had a 3-caliber, tangent ogive nose and a total length of 10.4 calibers (11.44 in.). A cylindrical afterbody, two solid flare afterbodies, and four split flare afterbodies were tested. All afterbodies were the same length (1.725 in.) with two base diameters used for the solid and split flare configurations (1.705 in. and 2.071 in.). The split flare afterbodies had either 6 or 12 petals, and one of the 6-petal configurations had partially filled slots or skirts. The model assembly is shown in Figure 2, and the afterbodies tested are shown in Figure 3. The plume simulator was located 0.73 in. behind the model base. Effective plume shape was controlled by regulating nitrogen flow through 12 holes, 5/64 in. diameter, equally spaced around the circumference of the simulator. The simulator had a total sonic jet orifice area of 6% of the model cross-sectional area and was 0.815 in. in diameter. Detailed descriptions of the plume simulator and all model parts are contained in MIRADCOM drawings TDK-13900 series.

<u>Model</u>	<u>Nomenclature</u>
C	Cylindrical afterbody
FD1	Small diameter solid flare afterbody
FD2	Large diameter solid flare afterbody
F6D2	Large diameter, 6-petal, split flare afterbody
F6D2S	Large diameter, 6-petal, split flare afterbody, skirt
F12D1	Small diameter, 12-petal, split flare afterbody
F12D2	Large diameter, 12-petal, split flare afterbody

#### III. TEST PROCEDURE

All configurations were tested at Mach numbers of 0.7, 1.05, 1.25, and 1.4. Data for a single run were obtained by varying angle of attack from  $-4^{\circ}$  to  $6^{\circ}$  while holding Mach number and plume simulator chamber pressure constant. The plume simulator nitrogen supply was adjusted to give the preselected chamber pressure that gave the desired radial thrust coefficient (CRT) for the tunnel test section conditions. Nominal test conditions are given in Table I, and the values for chamber pressure at specified values of CRT along with the expression for computation is contained in Table II. Zero roll position for the split flare configurations was with a petal flat up. Most of the runs were made at zero roll angle, but the effect of

roll on stability was investigated with the F6D2 configuration.

Shadowgraphs and oil flow photographs were taken at selected test points.

#### IV. DATA

All balance force coefficients are referenced to the cross-sectional area of the body, 0.95033 sq. in. The moment reference center is located at model station 5.83 inches aft of the nose (5.1 calibers forward of the body base). The moment coefficients are referenced to the body cross-sectional area times the body diameter (1.1 in.). The sign convention is the standard body axis system, positive nose up and right (climbing right turn). The two base pressures were averaged and ratioed to the free stream ambient pressure. Corrections to angle-of-attack were made for sting and balance deflections caused by aerodynamic loads and model weight.

The 2 $\sigma$  data uncertainties, calculated from the balance calibration, are shown in Table III.

#### V. DISCUSSION AND RESULTS

There are two primary geometry differences between the split flares and solid flares, and the effects of these differences are qualitatively easy but quantitatively difficult to predict. First, the split flares have less surface area than solid flares of the same length and diameter. Intuitively, the effect of this difference would be reduced stabilizing effectiveness for the split flare, but not a reduction equal to the surface area ratio, because of petal-to-petal interference.

Second, the split flare probably would not inhibit the onset of afterbody flow separation due to an underexpanded jet plume as well as the geometrically similar solid flare because of the high base pressure feeding up through the splits in the afterbody. In this study the effects of base diameter, number of petals, and a partial fill in skirt on split flare stabilizing effectiveness as compared to solid flares are investigated.

The basic longitudinal stability coefficients for all configurations tested are shown in Figure 4. Typical variation of base pressure with CRT is shown in Figure 5. The data in this figure was taken at Mach number 1.25 and zero angle of attack. A comparison of the plateau base pressure of the afterbodies tested gives an indication of their effectiveness in inhibiting flow separation, with a high plateau pressure indicating a good flow separation inhibitor.

As expected, the large diameter, solid flare, FD2, has the highest base pressure plateau and the cylindrical afterbody yields the lowest base pressure plateau. The data shows that the 6-petal configuration is more effective than the 12-petal configuration and that the skirt added to the 6-petal configuration causes little change in base pressure plateau.

Normal force coefficient and pitching moment coefficient versus angle of attack slopes at small angles of attack are shown as a function of CRT in Figure 6. Clearly, the large diameter, solid flare, FD2, is the most effective stabilizing afterbody tested. The 6-petal, large diameter split flare and the addition of the fill-in-skirt to the large diameter split flare increases its stabilizing effectiveness very little. Total axial force coefficients for all configurations tested are shown in Figure 7.

#### SUMMARY AND CONCLUSIONS

This report is a study of the aerodynamic stabilizing effectiveness of several split flare afterbodies suitable for use in tube launched, free rocket design. The split flares were compared to solid flares with the same base diameter and length in a transonic wind tunnel test. Mach number was varied from 0.7 to 1.4 and angle of attack from  $-4^{\circ}$  to  $6^{\circ}$ .

The following conclusions were drawn from this study:

- 1) The solid flares are more effective aerodynamic stabilizing devices than the split flares of the same base diameter and length.
- 2) The 6-petal split flare is a more effective aerodynamic stabilizing device than the 12-petal split flare.
- 3) The addition of partial fill-in-skirts to the 6-petal split flare design only caused a slight increase in aerodynamic stabilizing effectiveness.



## REFERENCE

1. "Test Facilities Handbook" (Tenth Edition), Propulsion Wind Tunnel Facility, Vol. 4, Arnold Engineering Development Center, May 1974.

## NOMENCLATURE

<u>SYMBOL</u>	<u>PLOT SYMBOL</u>	<u>DEFINITION</u>
$C_A$		total measured axial force coefficient
$C_m$	$C_{LM}$	pitching moment coefficient
$C_N$	$C_N$	normal force coefficient
$C_{m_\alpha}$	$C_{M\_ALPHA}$	pitching moment slope at zero angle of attack
$C_{N_\alpha}$	$C_{N\_ALPHA}$	normal force slope at zero angle of attack
CRT	CRT	radial thrust coefficient
FA		axial force
FN		normal force
FY		side force
$l_{ref}$	LREF	reference length, in.
$M_x$		rolling moment
$M_m$		pitching moment
$M_n$		yawing moment
$M_\infty$	MACH	tunnel test section Mach number
$P_b/P_\infty$		base to tunnel static pressure ratio
$P_t$		tunnel stagnation pressure, psfa

# NOMENCLATURE (Continued)

<u>SYMBOL</u>	<u>PLOT SYMBOL</u>	<u>DEFINITION</u>
$q_{\infty}$		tunnel test section dynamic pressure, psf
$R_N$		Reynolds number, per foot
$S_{ref}$	SREF	reference area used to reduce data to coefficient form, in.
$x_{mrp}$	XMRP	moment reference point on X axis
$\alpha$	ALPHA	angle of attack, degrees
$\phi$	PHI	angle of roll, degrees

TABLE 1. NOMINAL TEST CONDITIONS.

$M_\infty$	$P_t$ (psfa)	$q_\infty$ (psf)	$R_N \times 10^{-6}$ (per ft.)
0.7	2850	705	4.426
1.05	↓	1090	5.237
1.25		1204	4.999
1.4		1229	4.916

TABLE 2. NOMINAL PLUME SIMULATOR CHAMBER PRESSURE.

MACH	C/T											
	2.5	4.0	5.0	6.1	7.0	9.1	10.2	11.2	14.2	16.6	18.6	25.5
0.7				395			661				1190	1630
1.05	255			615				1120		1630		
1.25	280		557			1005			1580			
1.40	280	460			800			1265				

$$CRT = A_{nj} (0.5283 \times P_c (1.4 \times M_j^2 + 1) - P_s/144) / (A_{ref} \times q/144)$$

where

$A_{nj}$  = Total exit area, 12 orifices

$A_{nj}/A_{ref} = 0.06$

$M_j$  = Sonic jet ( $M=1.0$ )

$q$  = Free stream dynamic pressure, psf

$P_c$  = Chamber pressure in simulator, psi

$P_s$  = Tunnel static pressure, psf

$P_t$  = 2850 psf -- tunnel total pressure

TABLE 3. DATA UNCERTAINTY.

$2\sigma$  uncertainties calculated from the balance calibration

	Type of Loading			
	FN	FY	FA	M <sub>L</sub>
$\Delta FN$	0.06	0.02	0.06	0.12
$\Delta FY$	0.02	0.03	0.08	0.04
$\Delta FA$	0.03	0.10	0.06	0.05
$\Delta M_L$	0.02	0.02	0.01	0.04
$\Delta M_m$	0.04	0.05	0.08	0.15
$\Delta M_n$	0.04	0.08	0.09	0.09

TABLE 4. DATA SET SUMMARY.

TEST AEDC TM-359			TEST RUN NUMBERS																
Config	Mach No.	$\alpha$	$\phi$	0	2.5	4.0	5.0	6.1	7.0	9.1	10.2	11.2	14.2	16.6	18.6	25.5			
C	0.70	A	0	3				10			9				8	7			
C	1.05	A	0	11	12			18				16		25					
C	1.25	A	0	22	21		20			19			26						
C	1.40	A	0	27	31	30			29			28							
FD1	0.70	A	0	55				59			58				57	56			
FD1	1.05	A	0	53	60			50				49		48					
FD1	1.25	A	0	42	41		40			39			45						
FD1	1.40	A	0	34	38	37			36			35							
FD2	0.70	A	0	64				70			71				72	63			
FD2	1.05	A	0	65	69			68				67		66					
FD2	1.25	A	0	75	79		78			77			76						
FD2	1.40	A	0	80	84	83			82			81							
F6D2S	0.70	A	0	104				108			107				106	105			
F6D2S	1.05	A	0	103	113			112				111		101					
F6D2S	1.25	A	0	97	96		95			94			93						
F6D2S	1.40	A	0	92	91	90			88			87							
F12D1	0.70	A	0	117				125			124				123	116			
F12D1	1.05	A	0	118	122			121				120		119					
F12D1	1.25	A	0	133	132		131			126			129						
F12D1	1.40	A	0	134	138	137			136			135							
F12D2	0.70	A	0	160				164			163				162	151			
F12D2	1.05	A	0	155	152			153				154		159					
F12D2	1.25	A	0	147	151		156			149			148						
F12D2	1.40	A	0	145	144	143			142			141							
F6D2	0.70	A	0	167				171			170				169	168			
F6D2	1.05	A	0	175	174			173				172		173					
F6D2	1.25	A	0	184	183		182			161			180						
F6D2	1.40	A	0	185	185	188			187			186							
F6D2	0.70	A	30	206				210			209				208	207			
F6D2	1.05	A	30	205	213			212				211		204					
F6D2	1.25	A	30	197	198		199			200			203						
F6D2	1.40	A	30	192	196	195			194			193							
F6D2	0.70	A	180	215				218											
F6D2	1.05	A	180	219				220											

A = -4, -2, -1, -0.25, 0, 0.25, 0.5, 1.0, 2.0, 4.0, & 6.0

A = -4, -2, -1, -0.25, 0, 0.25, 0.5, 1.0, 2.0, 4.0, &amp; 6.0

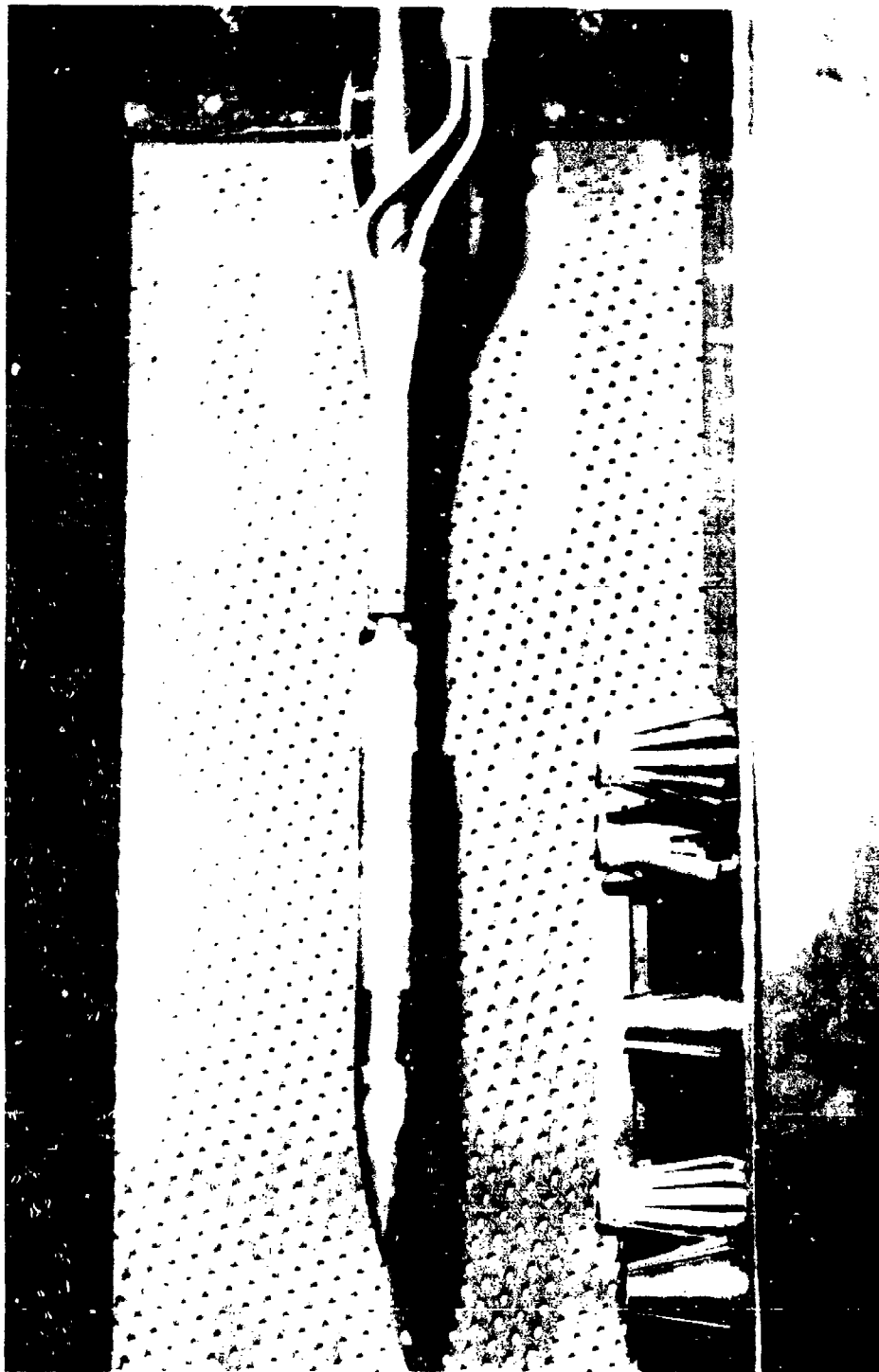


Figure 1. Model installation photograph.

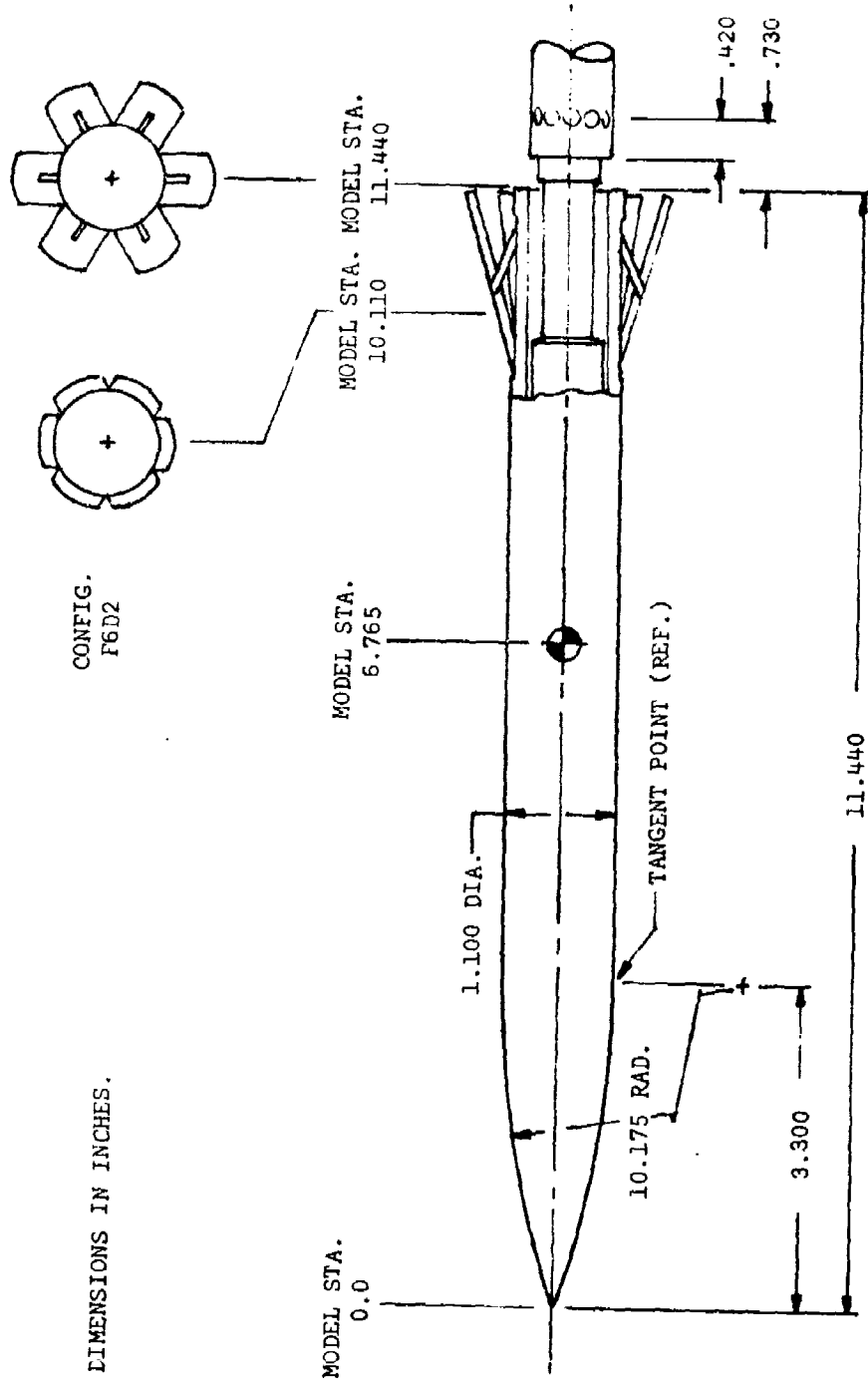
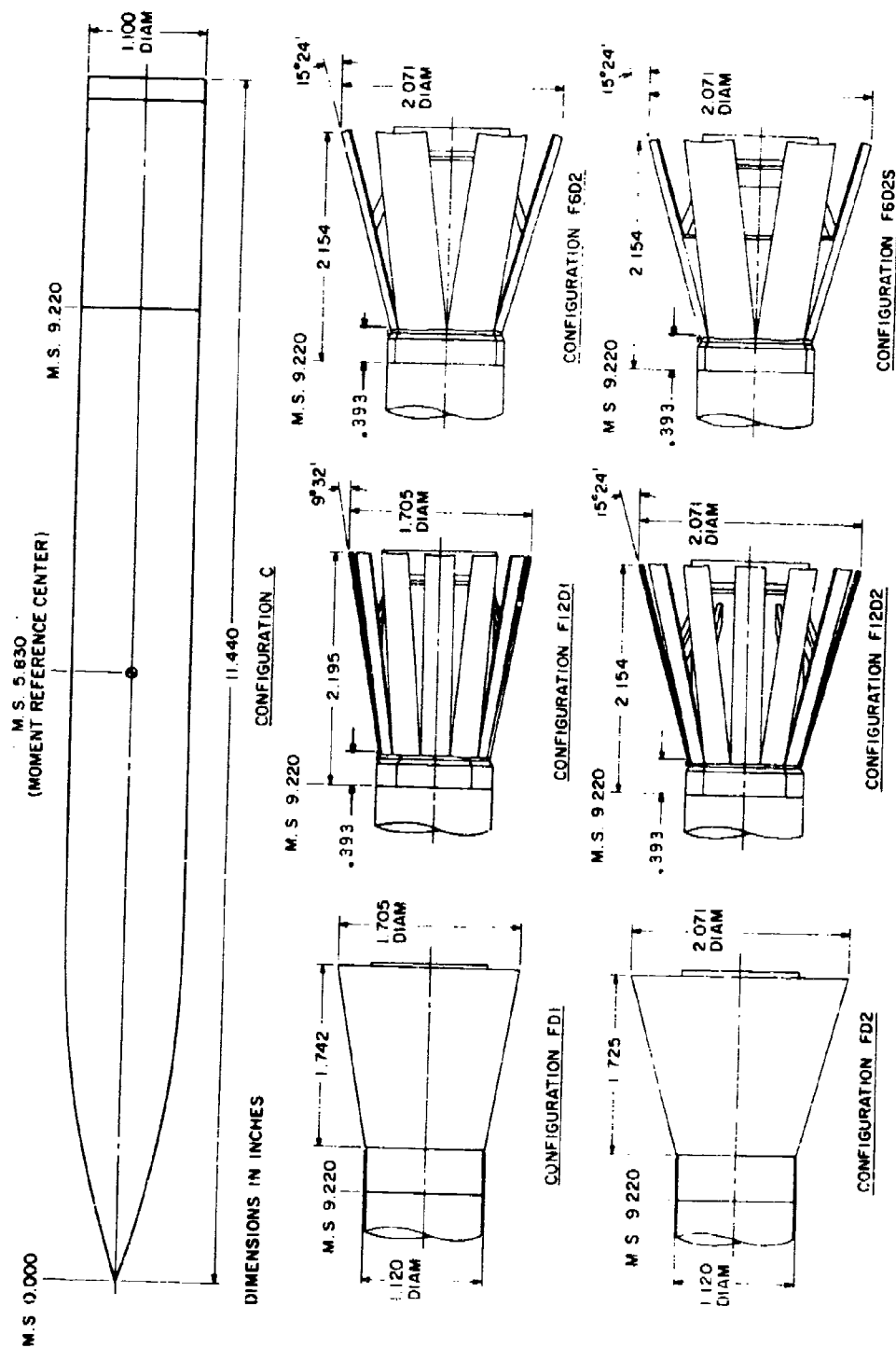


Figure 2. Model assembly.



REFERENCE AREA (S): 0.950 in.<sup>2</sup> REFERENCE LENGTH: 1.100 in.

Figure 3. Model details and identification.



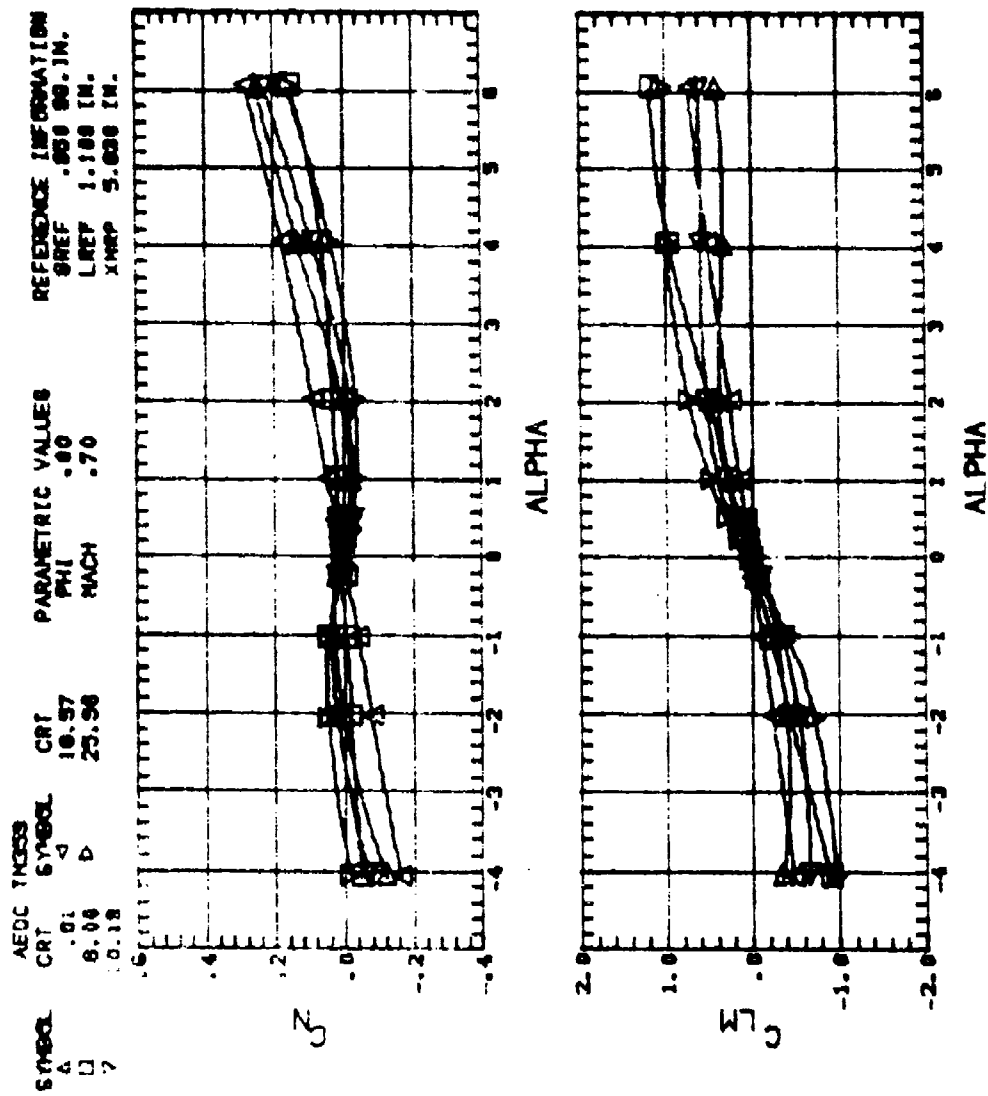


Figure 4. Thrust effects on stability coefficients. C

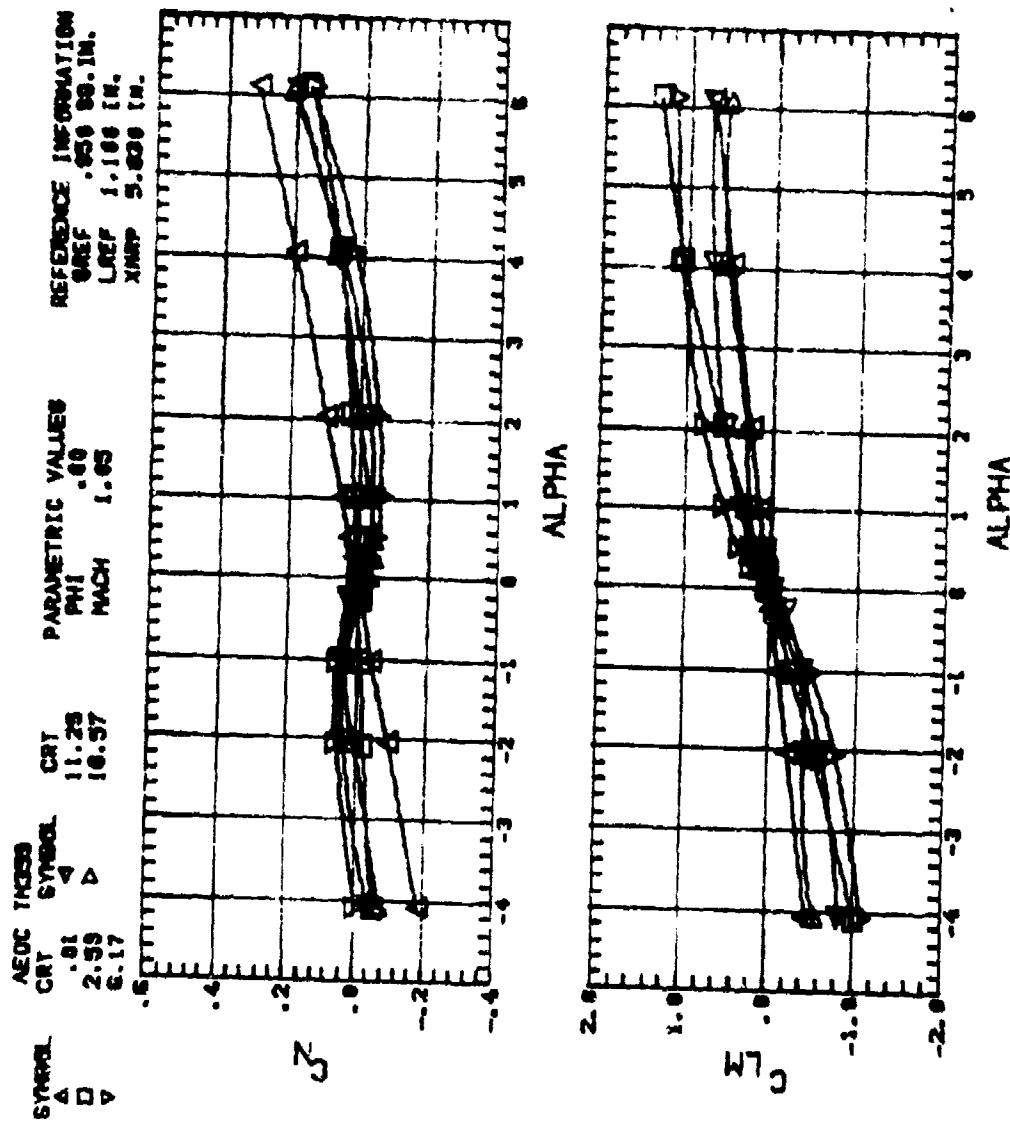


Figure 4. Continued. C

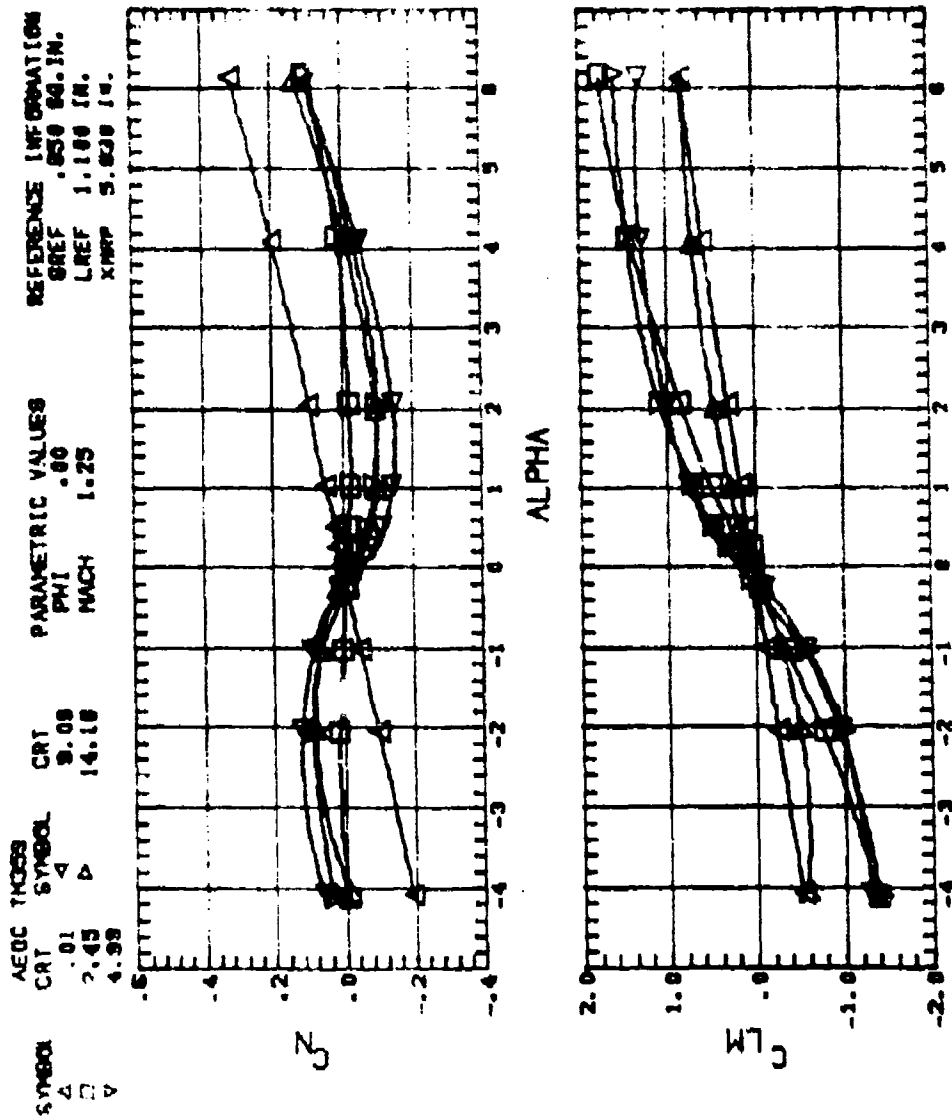


Figure 4. Continued. C

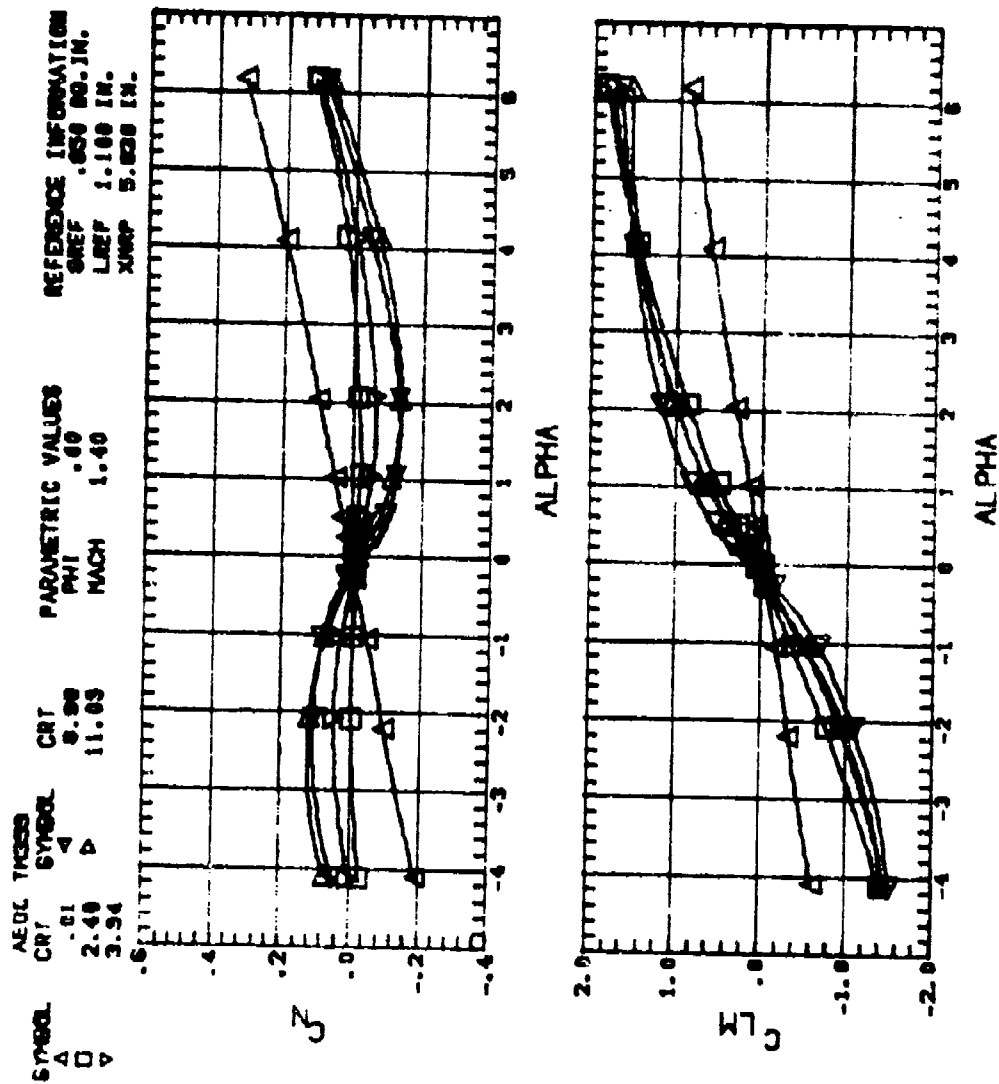


Figure 4. Continued. C

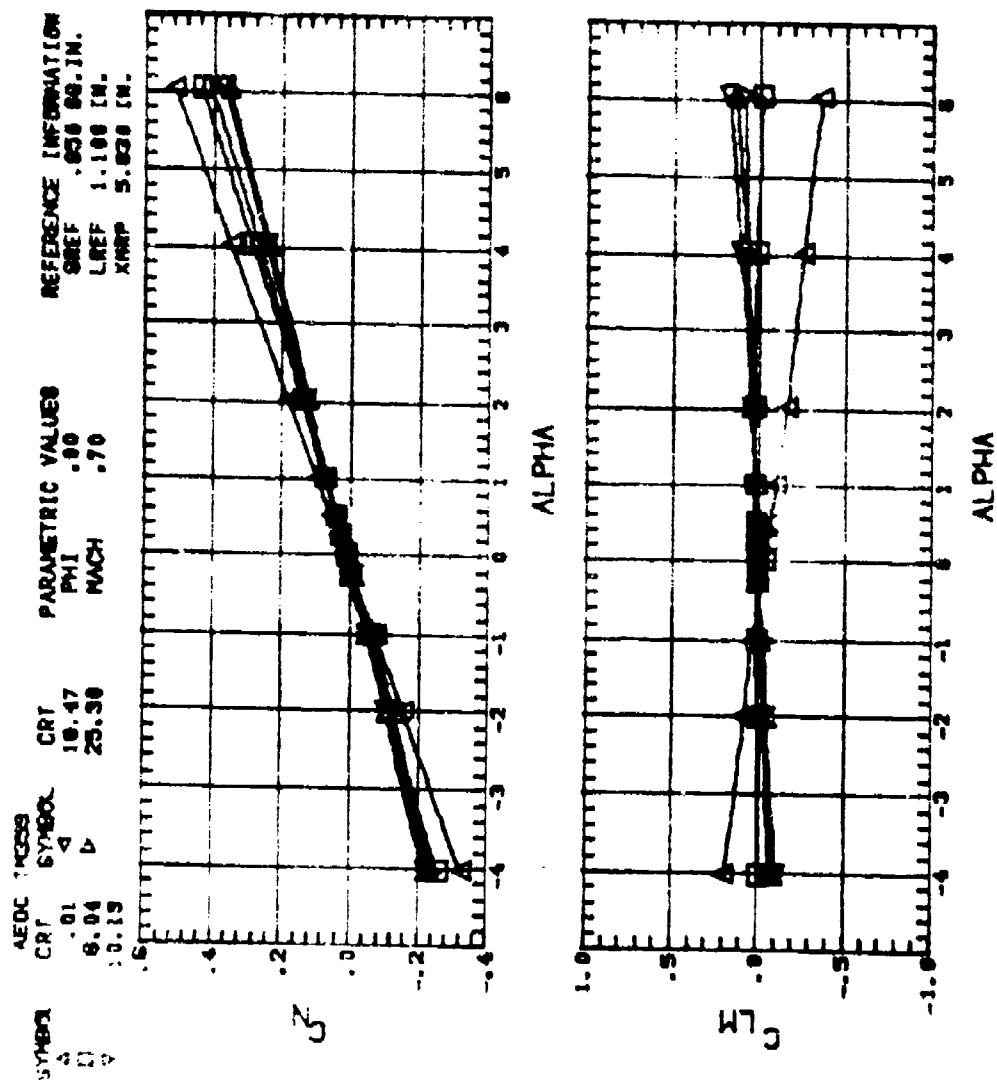


Figure 4. Continued. FD1

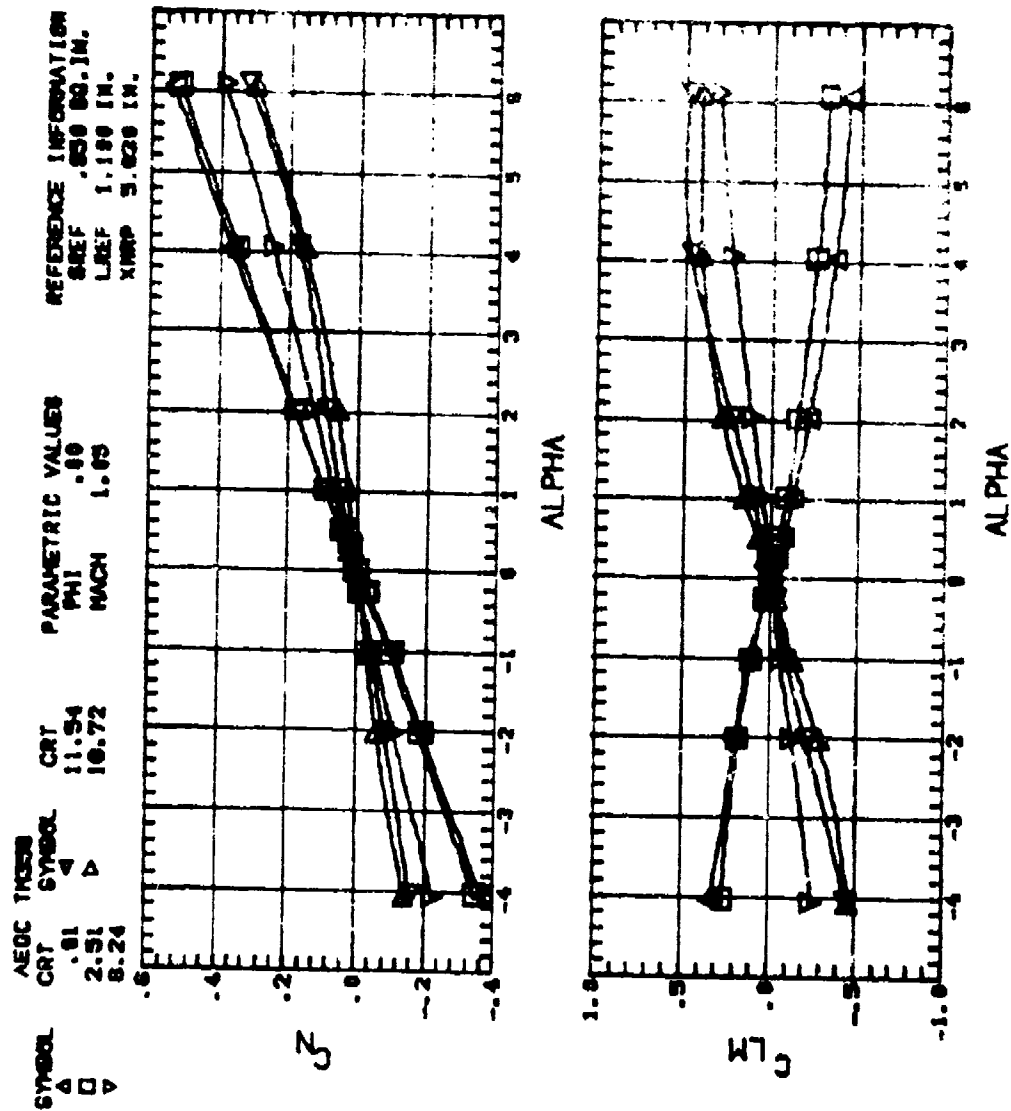


Figure 4. Continued. FDI

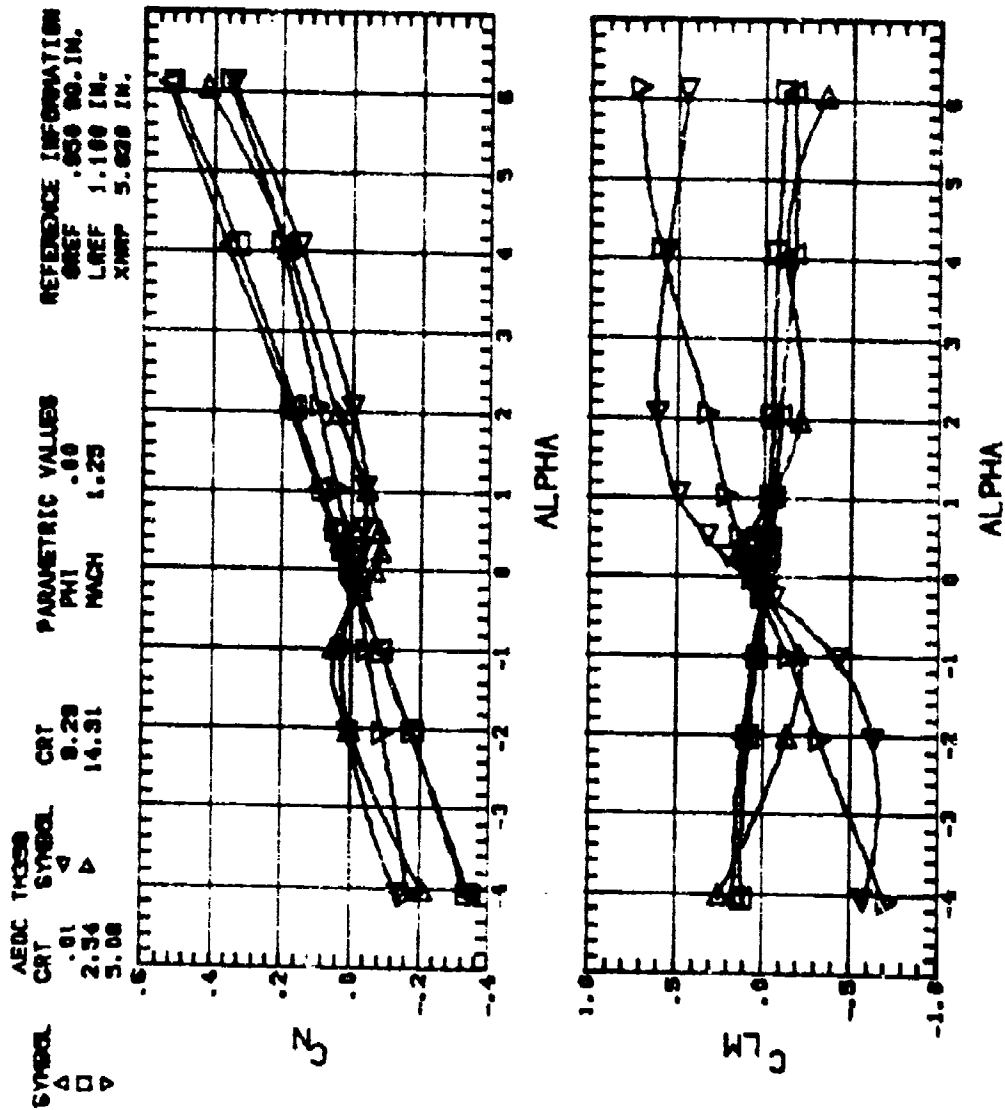


Figure 4. Continued. FDI

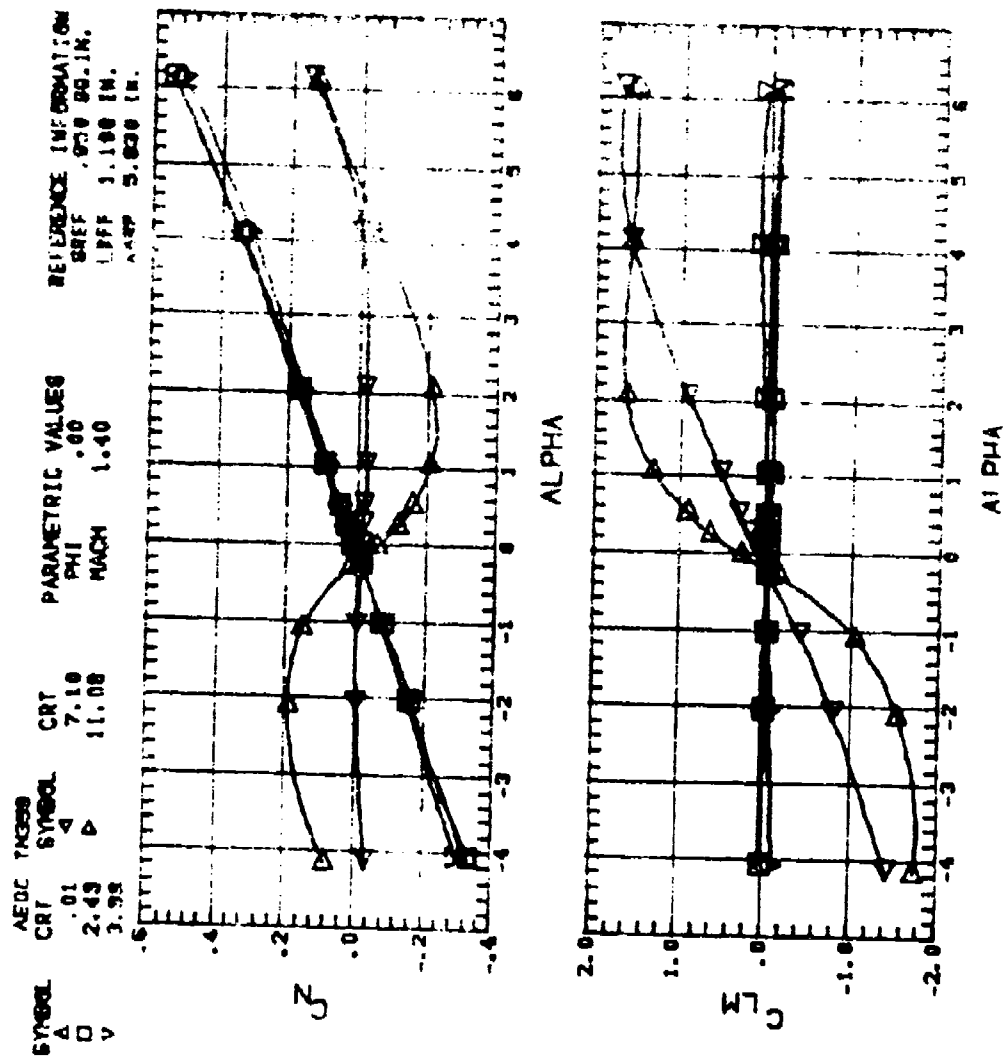


Figure 4. Continued. FDI



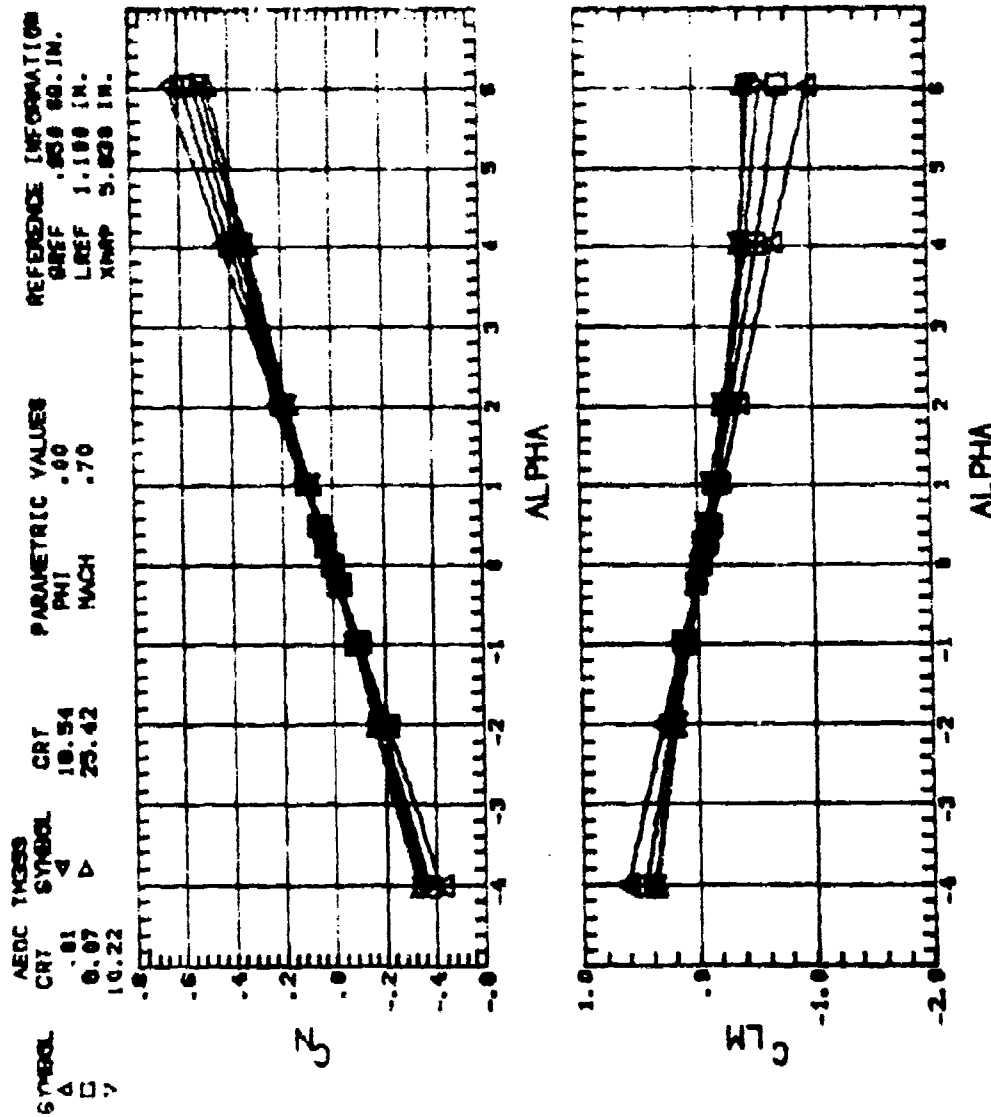


Figure 4. Continued. FD2

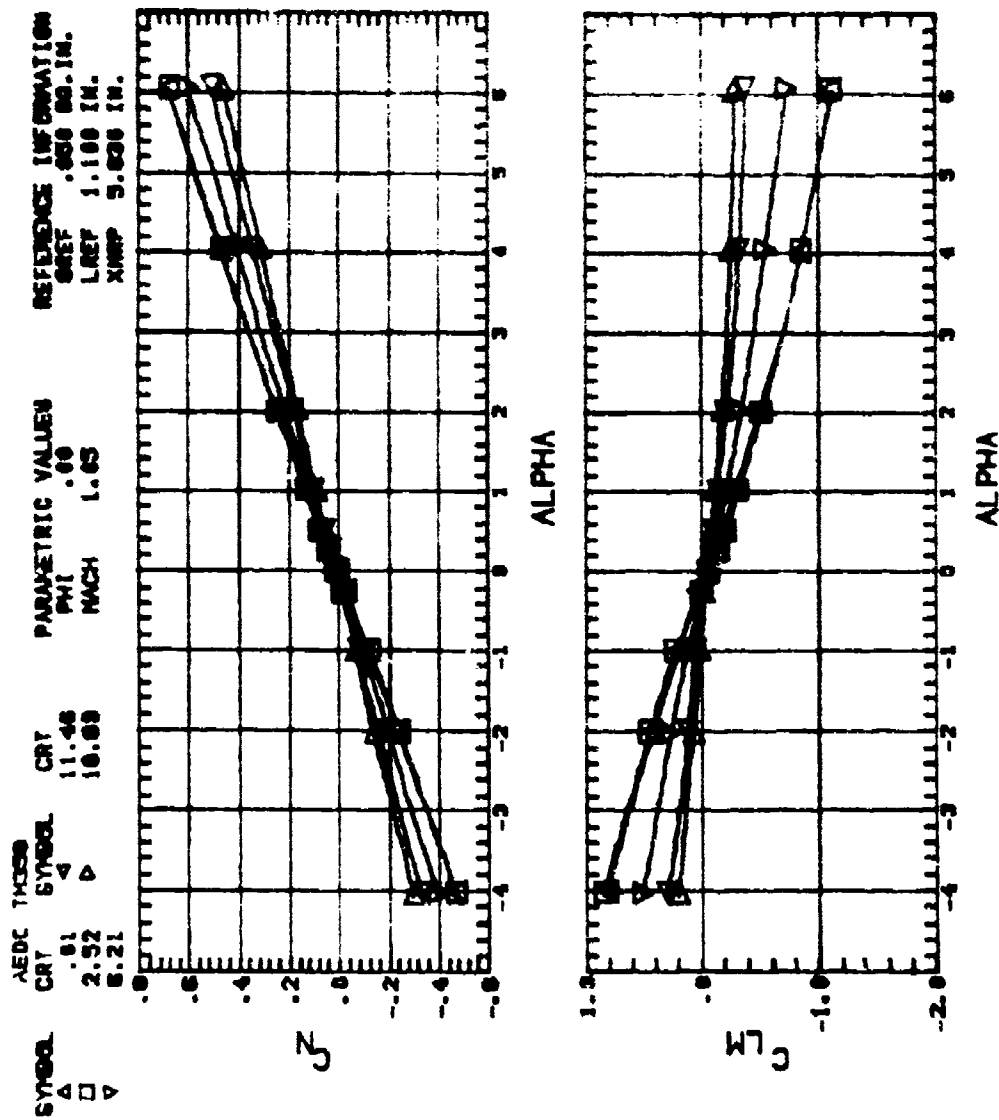


Figure 4. Continued. FD2

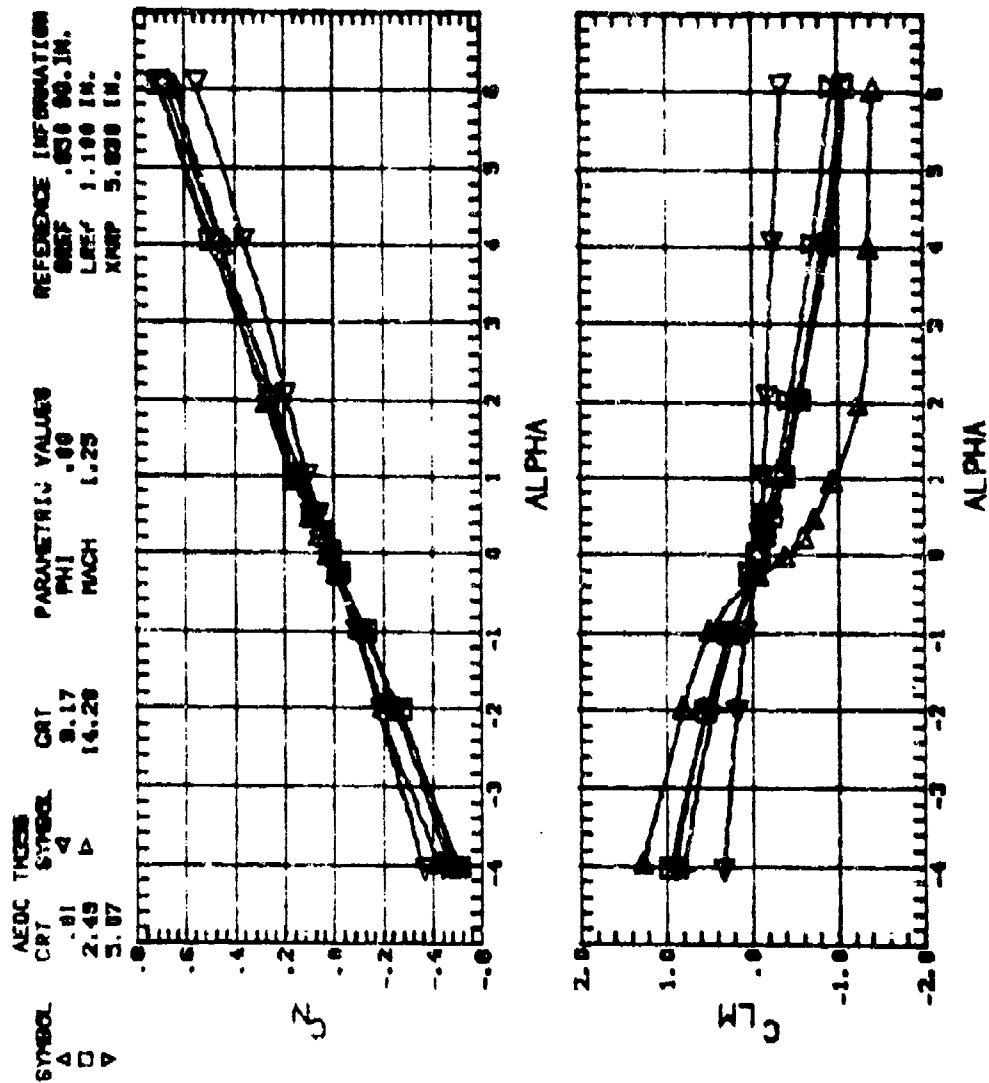


Figure 4. Continued. FD2

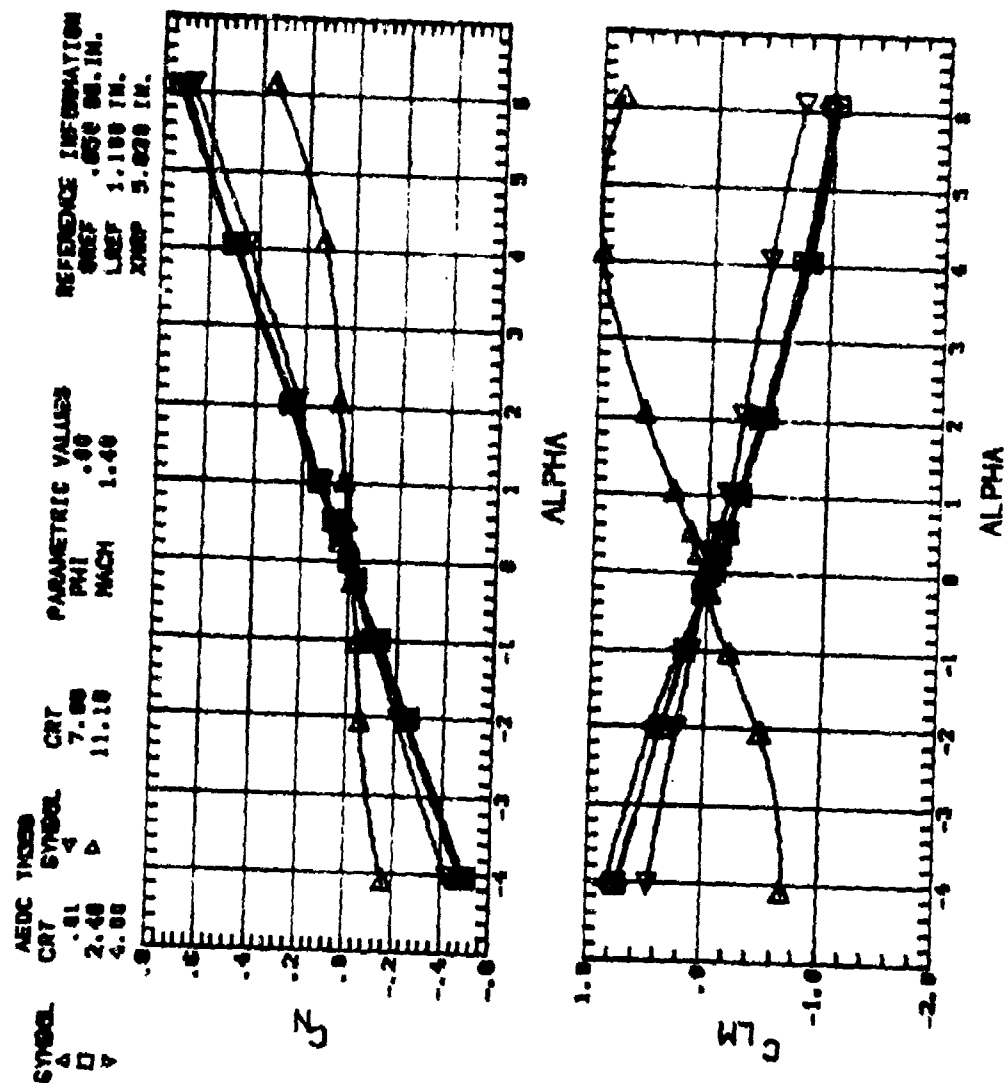


Figure 4. Continued. FD2

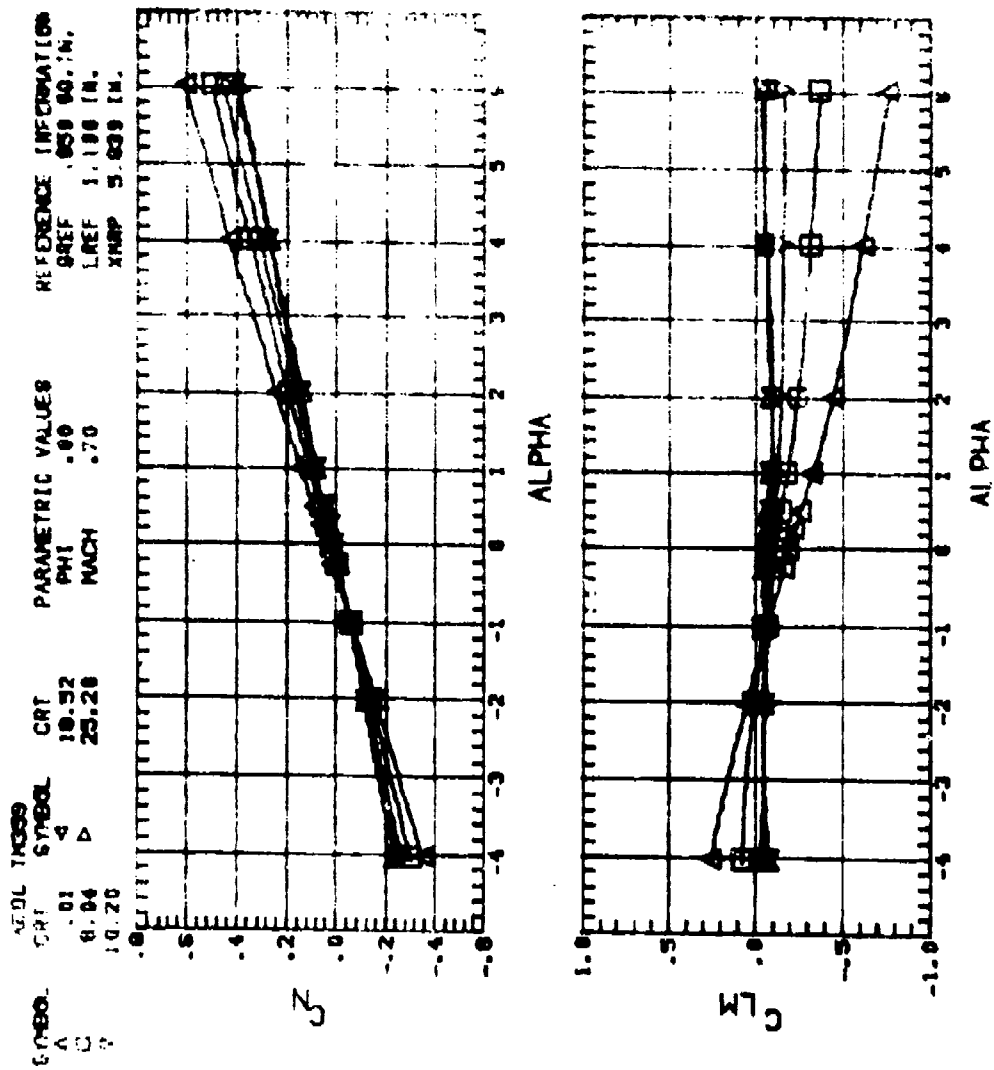


Figure 4. Continued. F6D2S

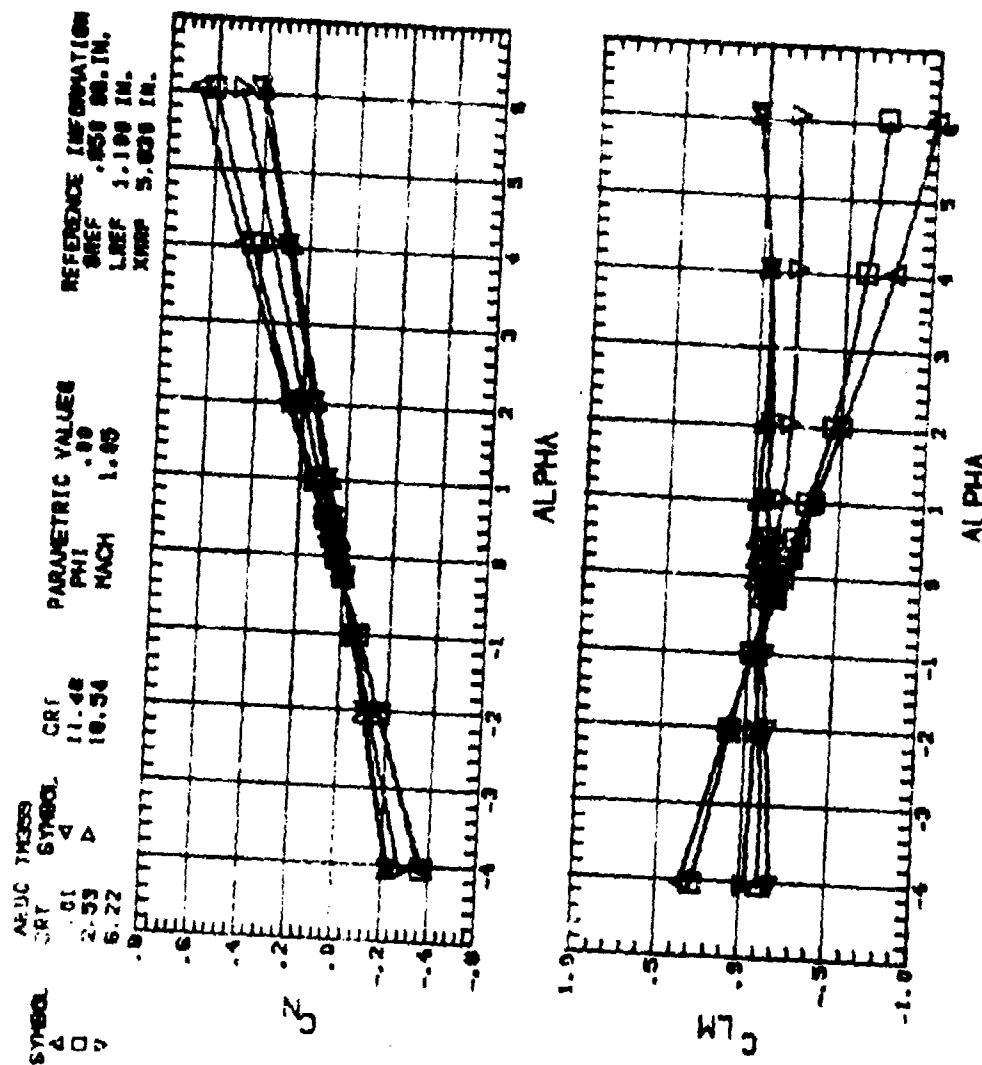


Figure 4. Continued. F6D2S

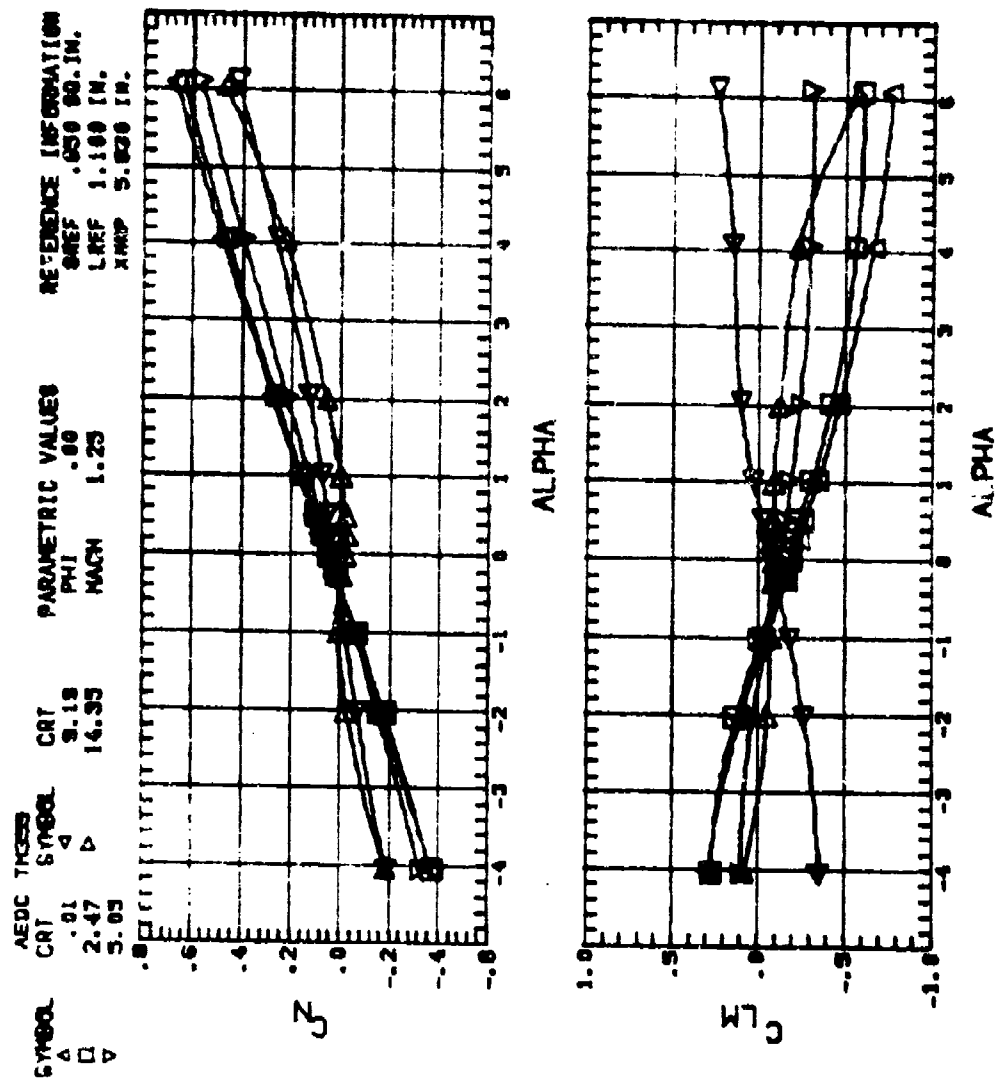


Figure 4. Continued. F6D2S

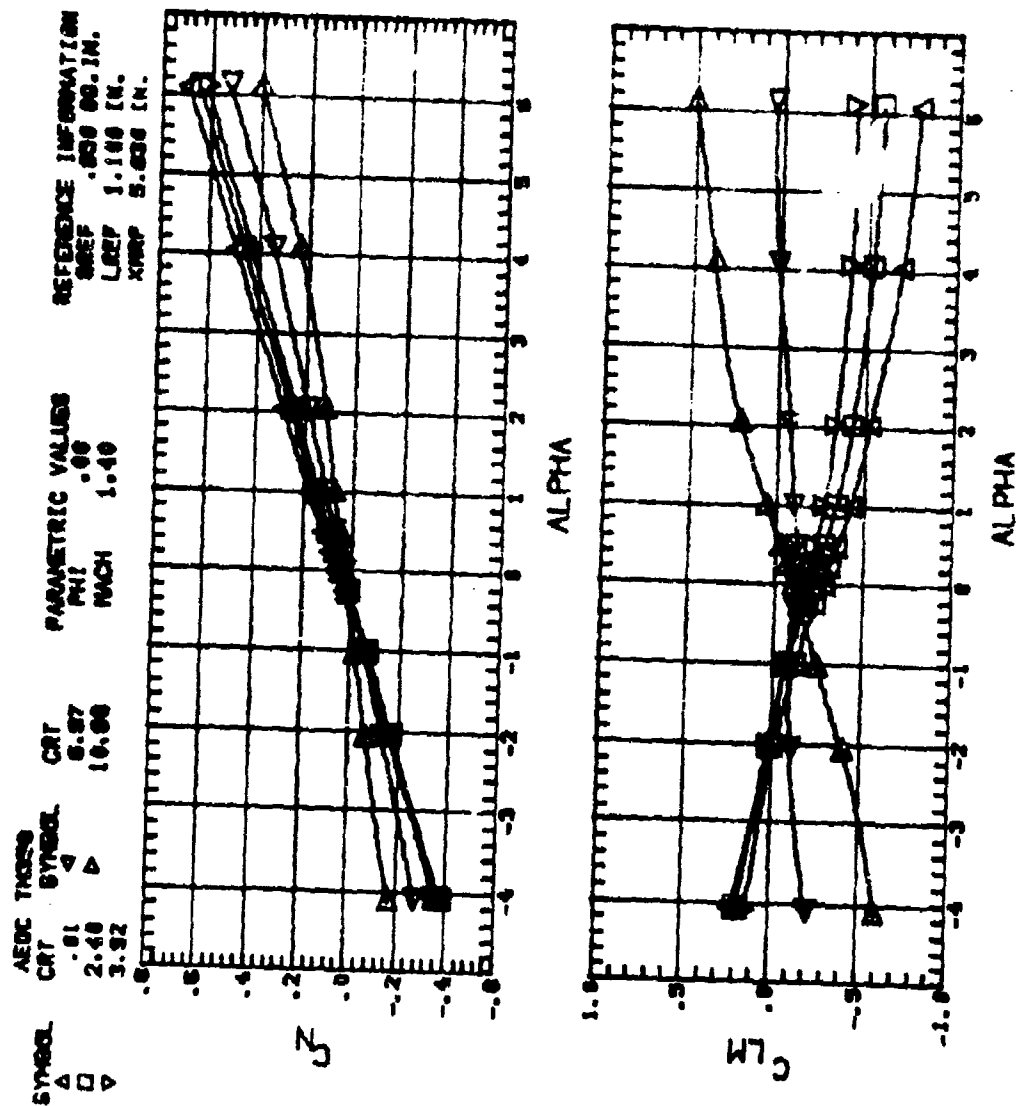


Figure 4. Continued. F6D2S



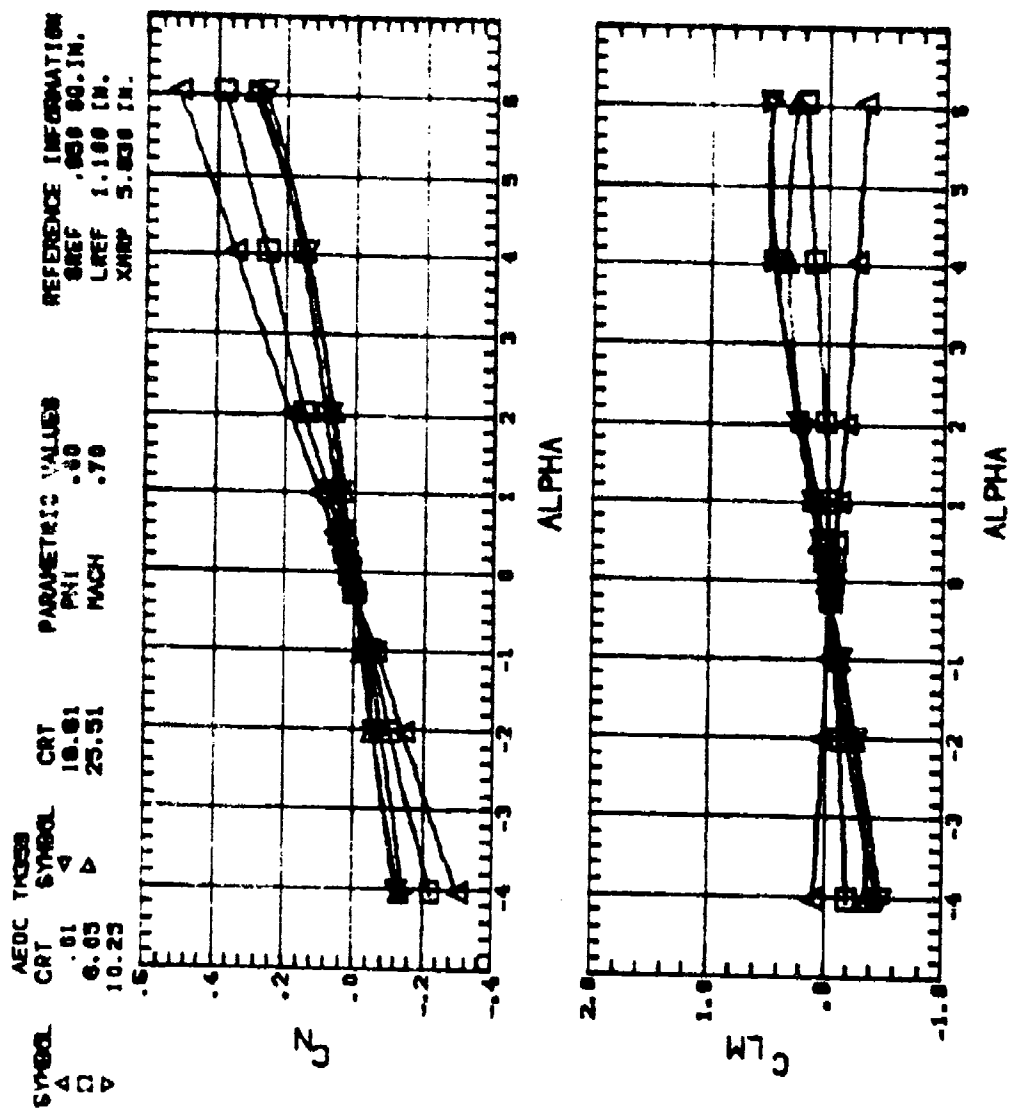


Figure 4. Continued. F12D1

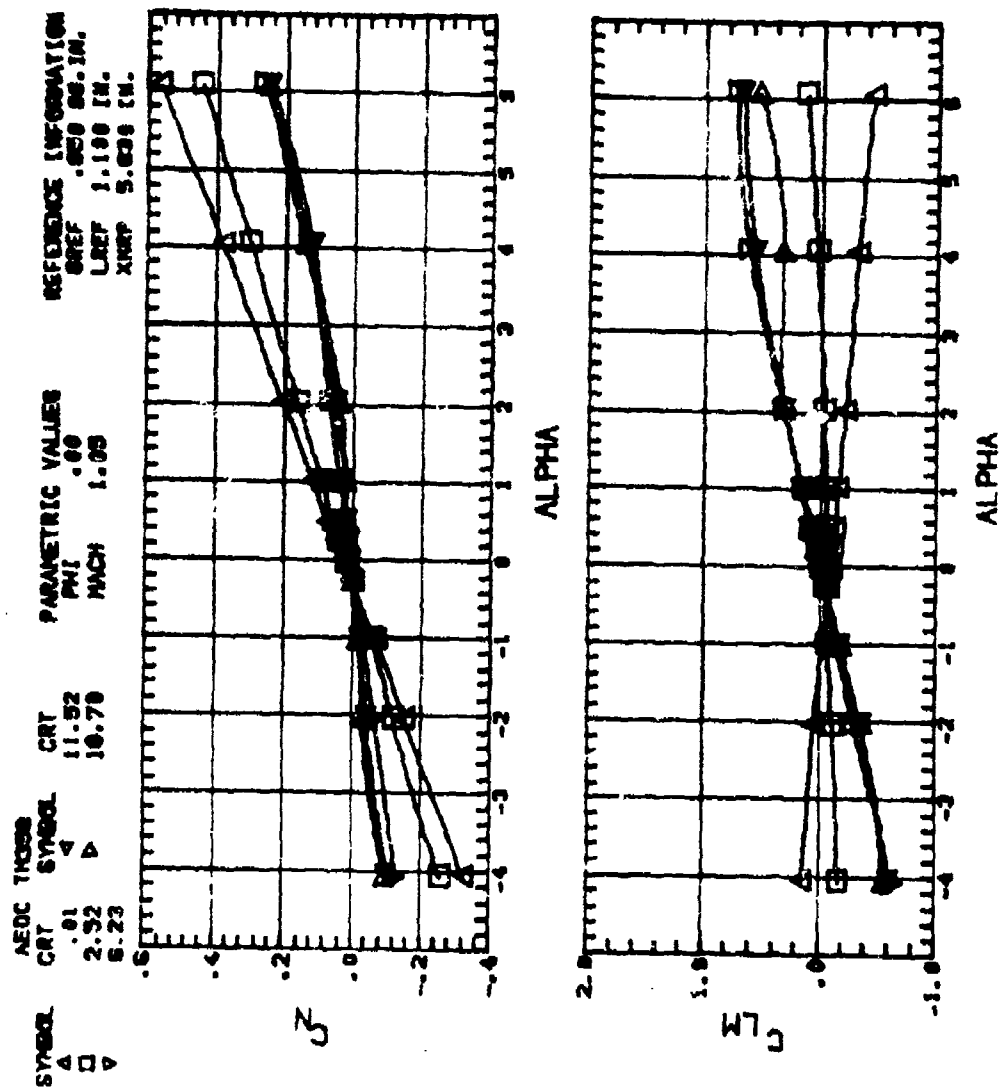


Figure 4. Continued. F12D1

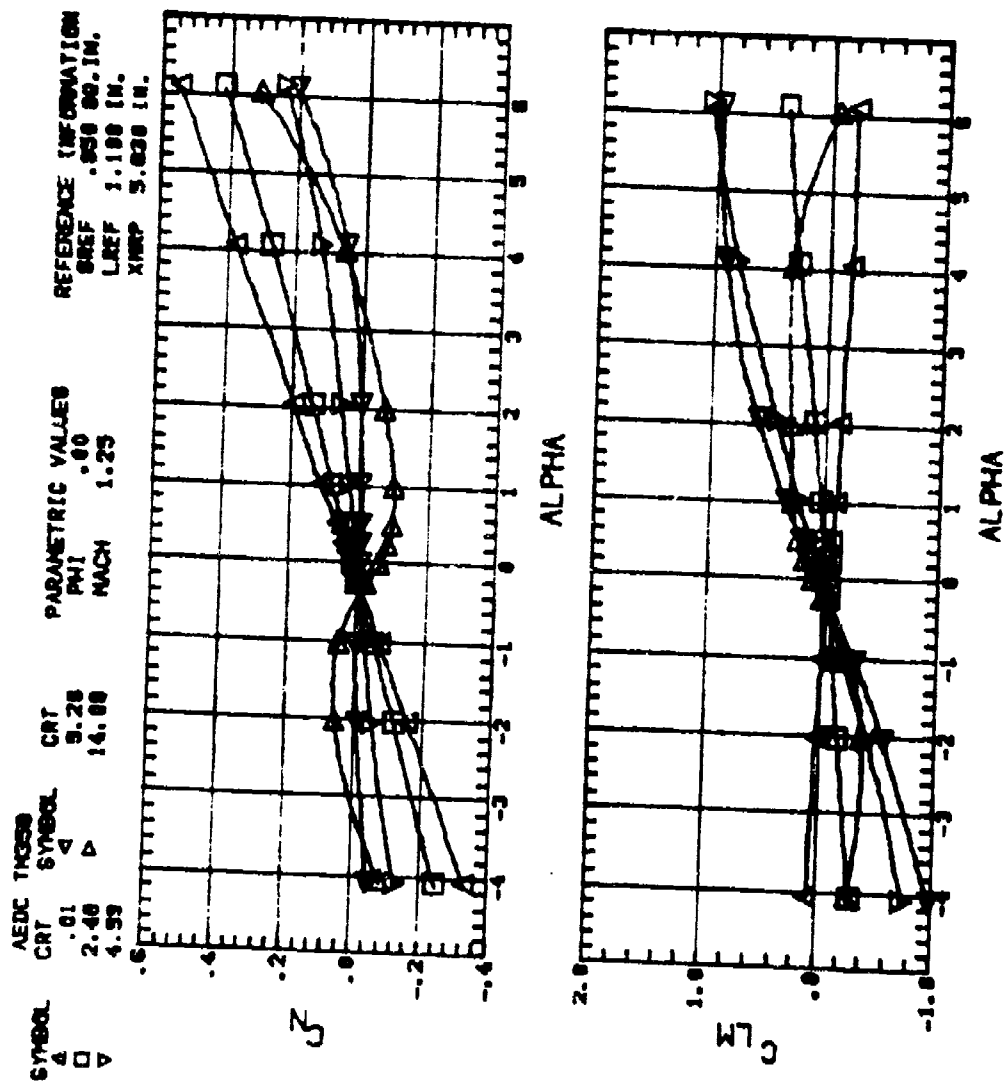


Figure 4. Continued. F12D1

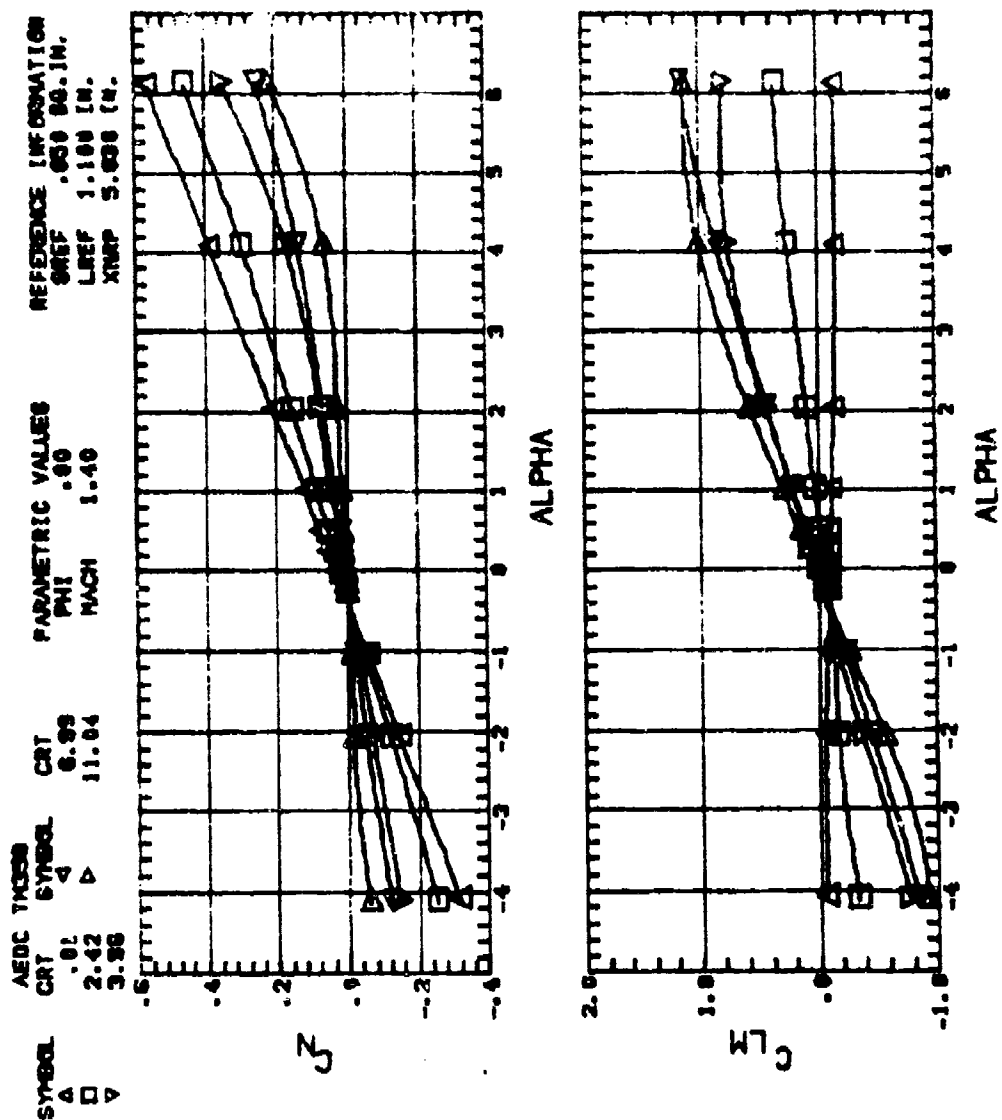


Figure 4. Continued. F12D1

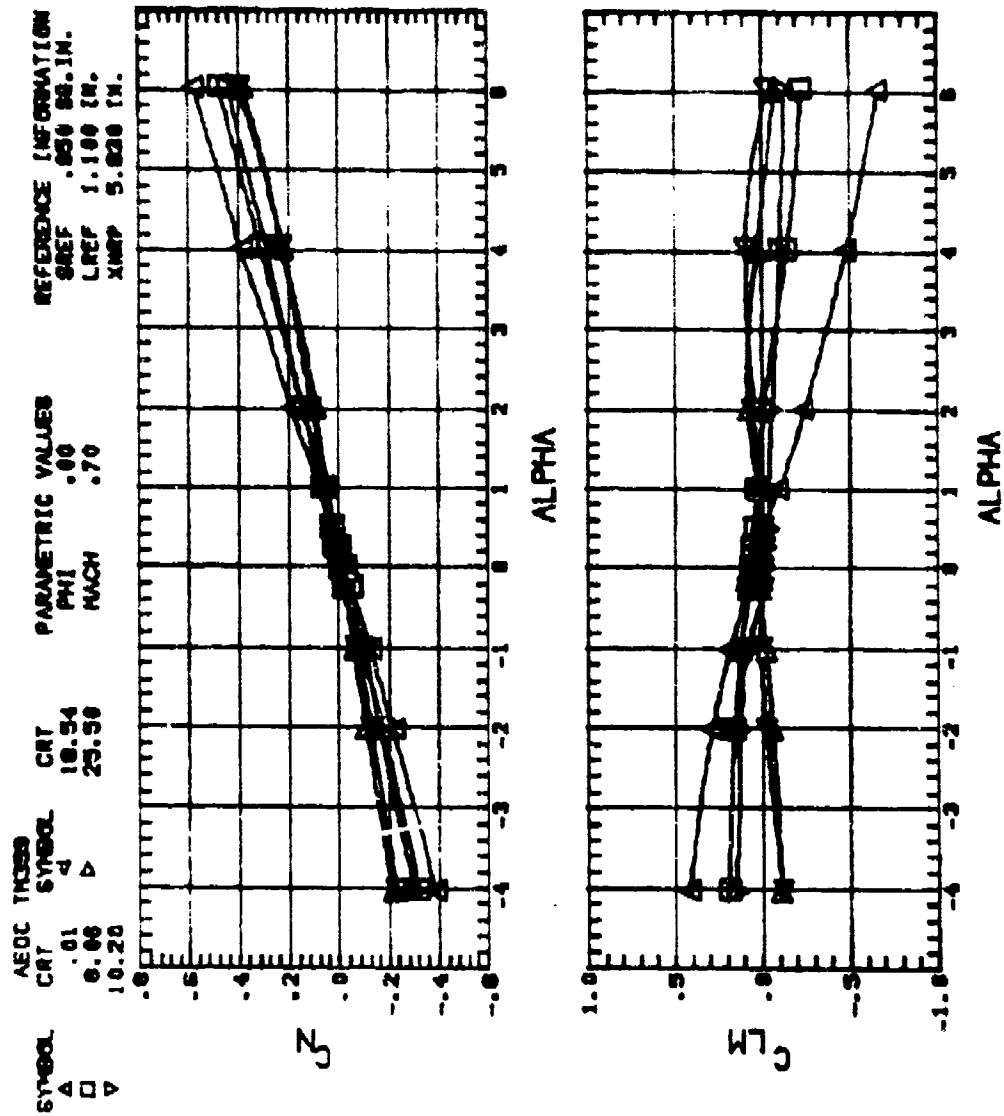


Figure 4. Continued. F12D2

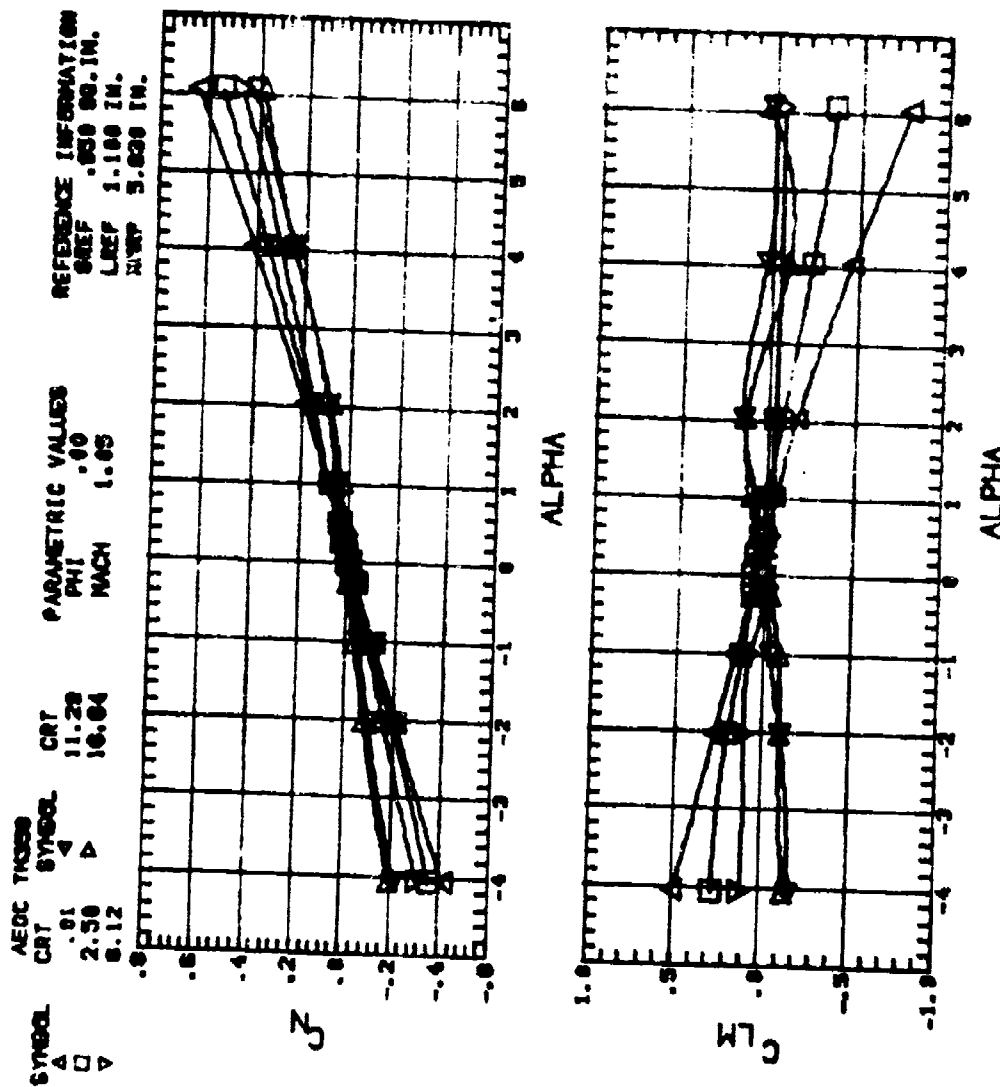


Figure 4. Continued. F12D2

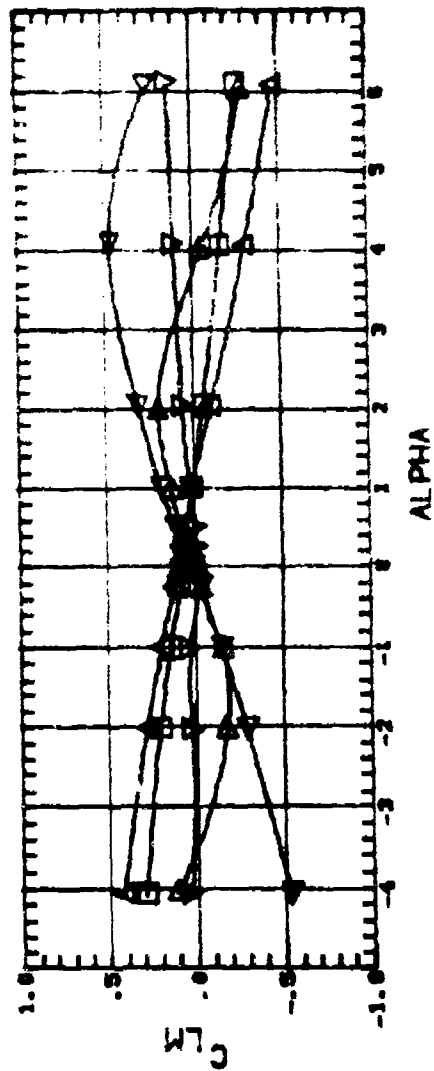
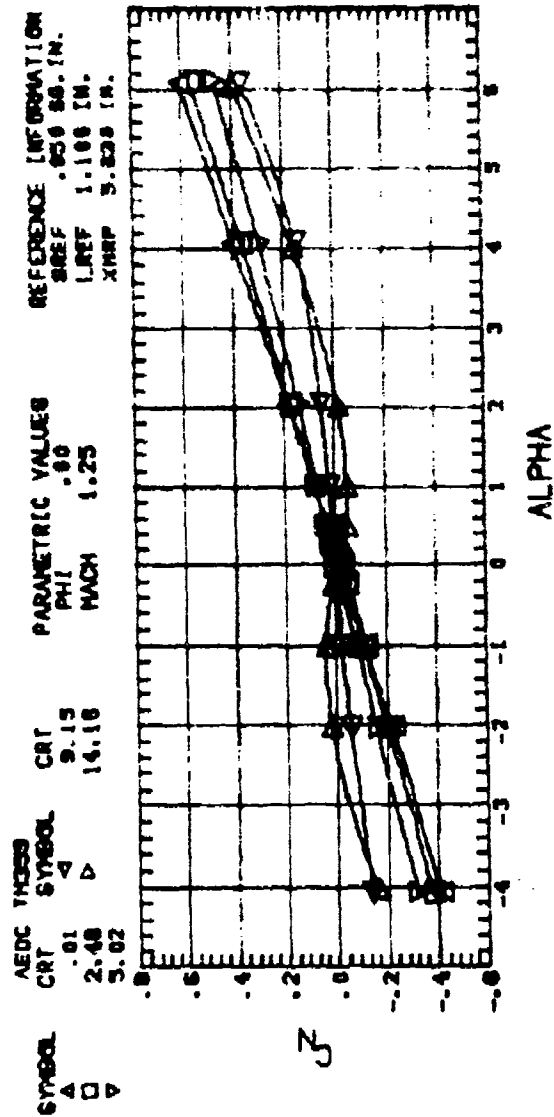


Figure 4. Continued. F12D2

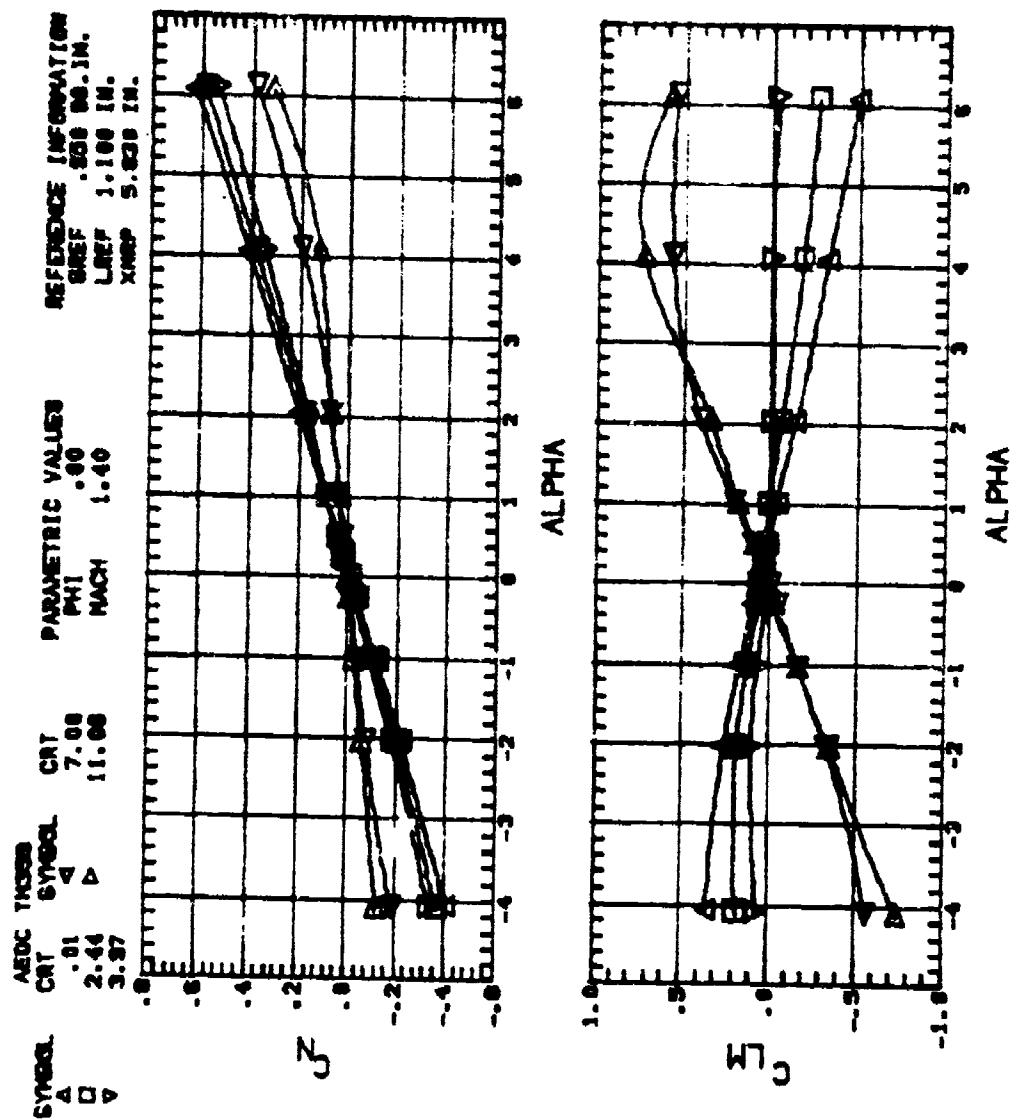


Figure 4. Continued. F12D2



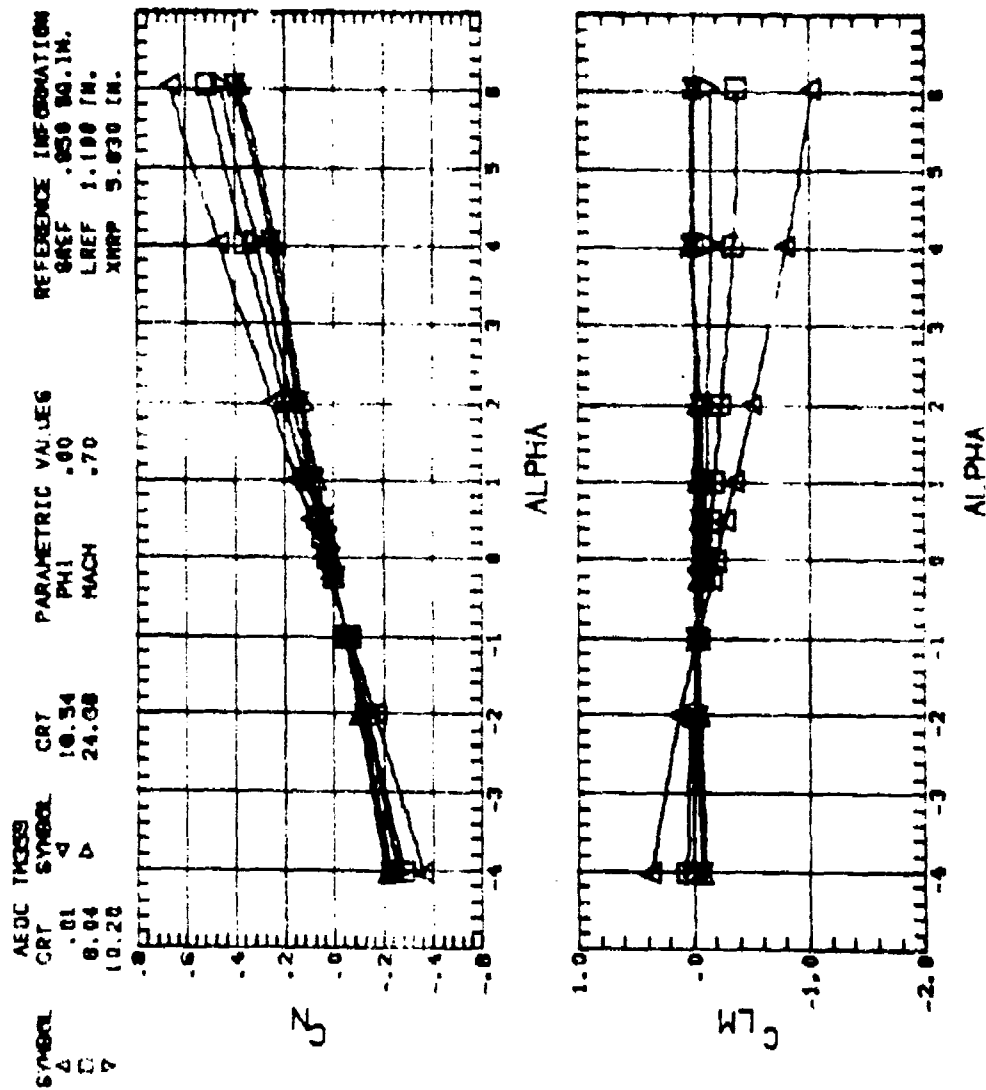


Figure 4. Continued. F6D2

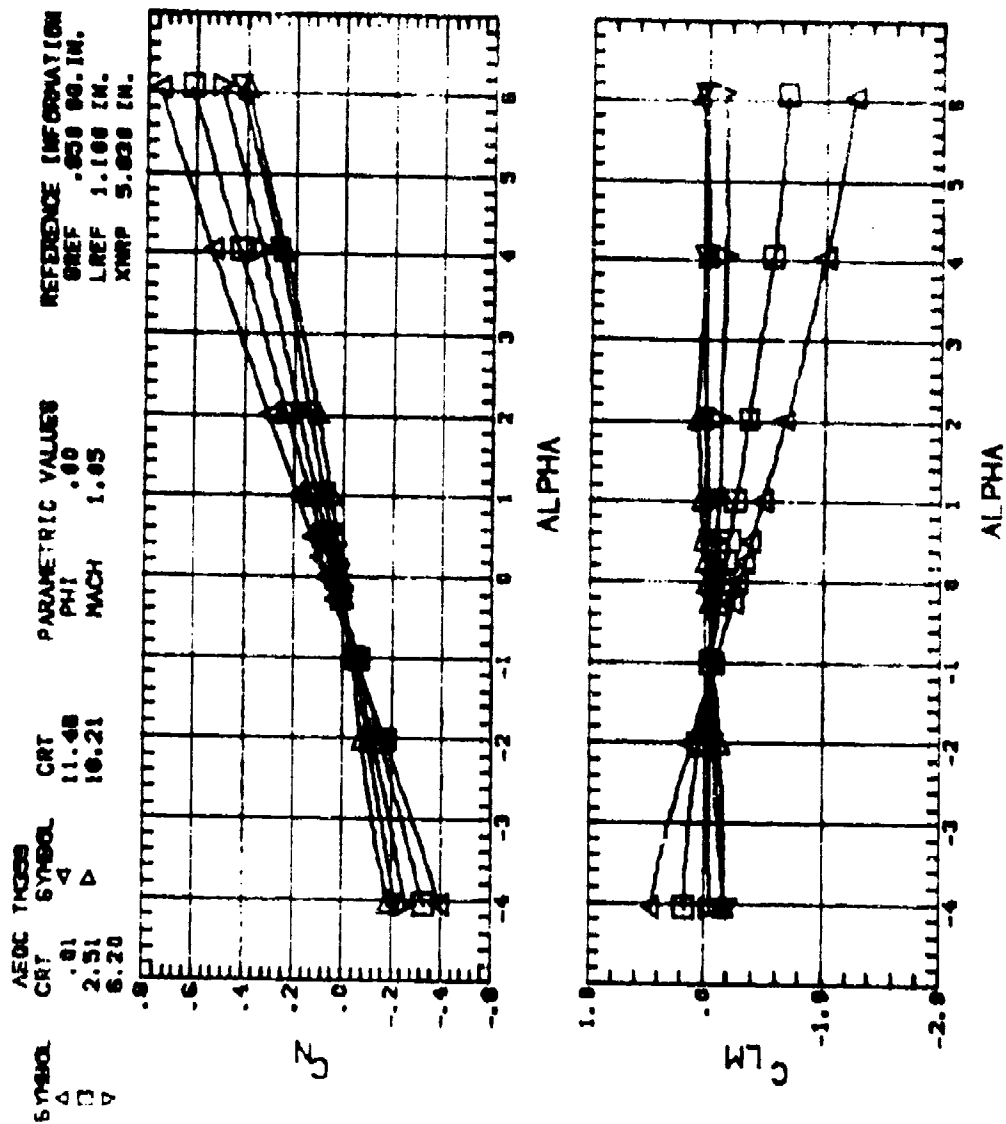


Figure 4. Continued. F6D2

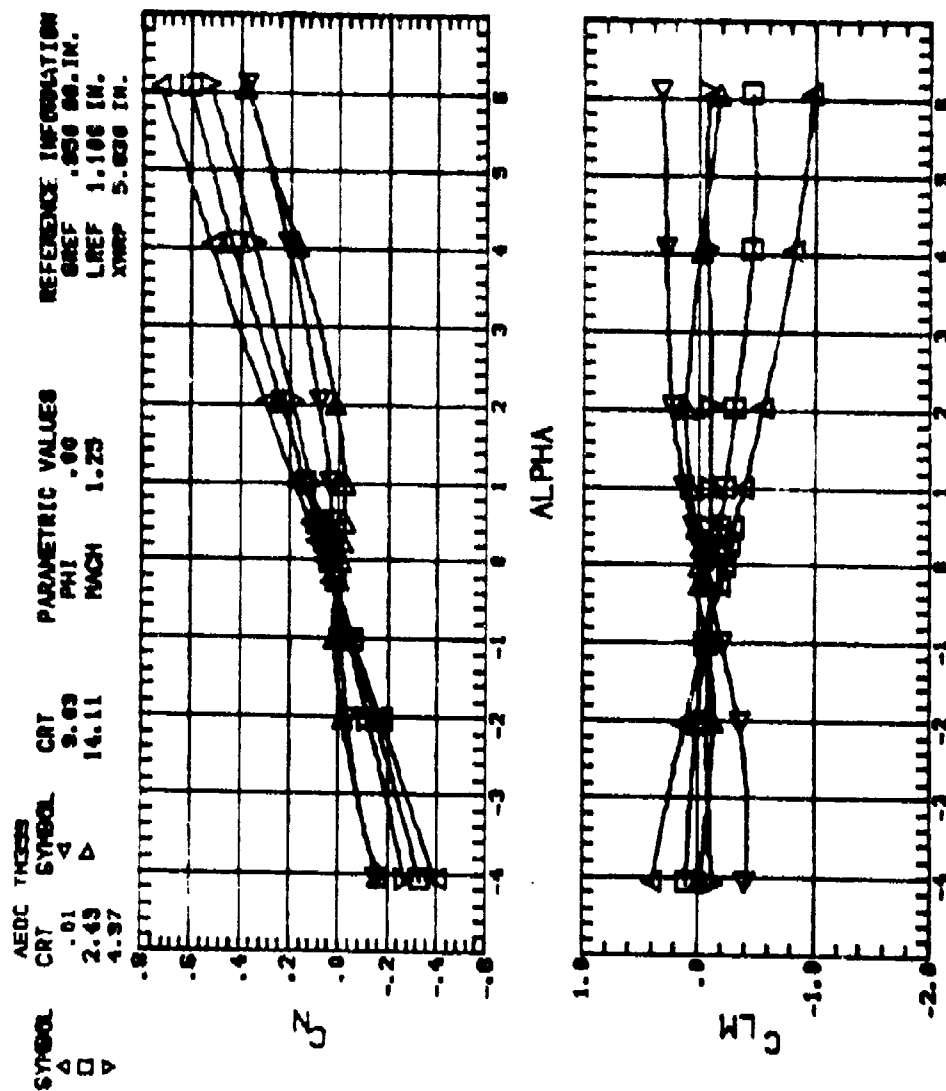


Figure 4. Continued. F6D2

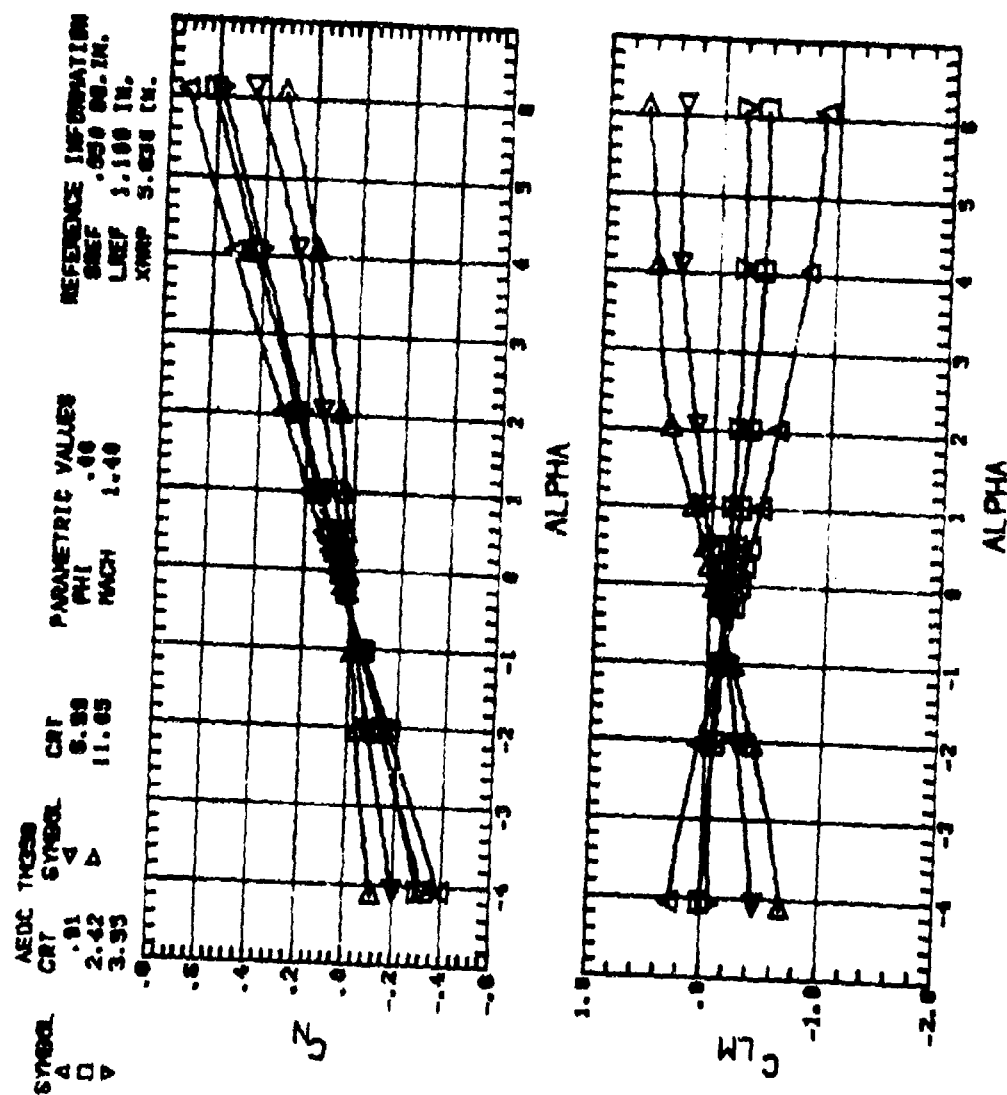


Figure 4. Continued. F6D2

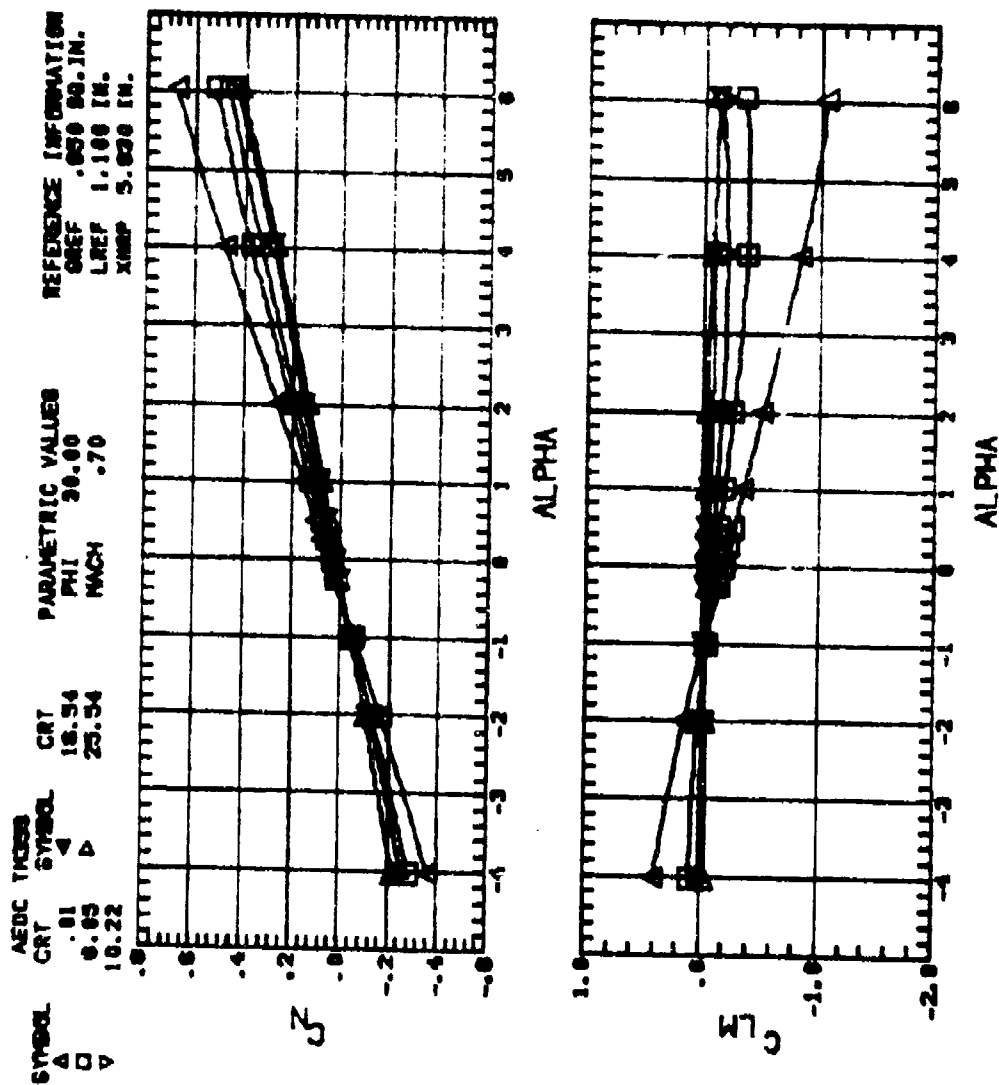


Figure 4. Continued. F6D2, PHI=30 DEG

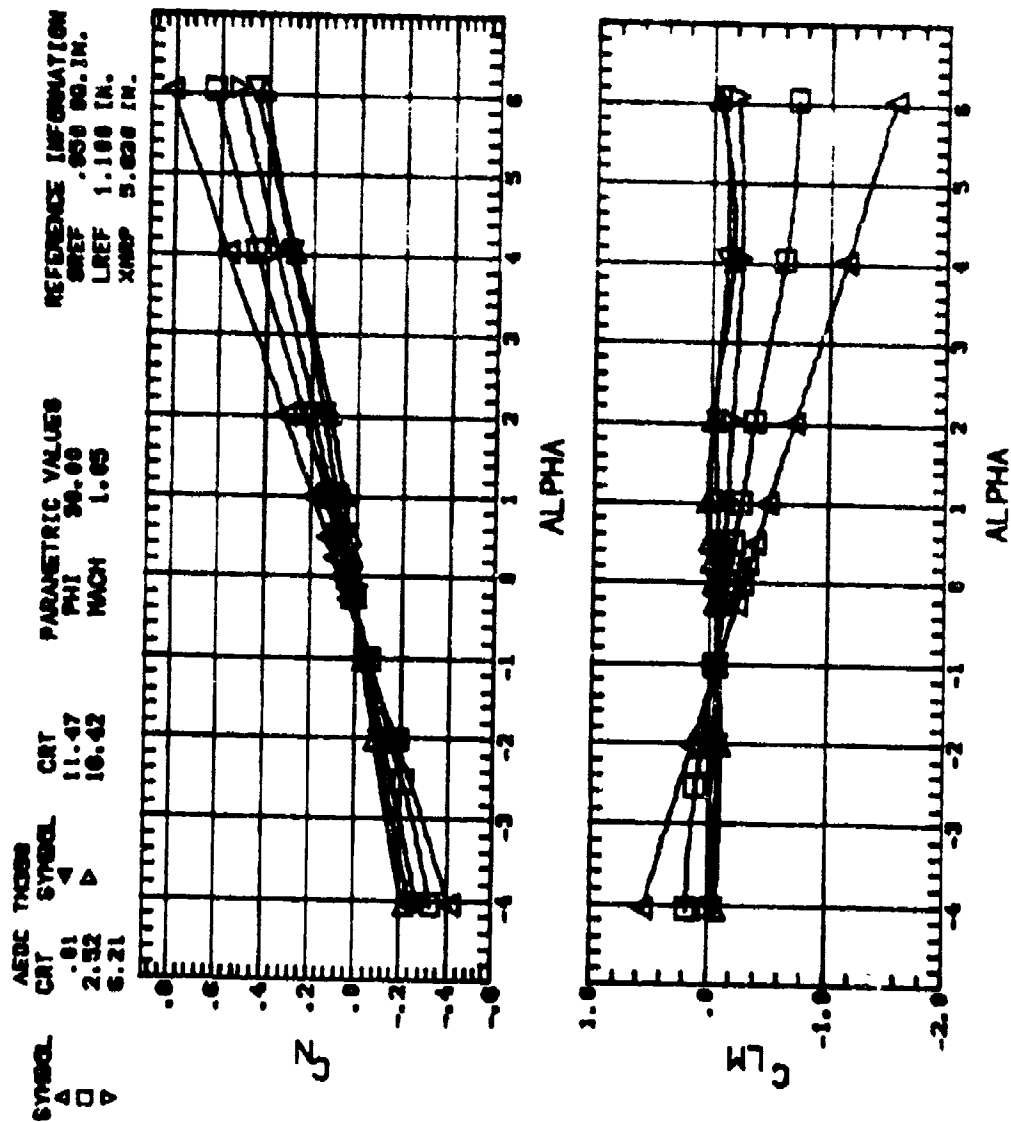


Figure 4. Continued. F6D2, PHI=30 DEG

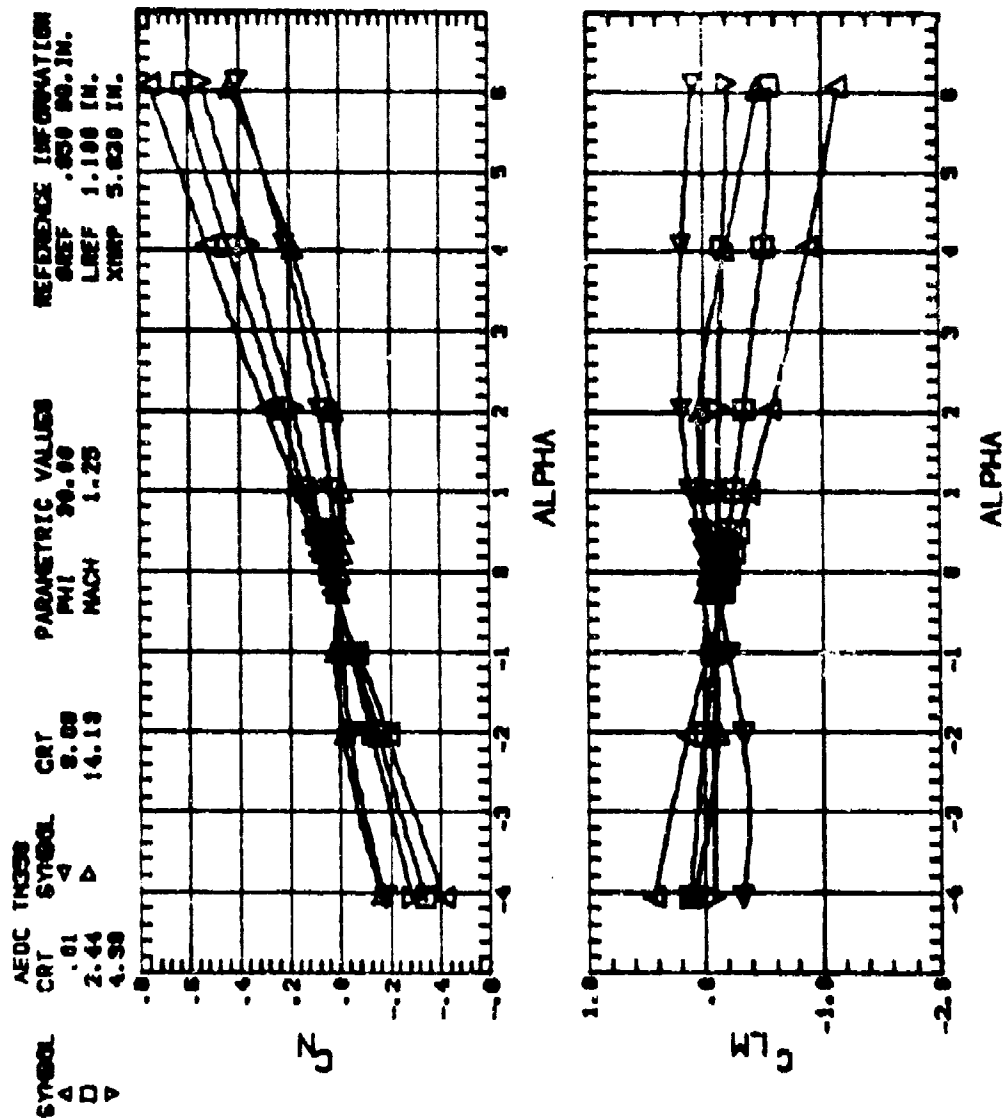


Figure 4. Continued. F6D2, PHI=30 DEG









SYMBOL	CONFIG	REFERENCE INFORMATION
○	C	SREF .950 SQ. IN.
□	FD2	LREF 1.100 IN.
△	F6D2	XMRP 5.830 IN.
▽	FL2D2	
◇	F6D2S	

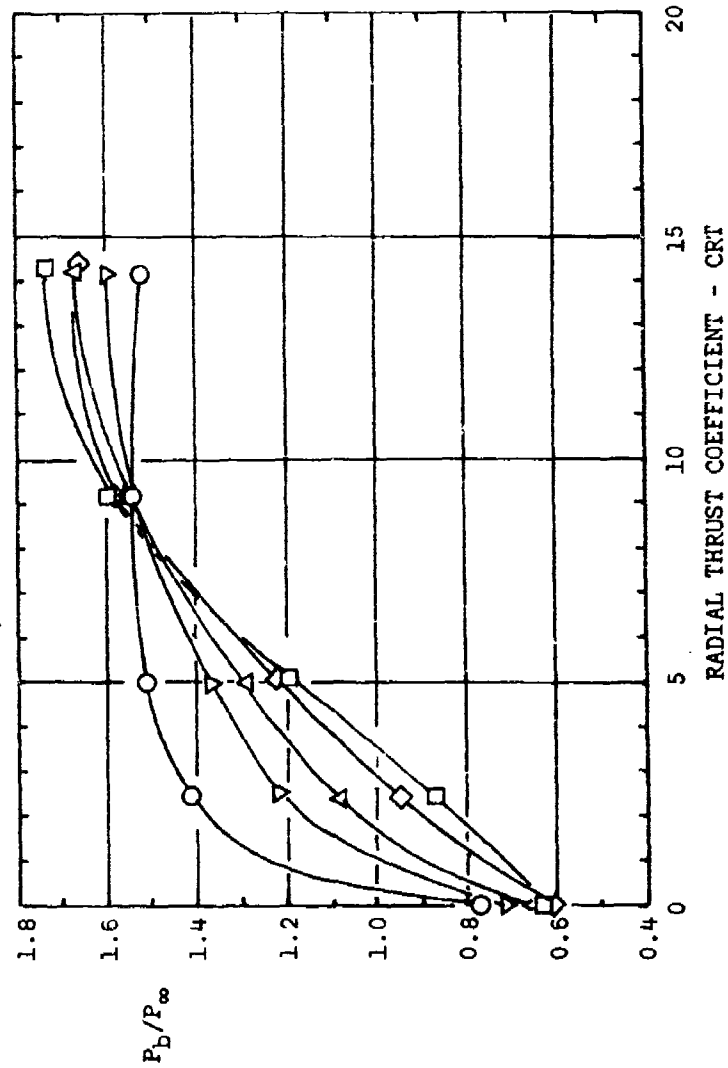


Figure 5. Typical thrust effect on base pressure ratio  $-M_\infty = 1.25$ ,  $\alpha = 0^\circ$ .

AEDC TM-359

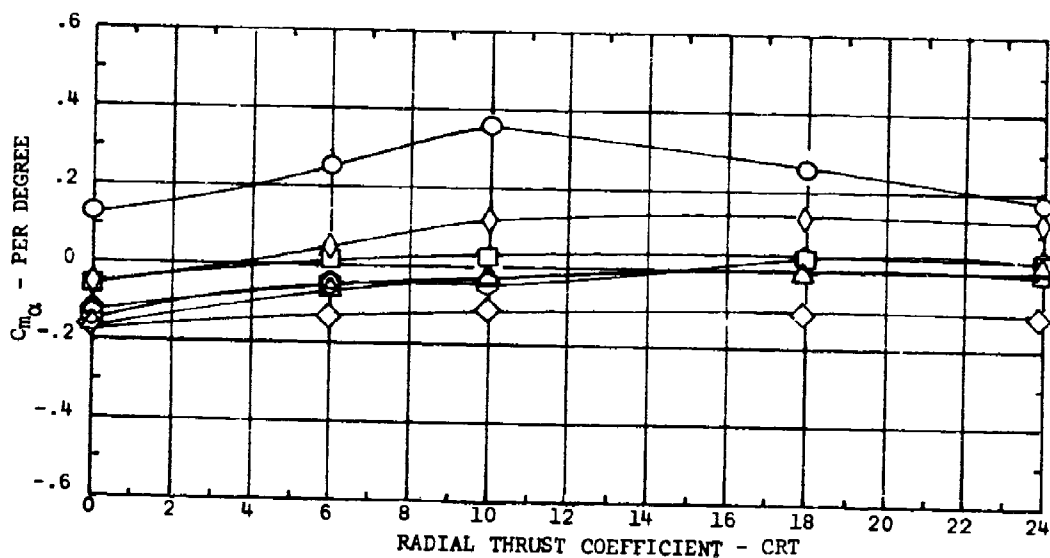
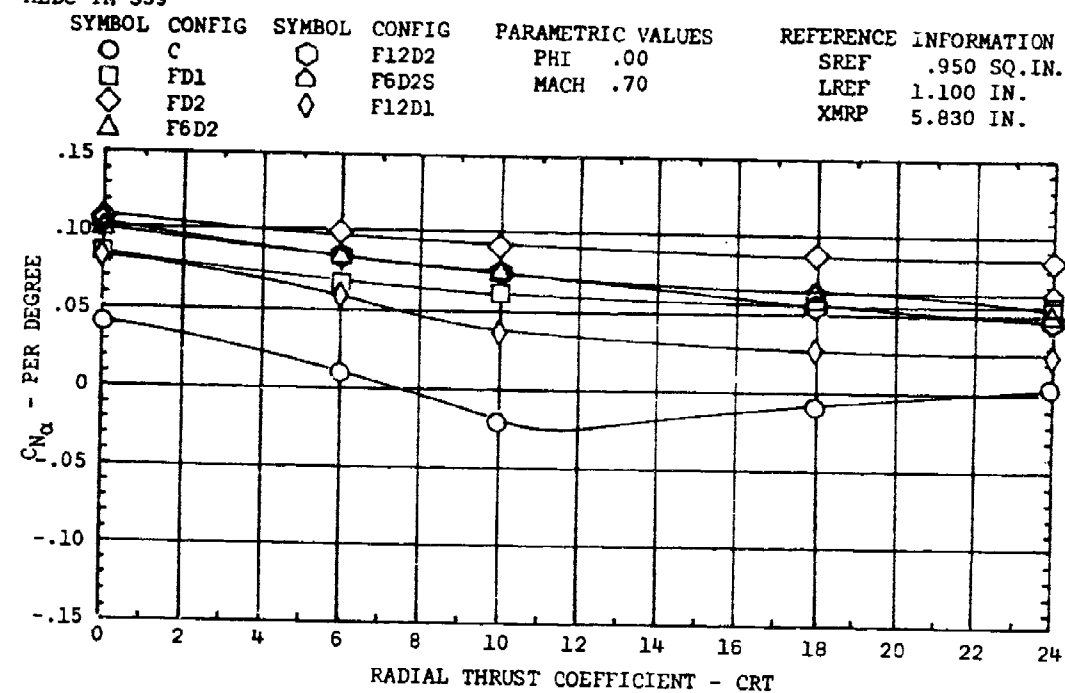


Figure 6. Thrust effects on initial normal force and pitching moment coefficient slopes.

SYMBOL	CONFIG	SYMBOL	CONFIG	PARAMETRIC VALUES	REFERENCE INFORMATION
○	C	○	F12D2	PHI .00	SREF .950 SQ. IN.
□	FD1	□	F6D2S	MACH 1.05	LREF 1.100 IN.
◇	FD2	◇	F12D1		XMR? 5.830 IN.
△	F6D2				

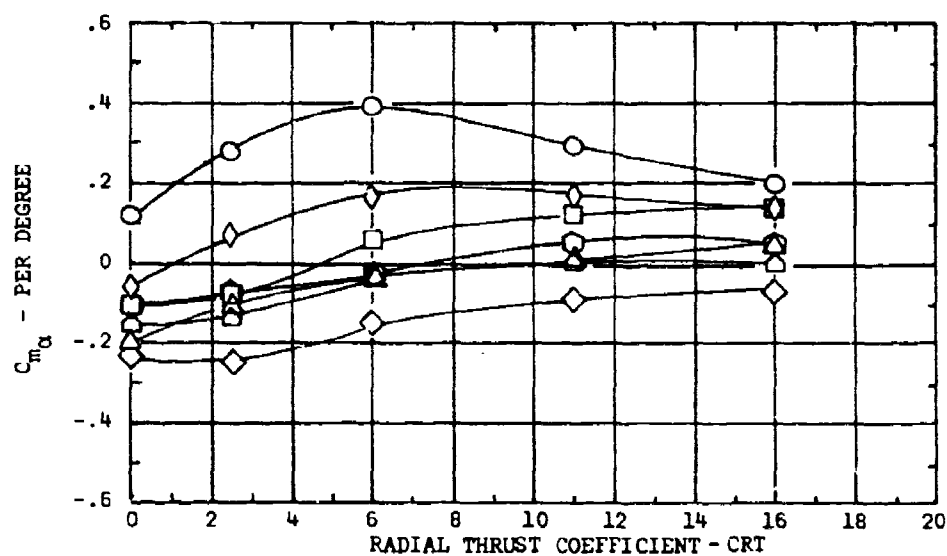
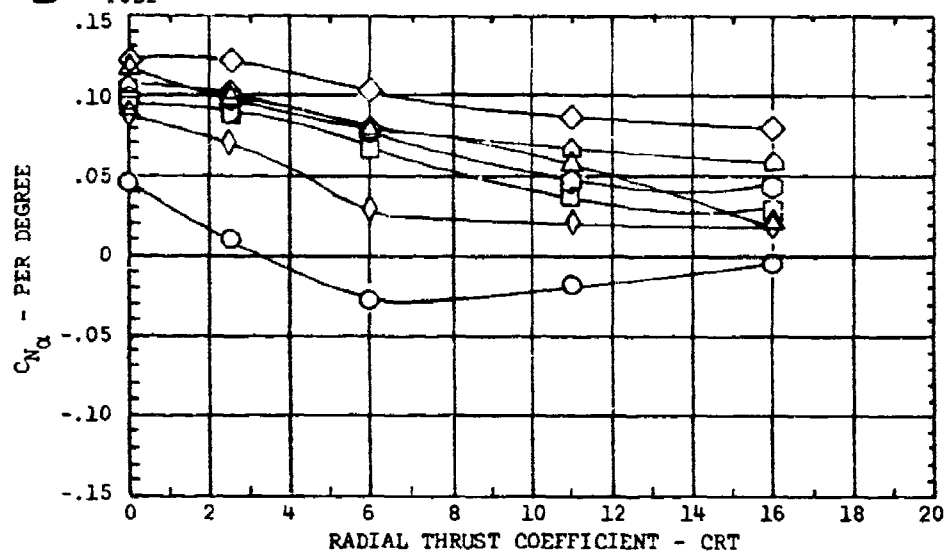


Figure 6. Continued.

AEDC TM-359

SYMBOL	CONFIG	SYMBOL	CONFIG	PARAMETRIC VALUES	REFERENCE LINE
○	C	○	F12D2	PHI .00	SRE
□	FD1	△	F6D2S	MACH 1.25	LREF
◇	FD2	◇	F12D1		XMRP 5.830 IN.
△	F6D2				

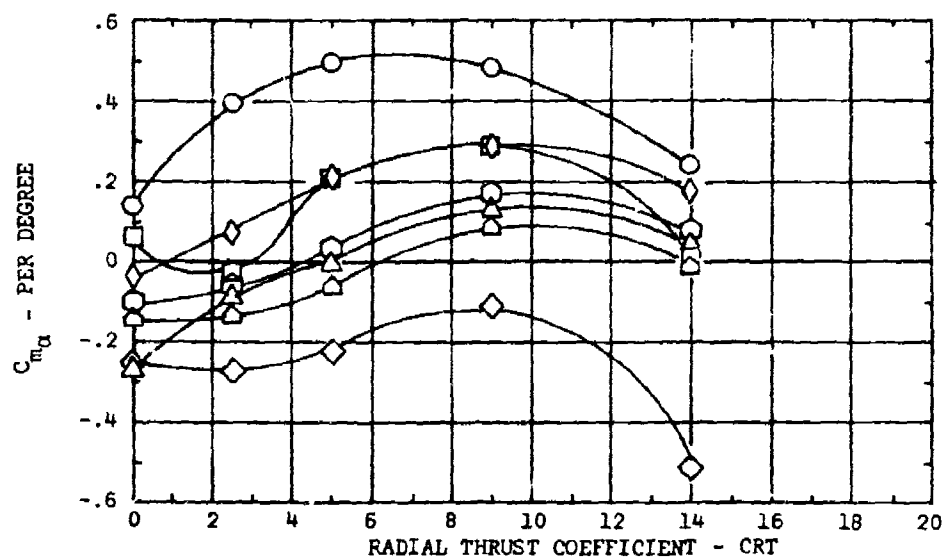
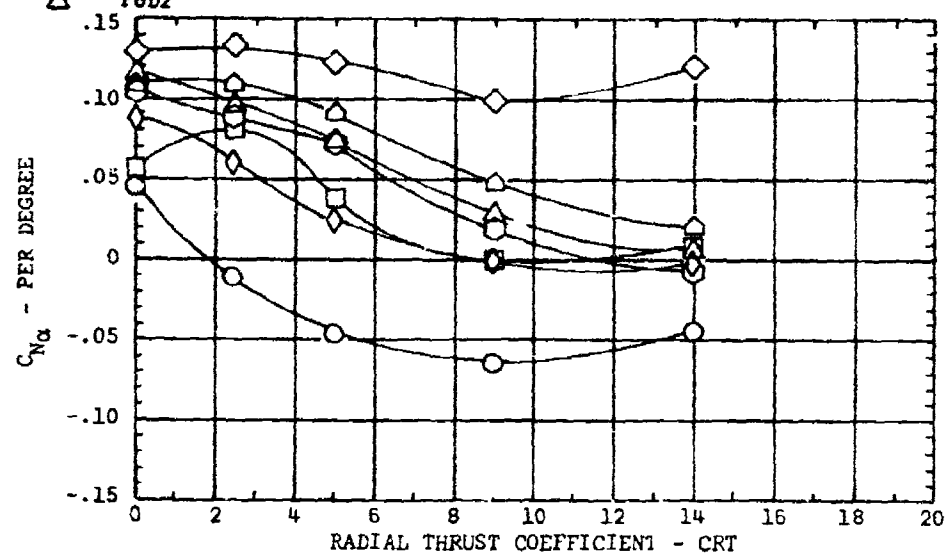


Figure 6. Continued.

## PARAMETRIC VALUES

PHI .00  
MACH 1.40

## REFERENCE INFORMATION

SREF .950 SQ. IN.  
LREF 1.100 IN.  
XMRP 5.830 IN.

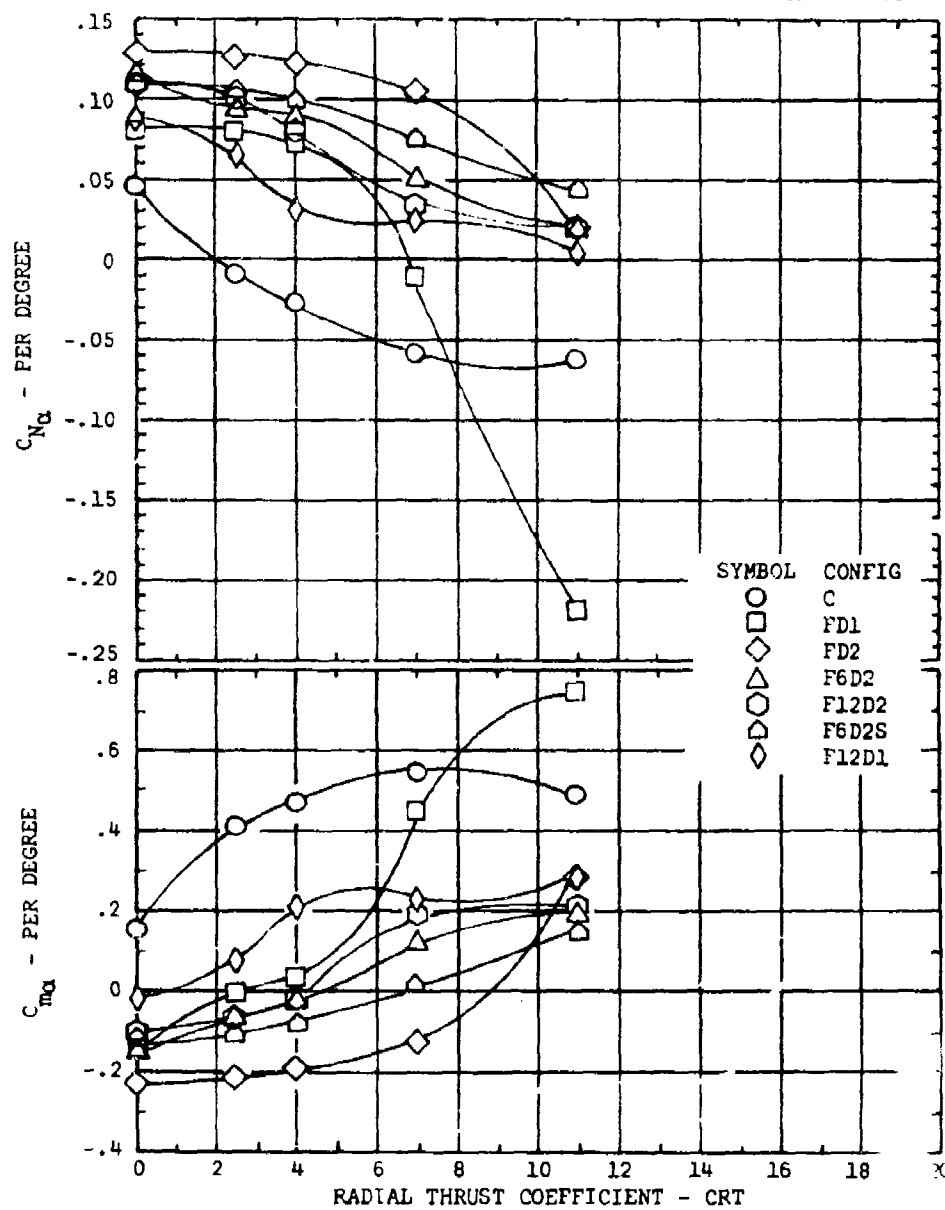


Figure 6. Concluded.

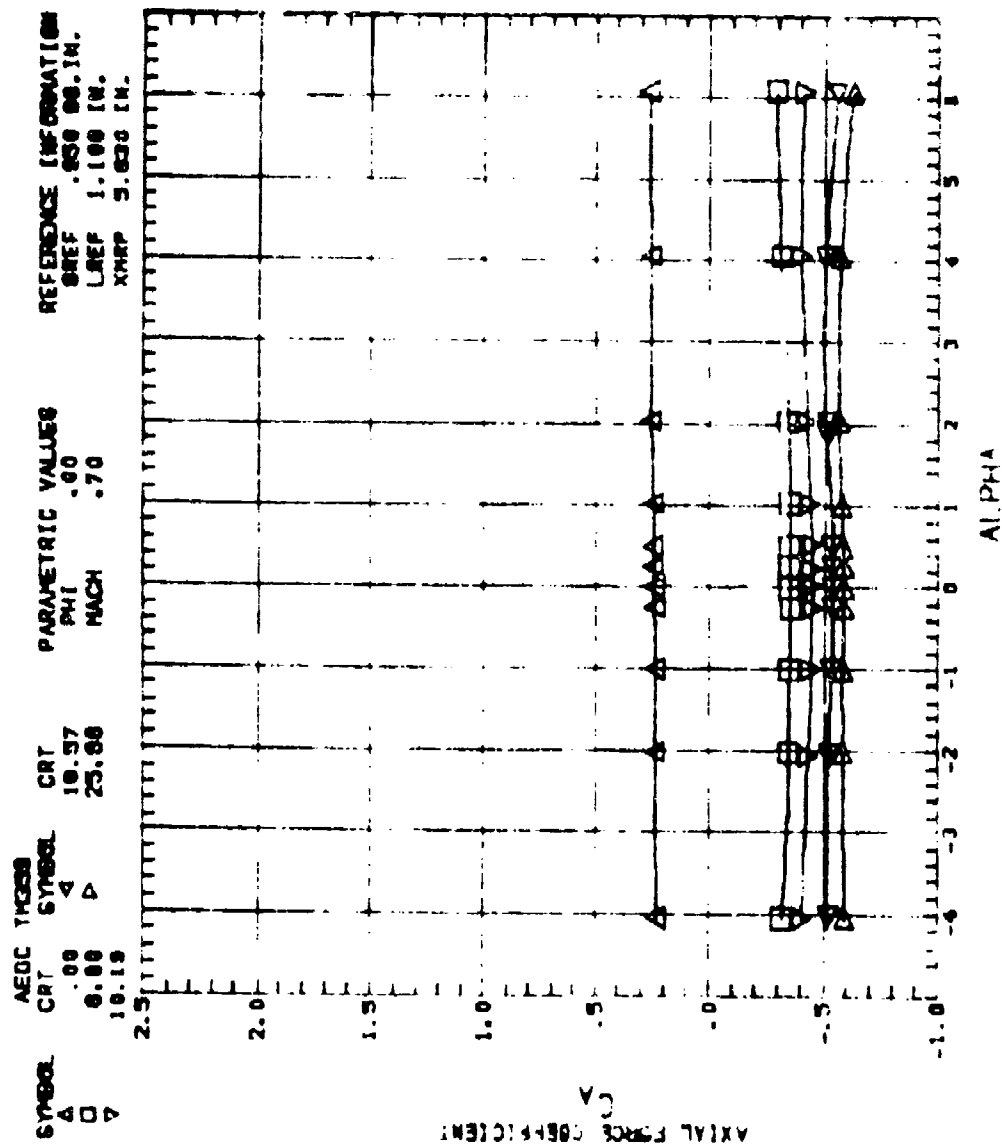


Figure 7. Thrust effects on axial force coefficient. C



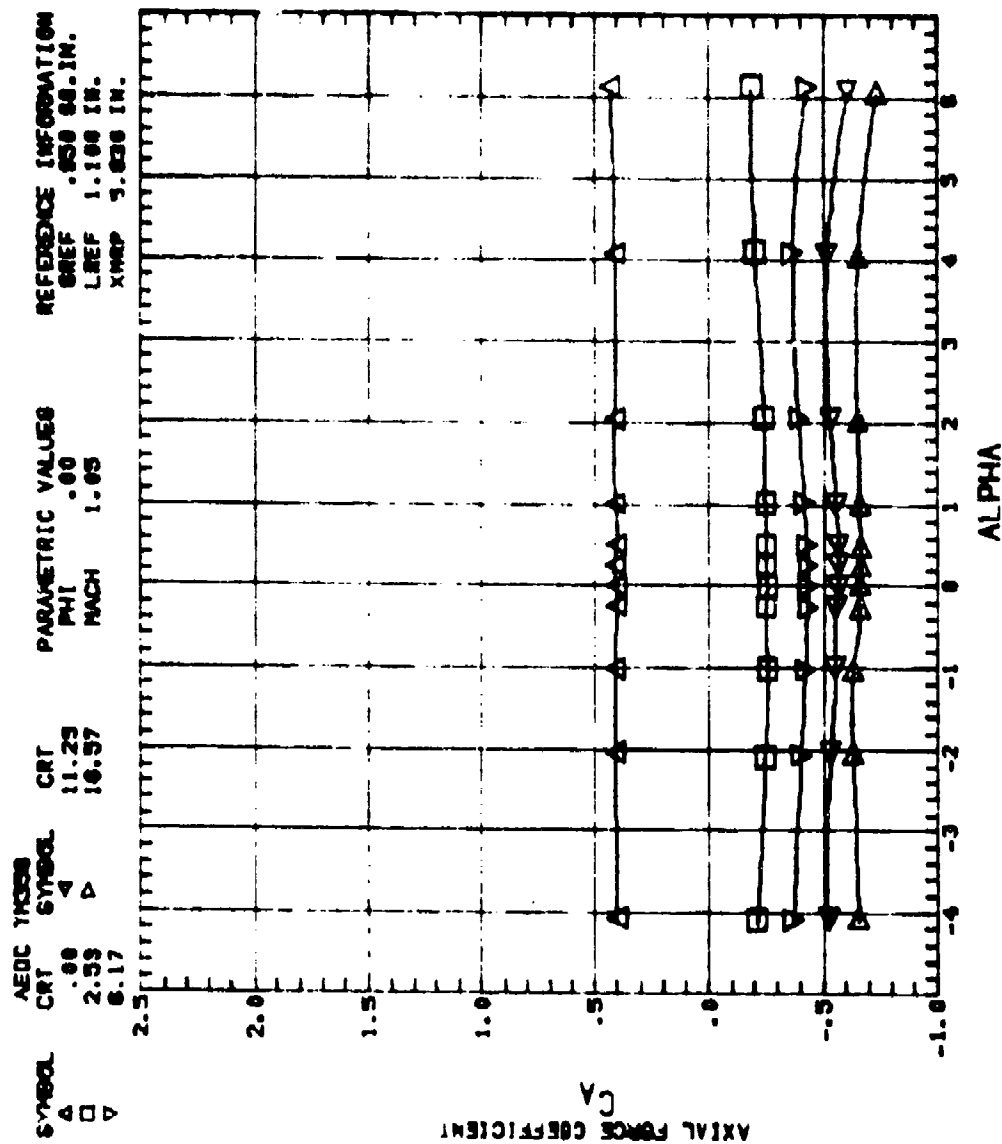


Figure 7. Continued. C

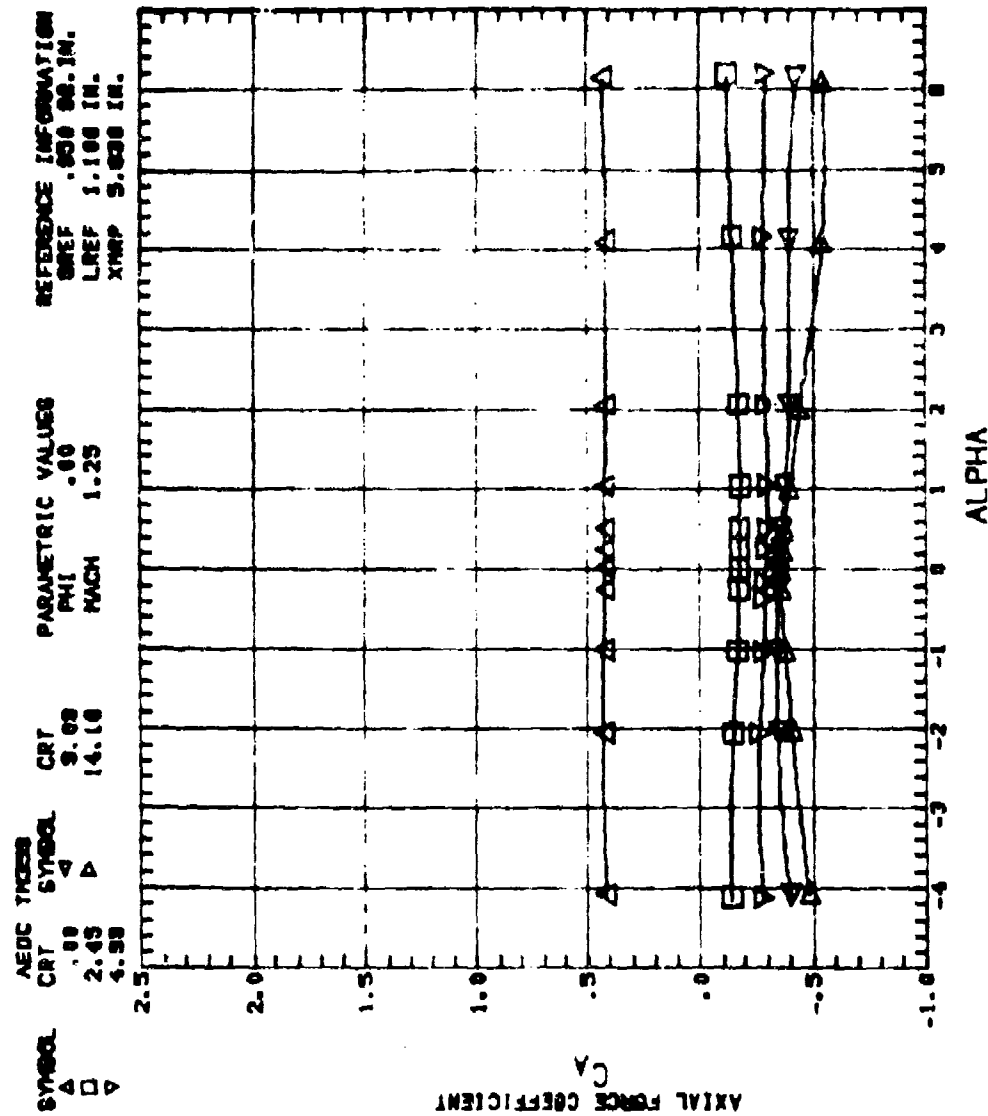


Figure 7. Continued. C

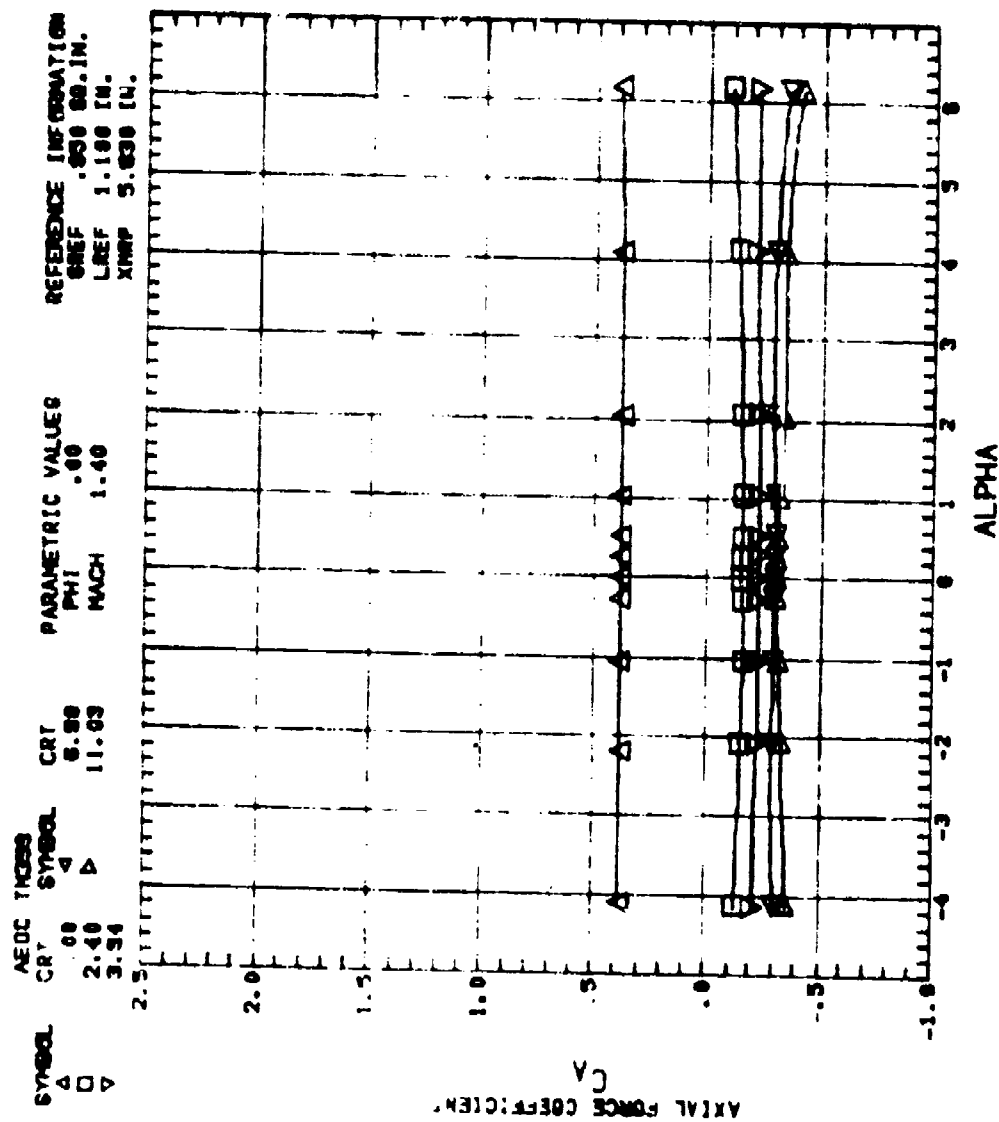


Figure 7. Continued. C

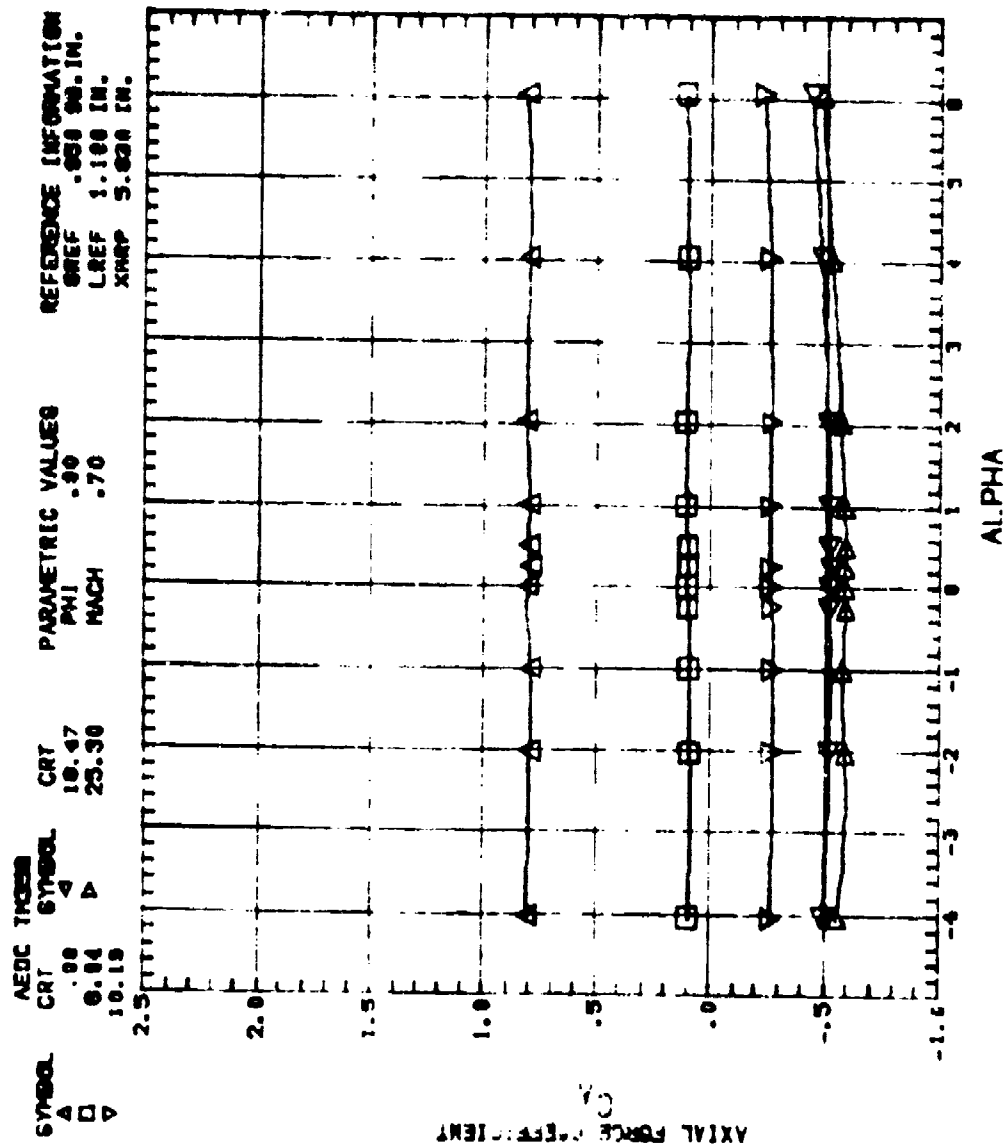


Figure 7. Continued. FDI

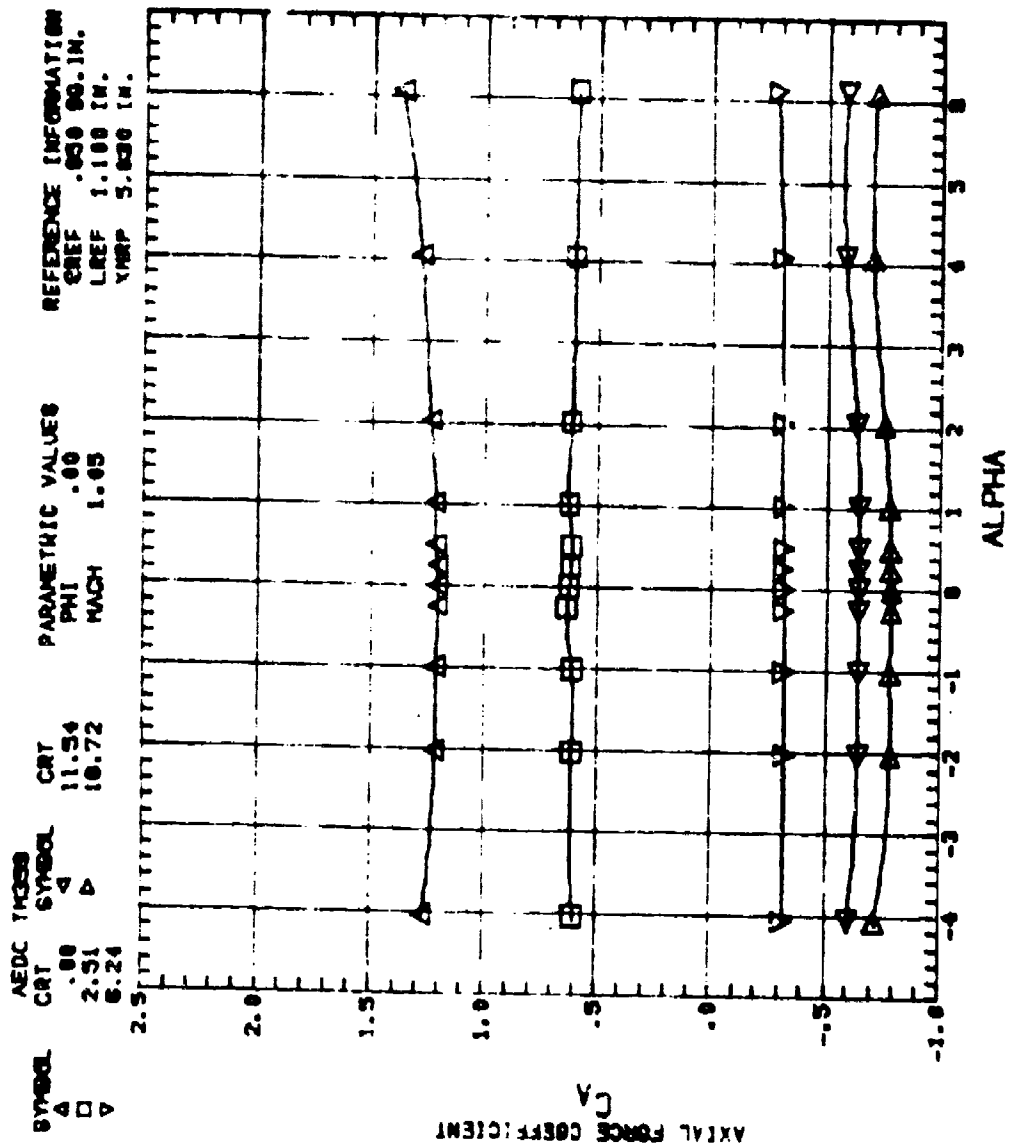


Figure 7. Continued. FD1

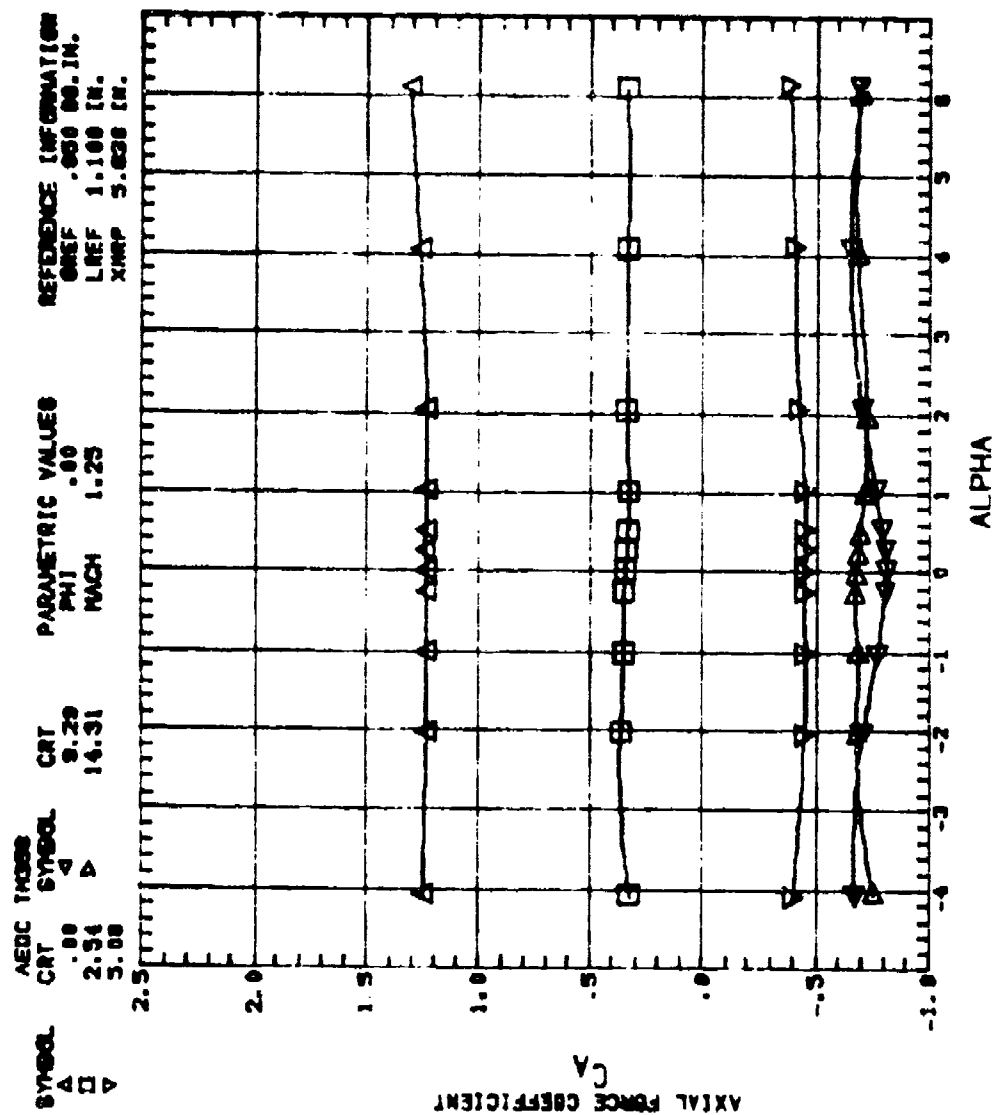


Figure 7. Continued. FD1

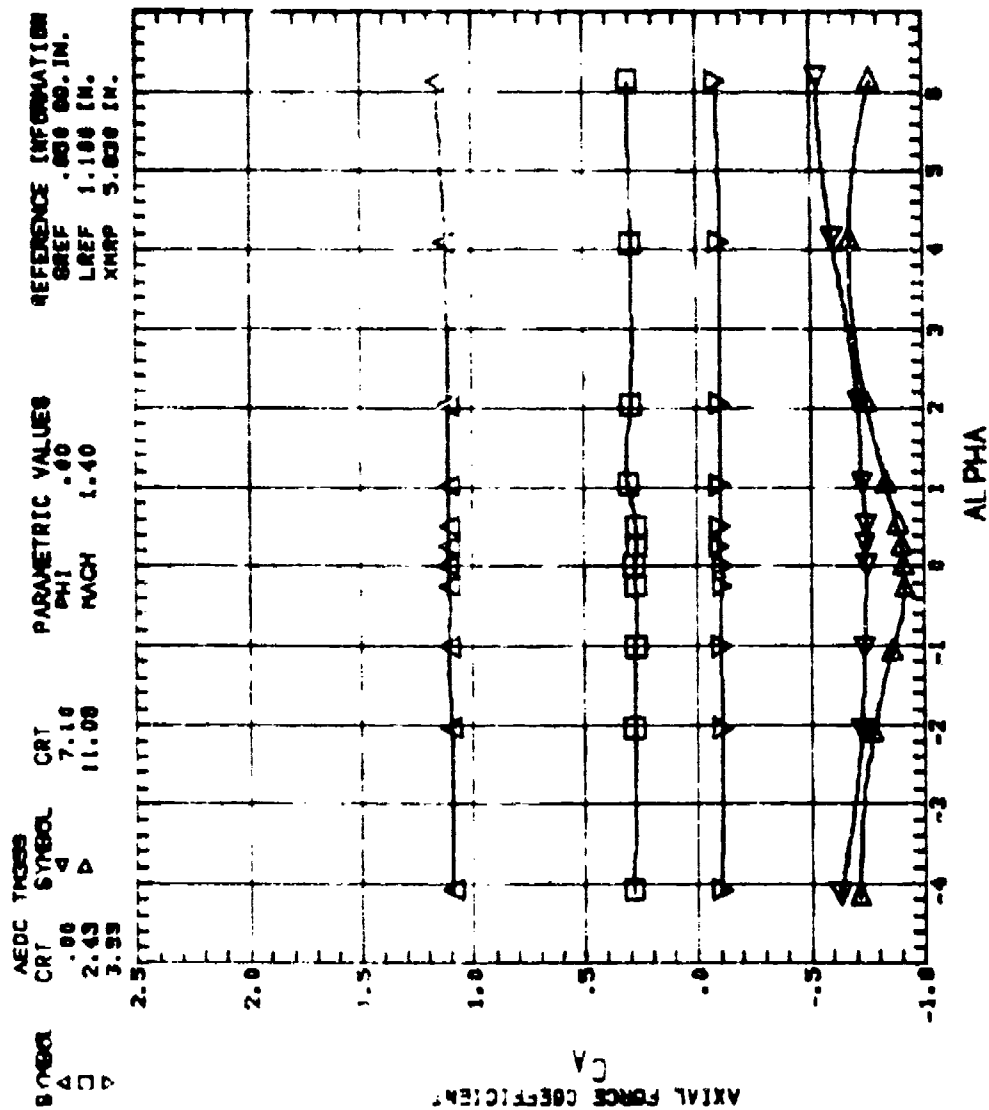


Figure 7. Continued. FD1

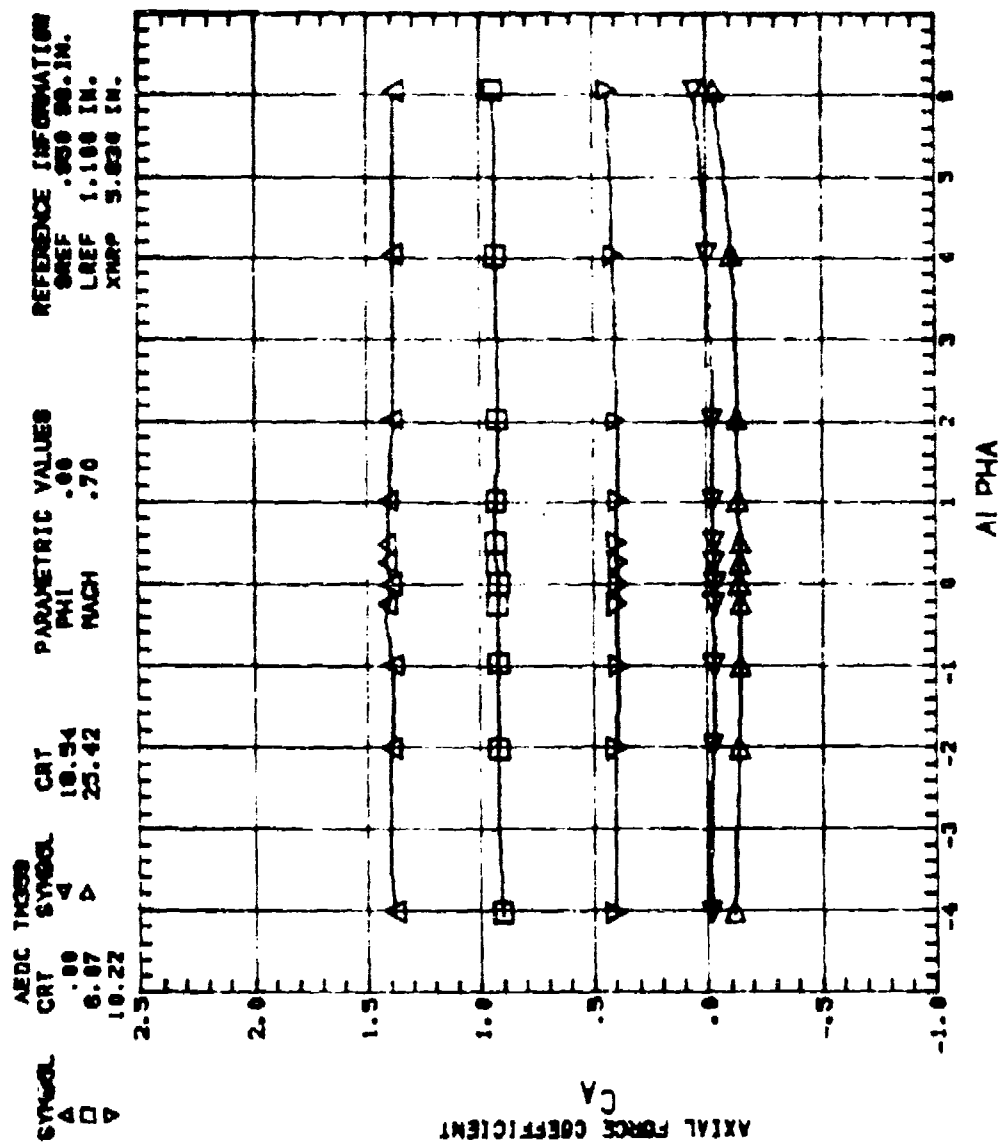


Figure 7. Continued. FD2



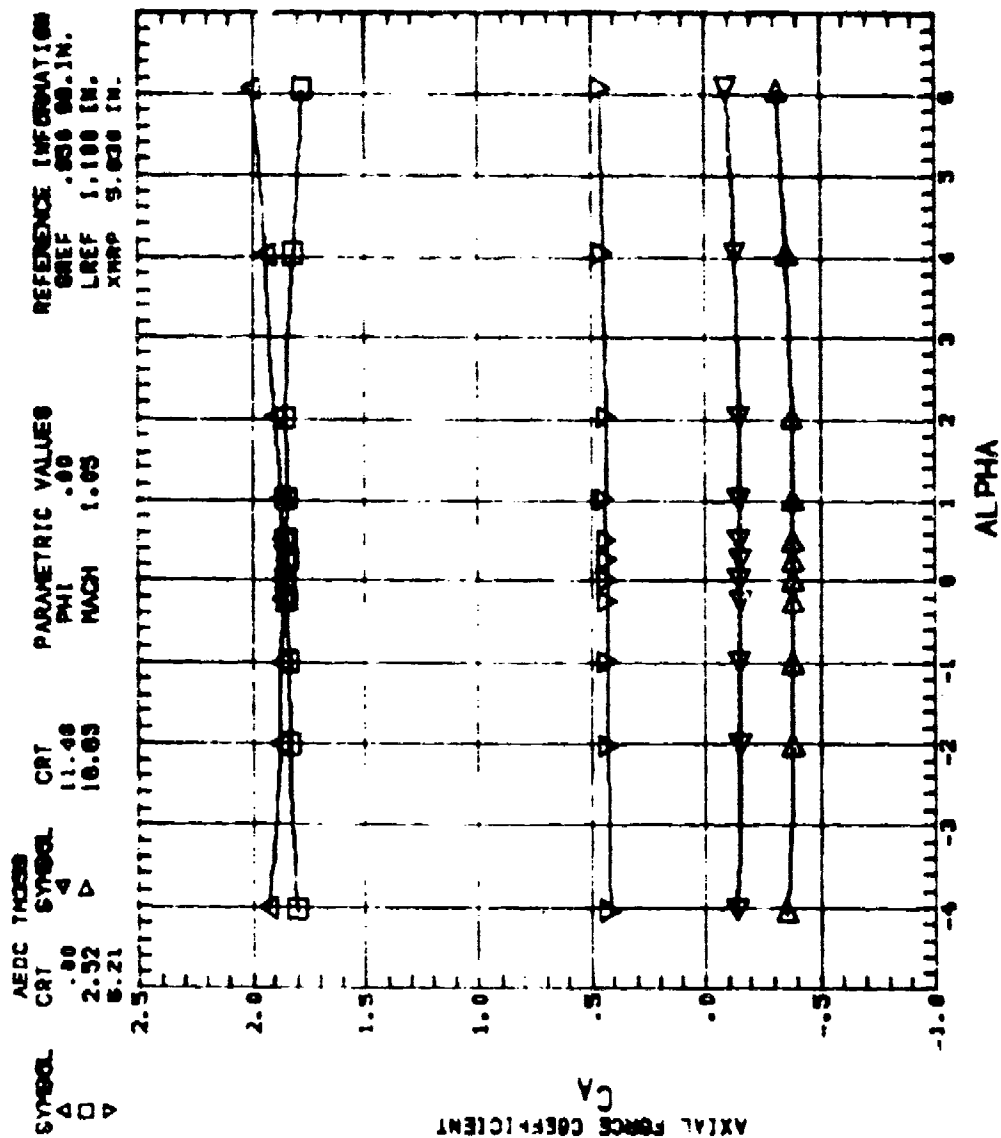


Figure 7. Continued. FD2

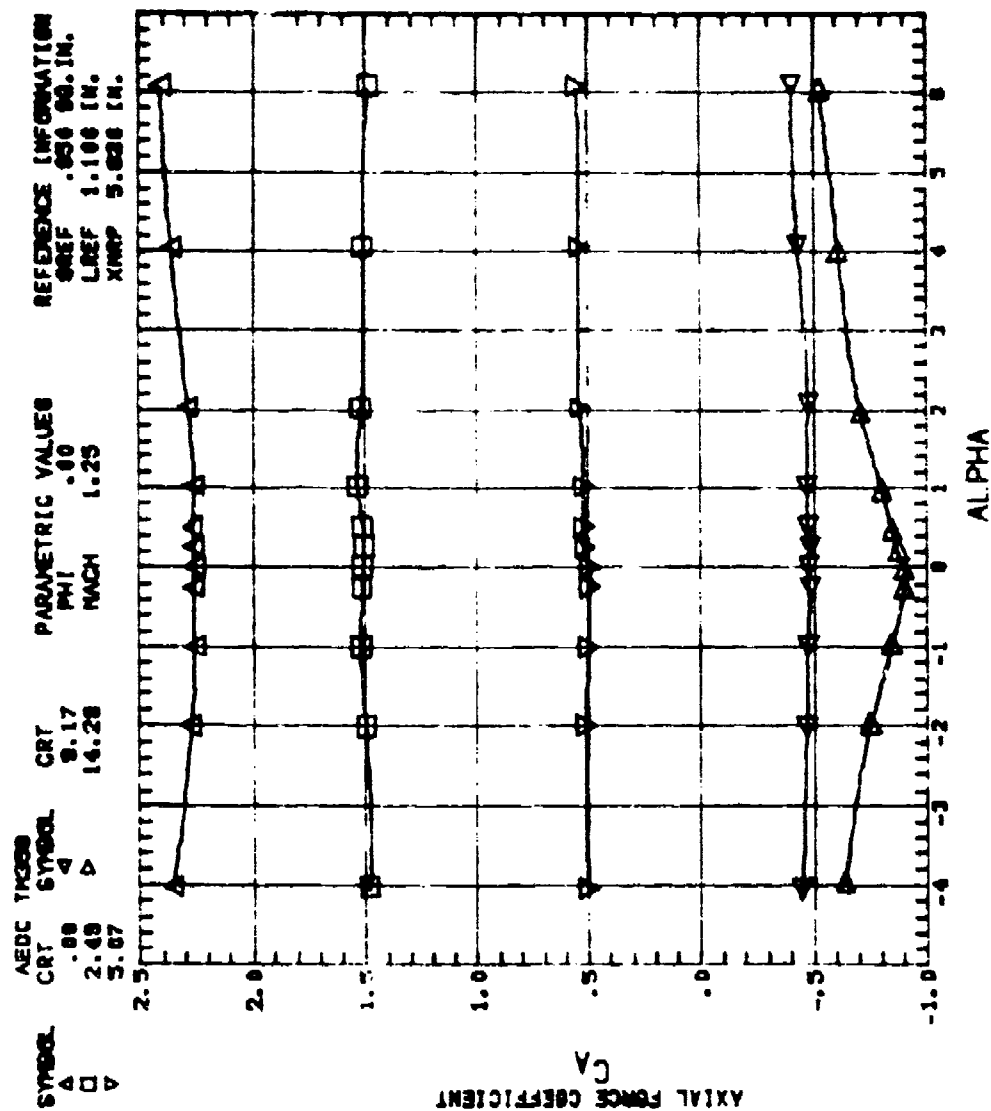


Figure 7. Continued. FD2

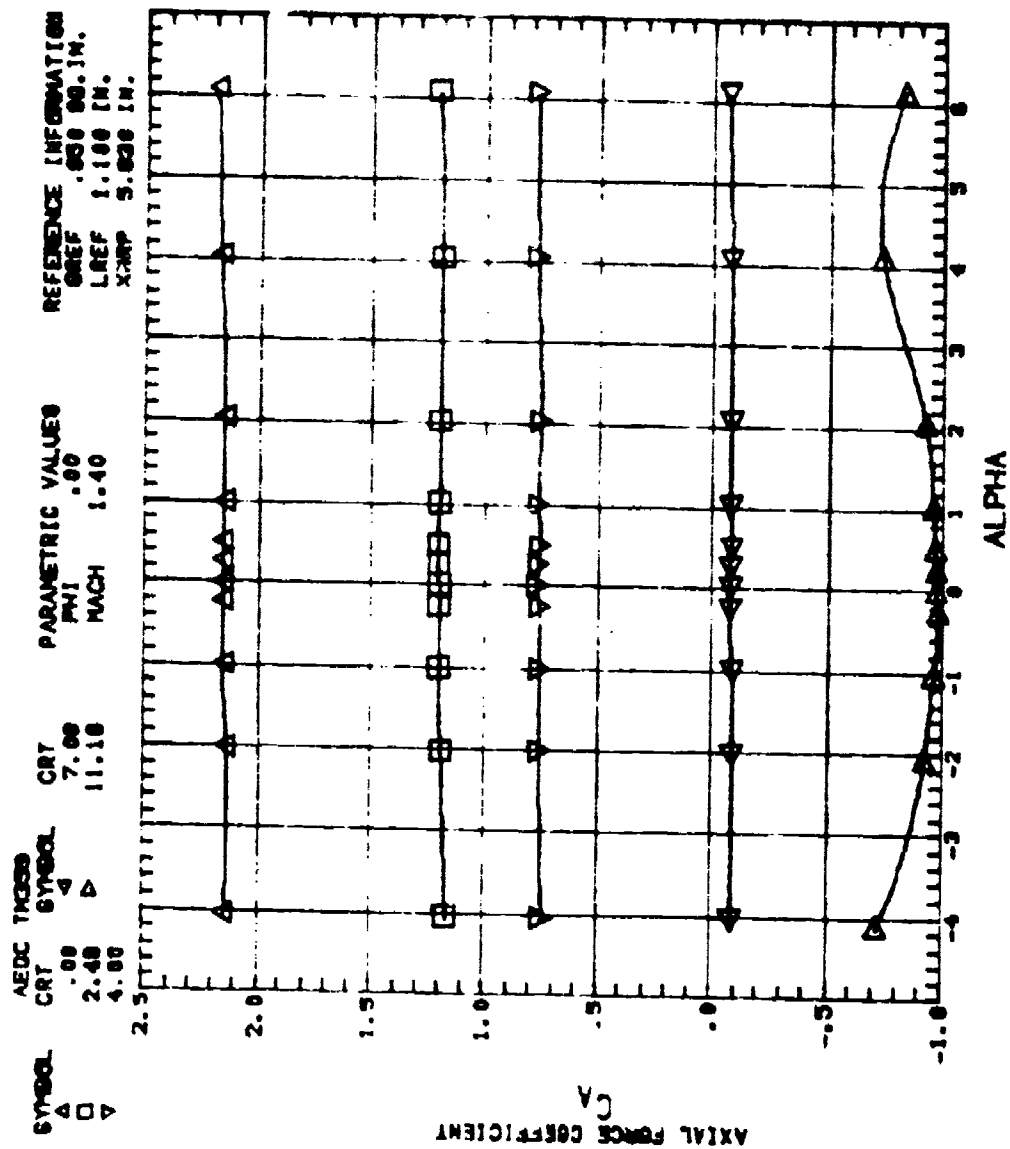


Figure 7. Continued. FD2

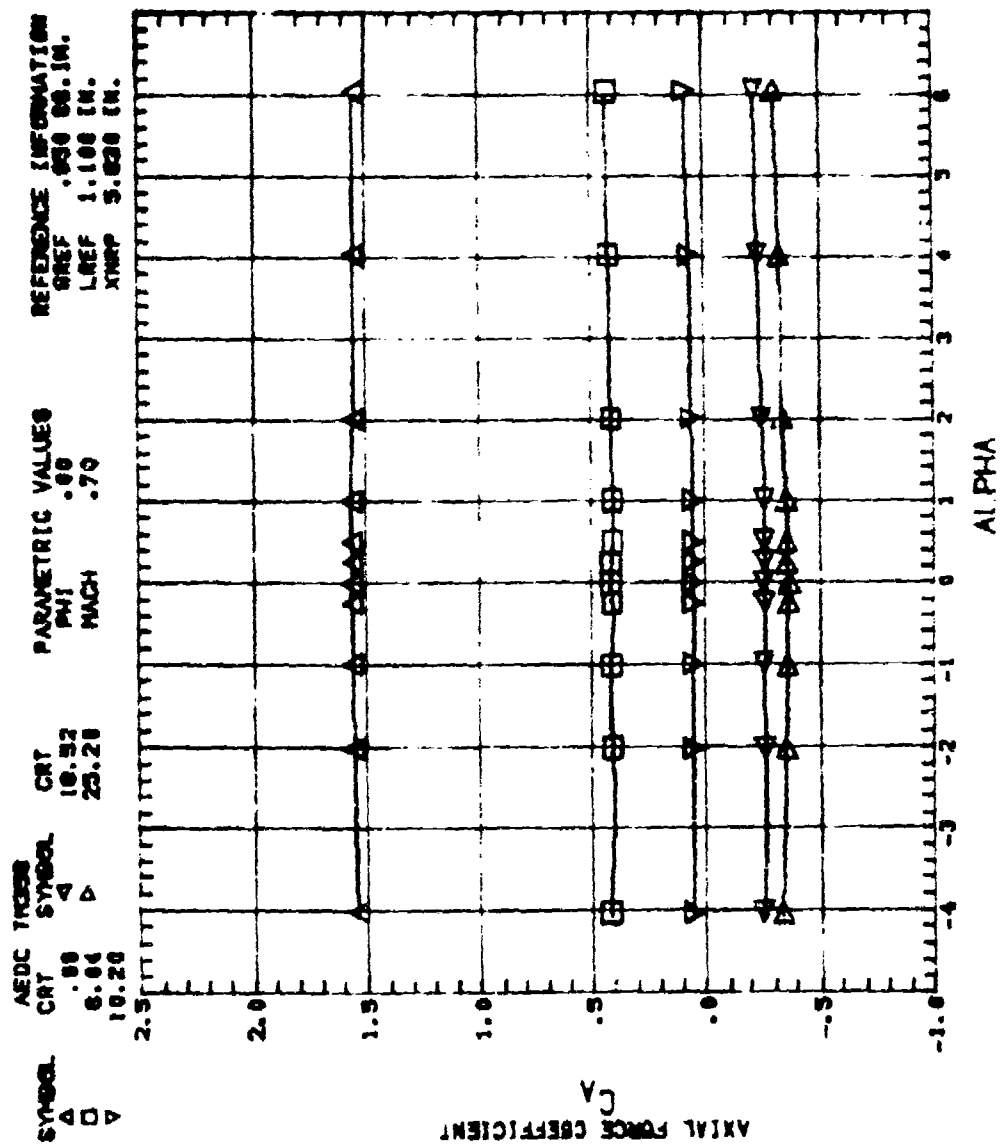


Figure 7. Continued. F6D2S

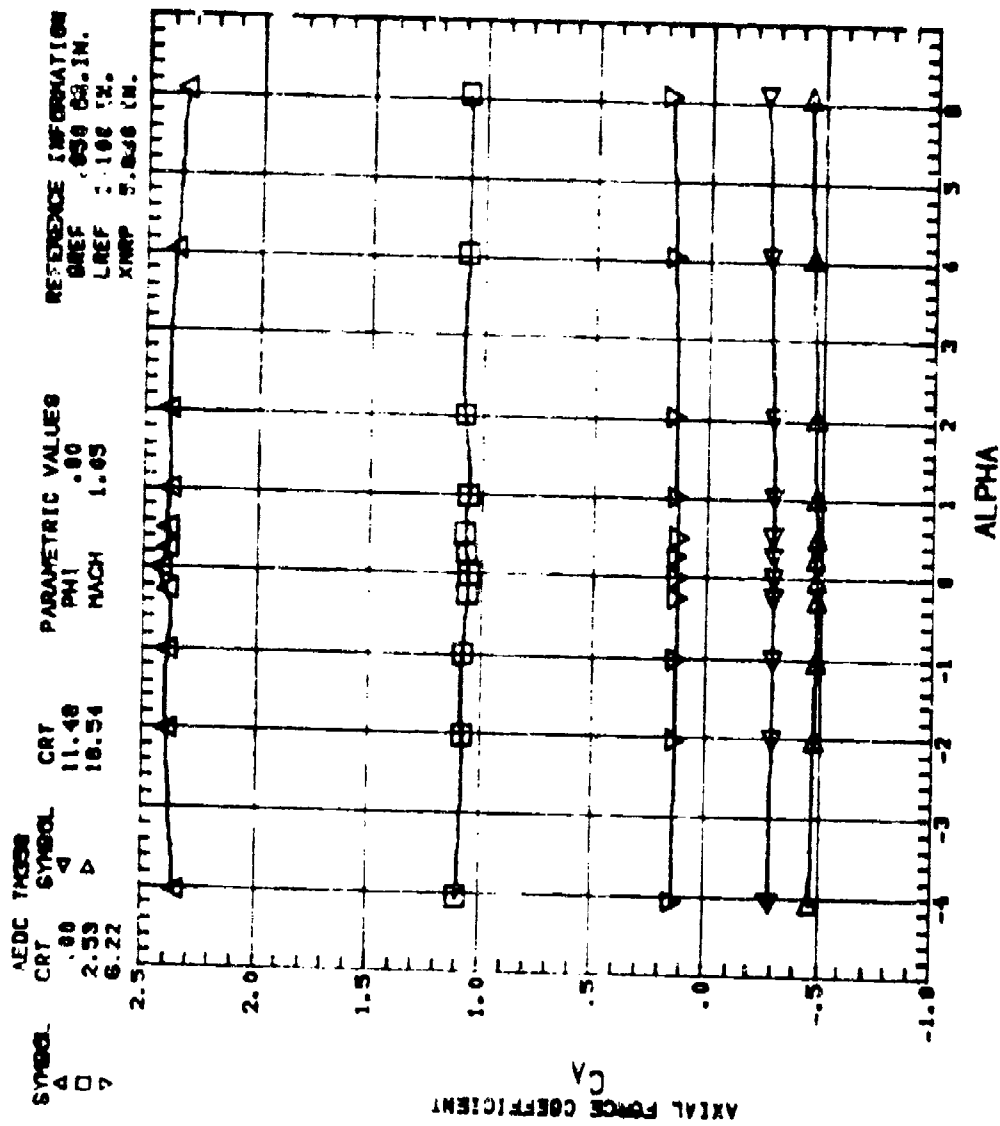


Figure 7. Continued. F6D2S

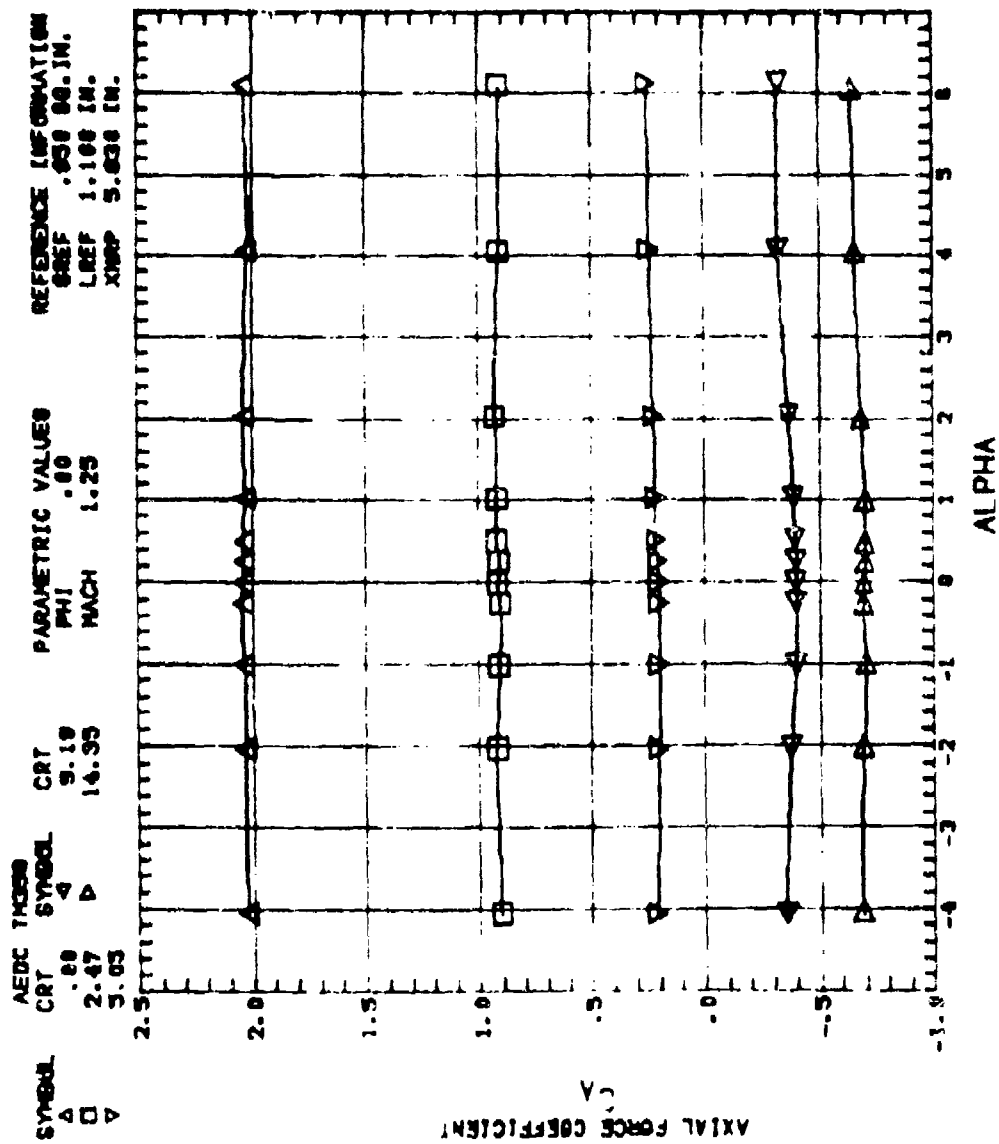


Figure 7. Continued. F6D2S

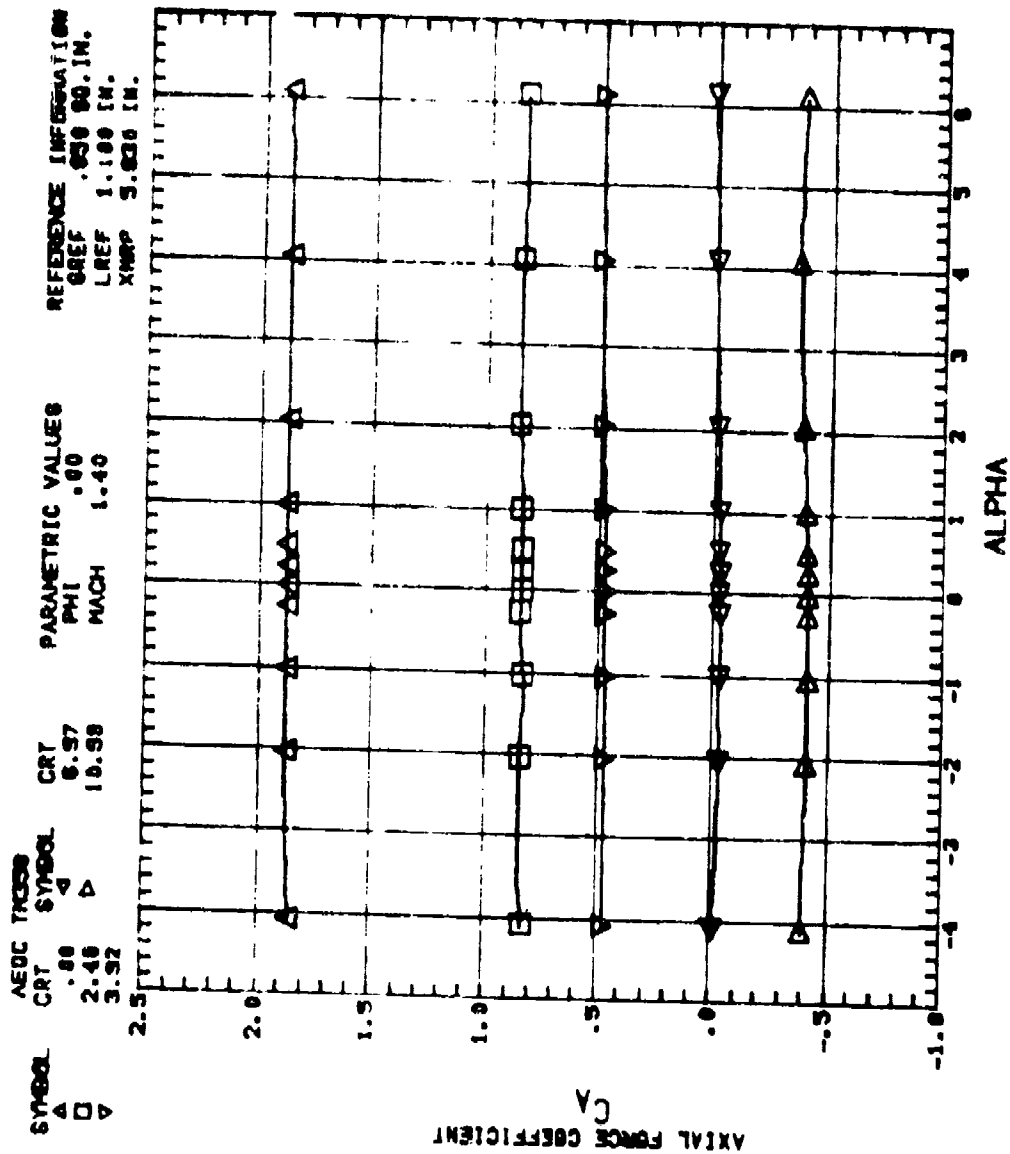


Figure 7. Continued. F6D2S

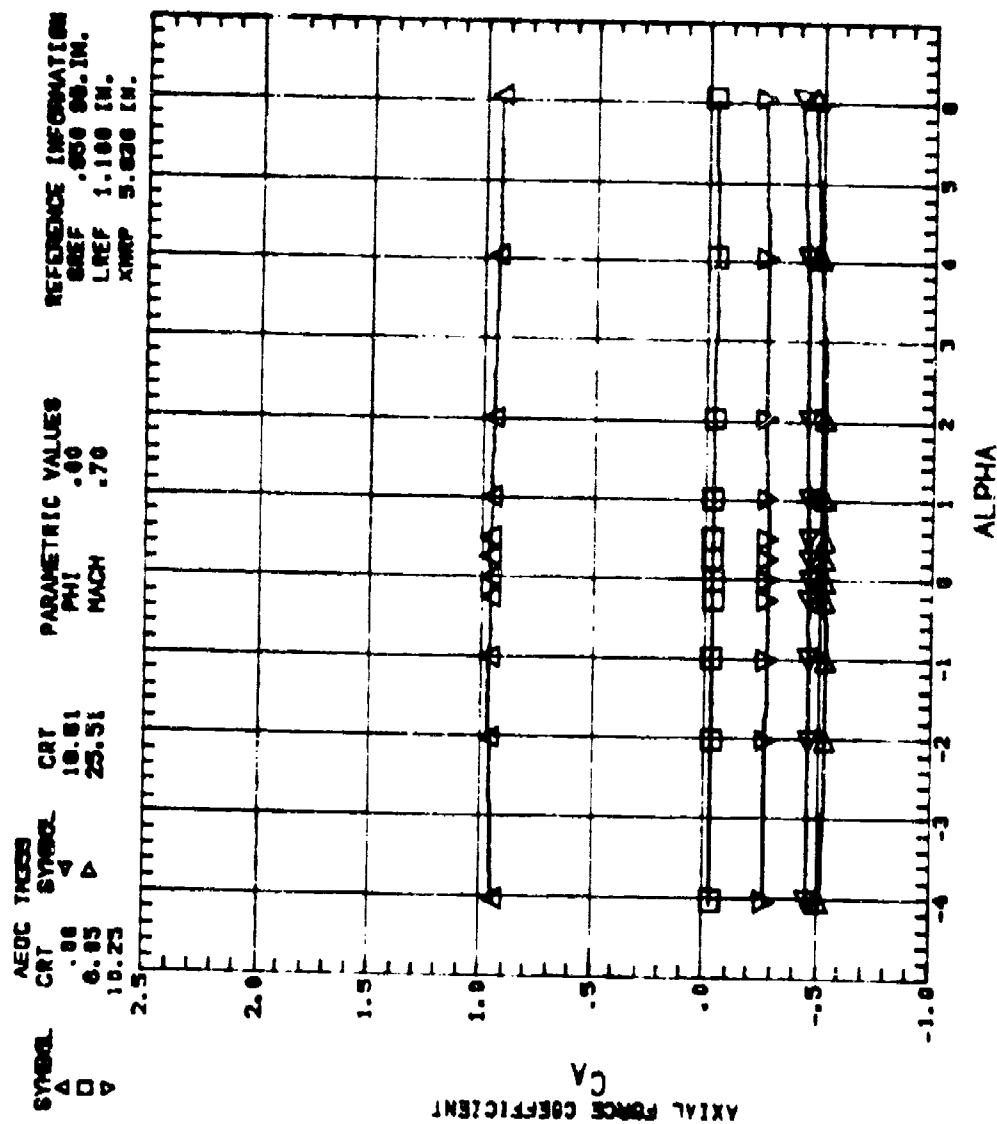


Figure 7. Continued. FL 41



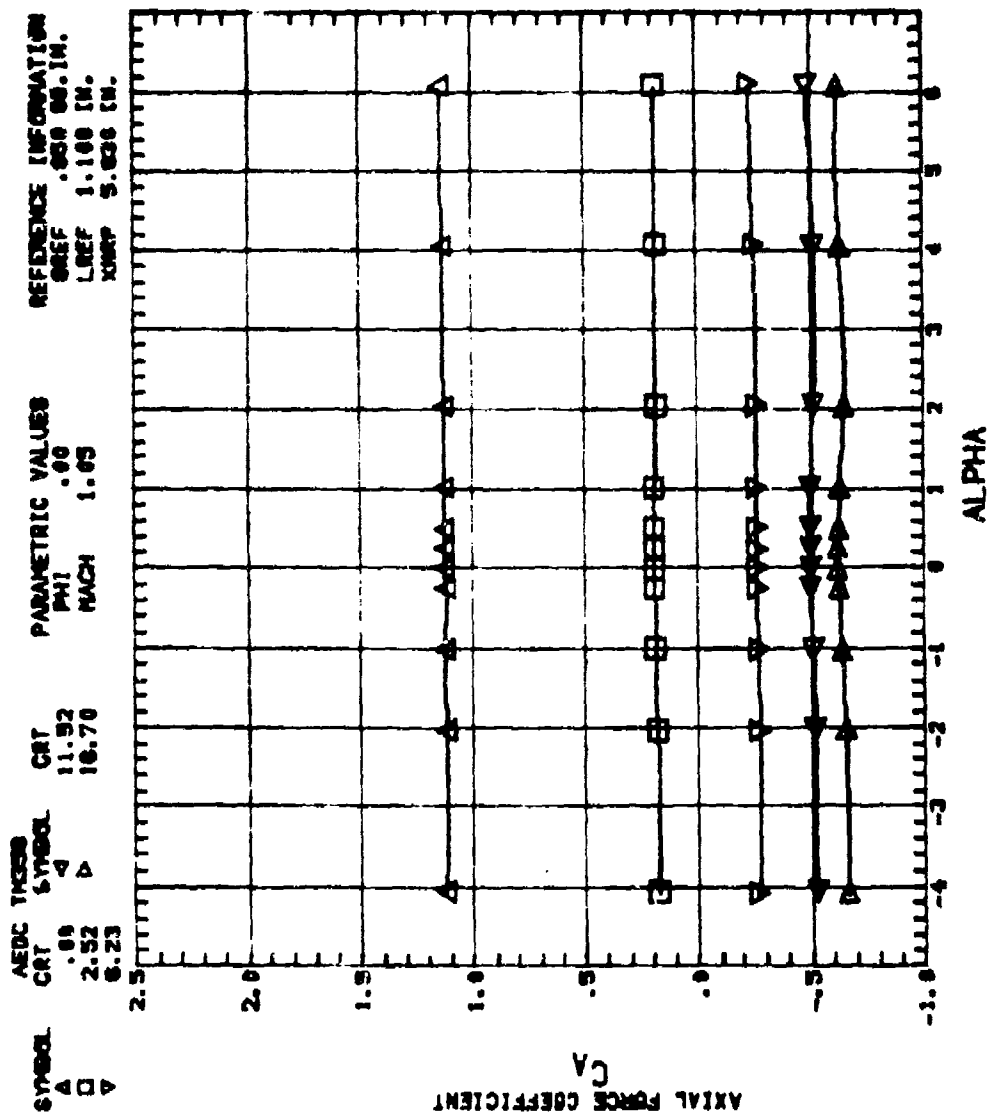


Figure 7. Continued. F12D1

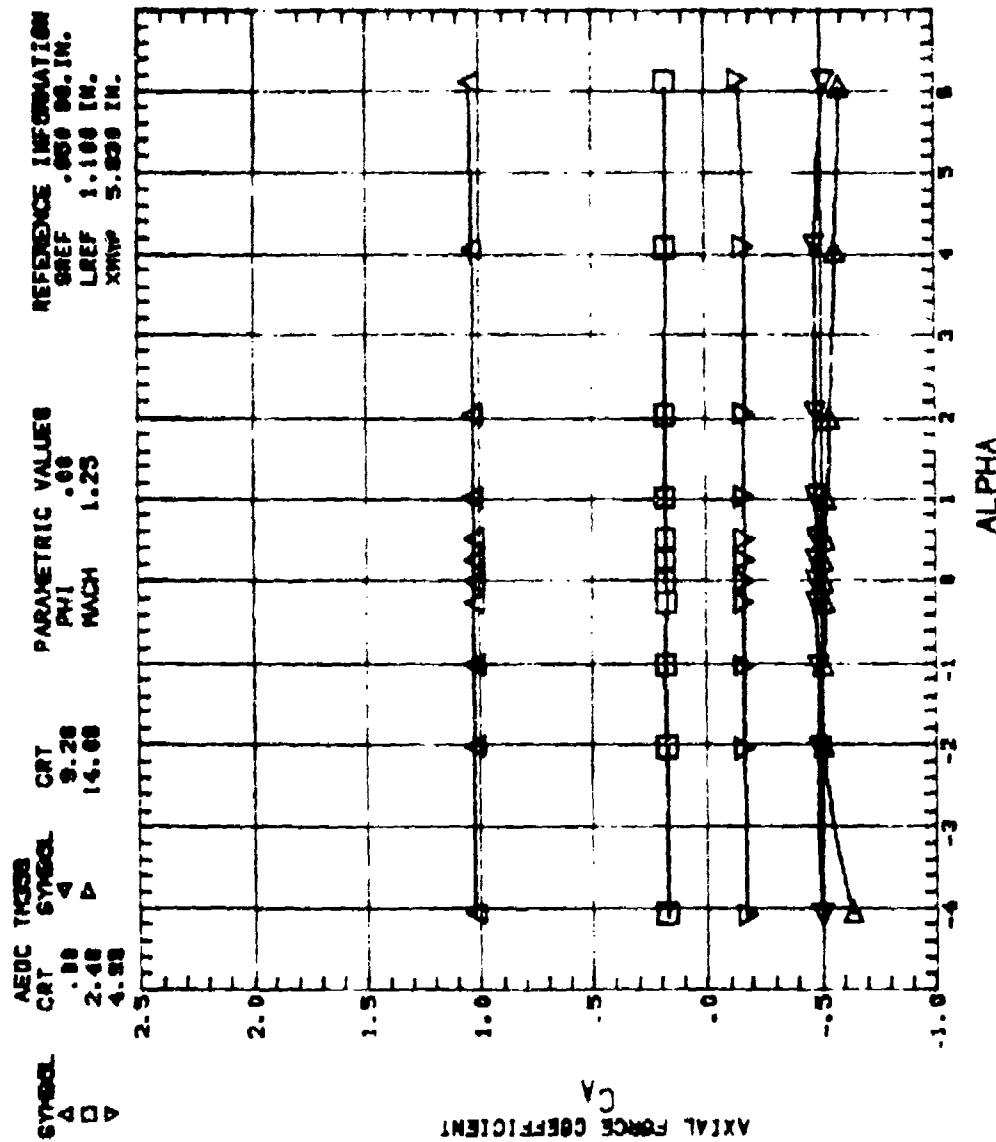


Figure 7. Continued. FI2D1

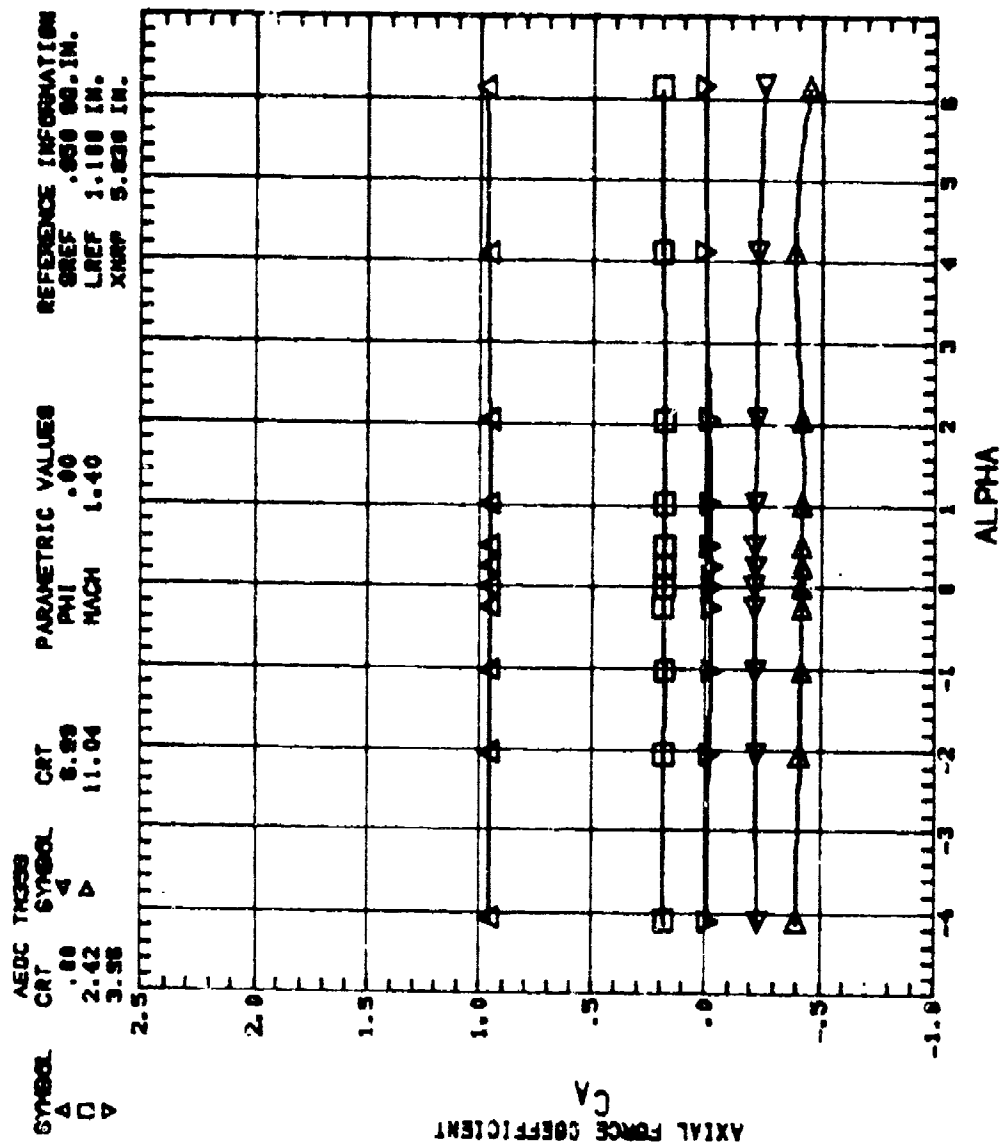
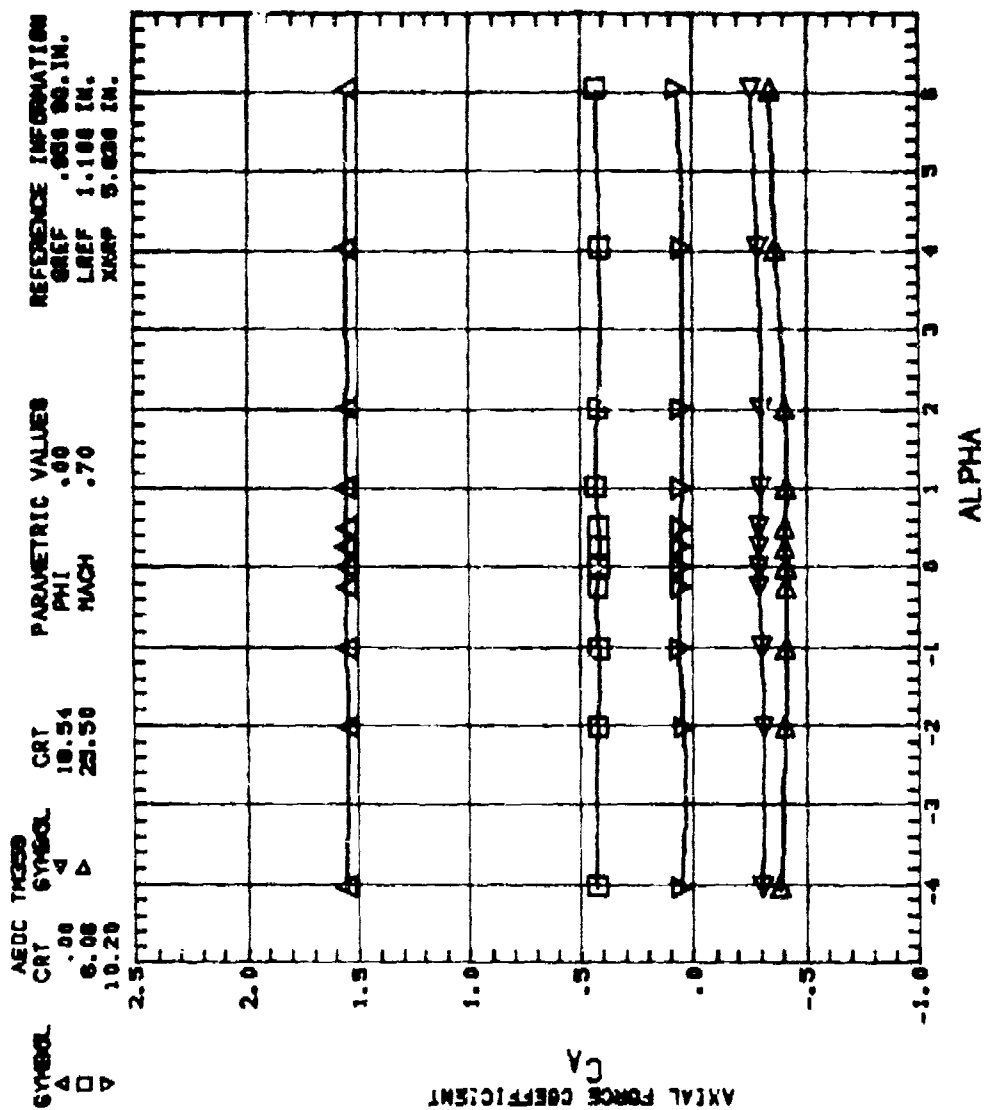


Figure 7. Continued. F12D1



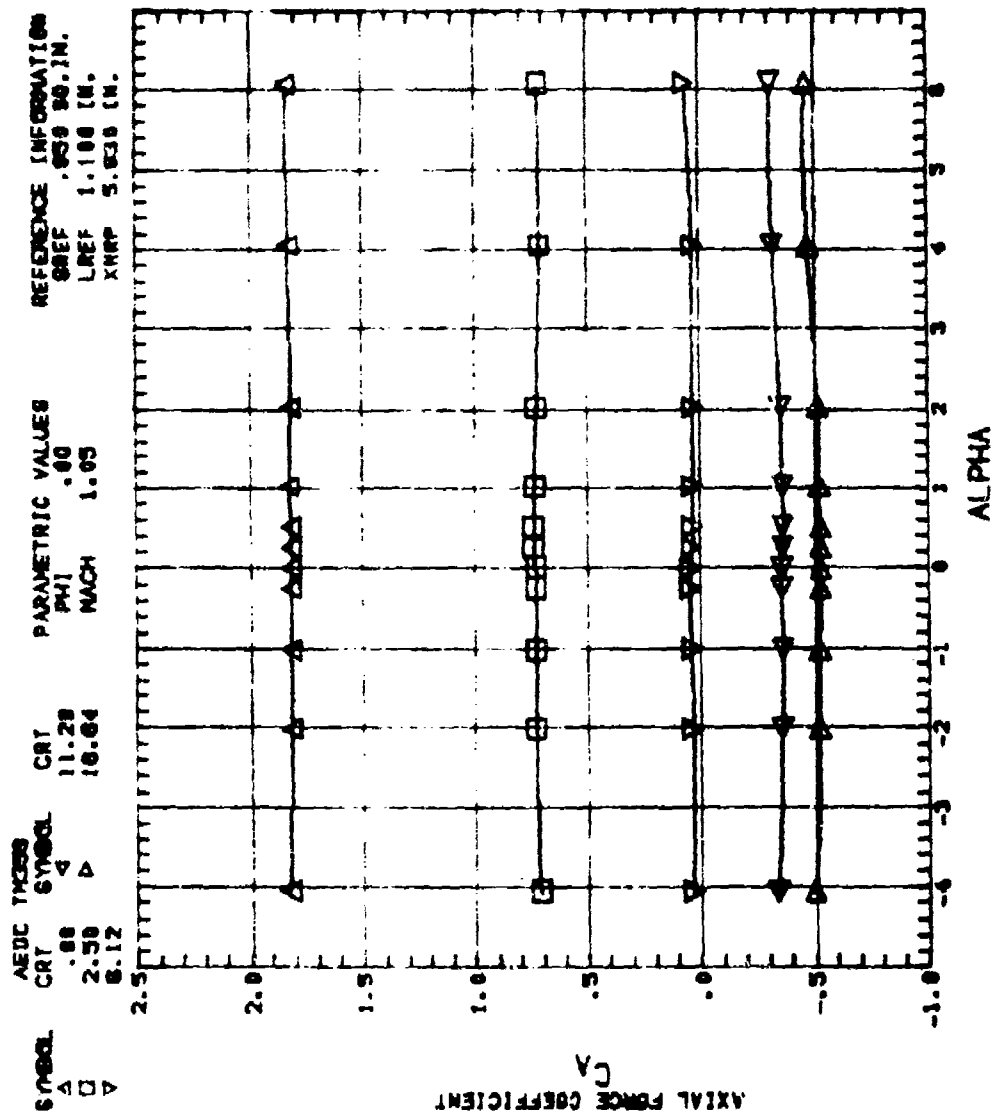


Figure 7. Continued. F12D2

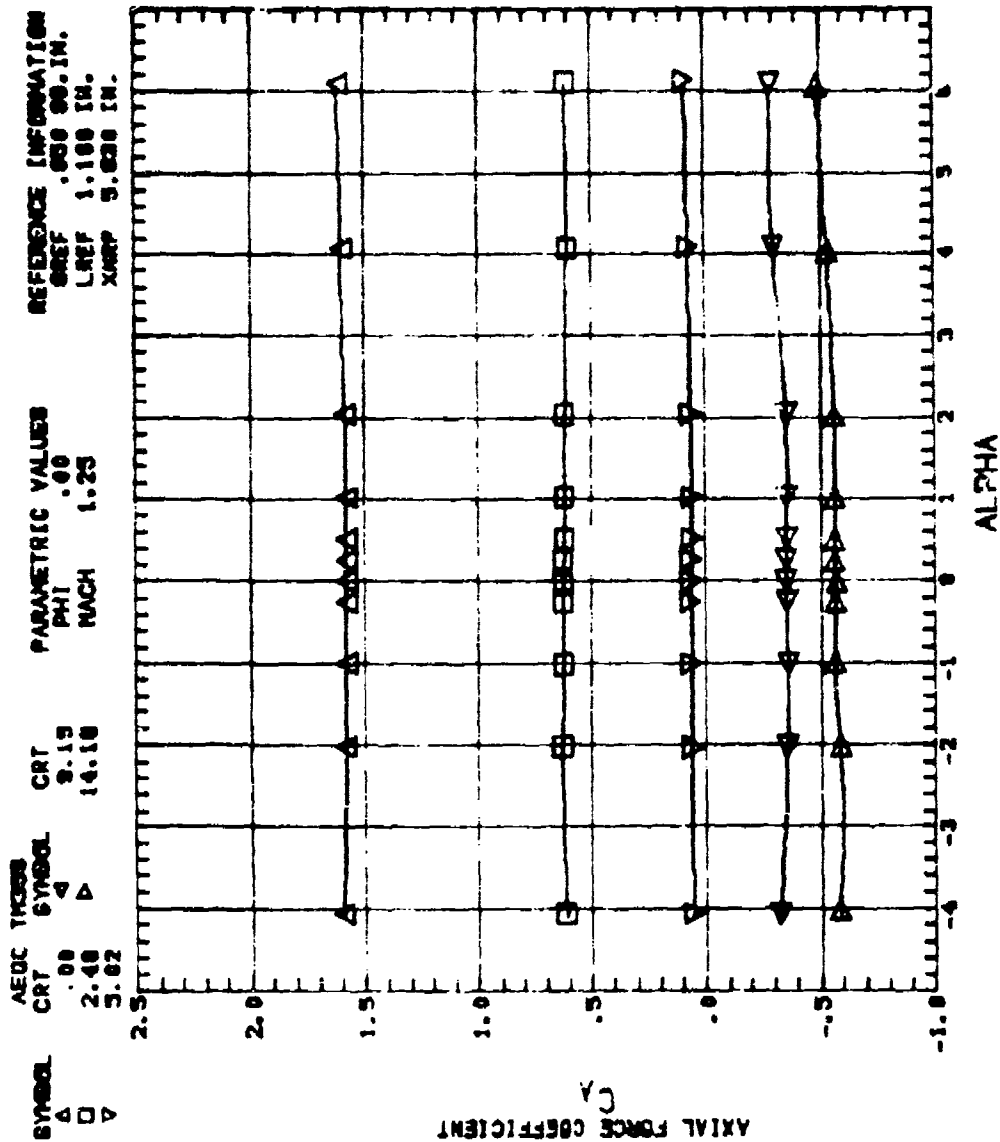


Figure 7. Continued. F12D2

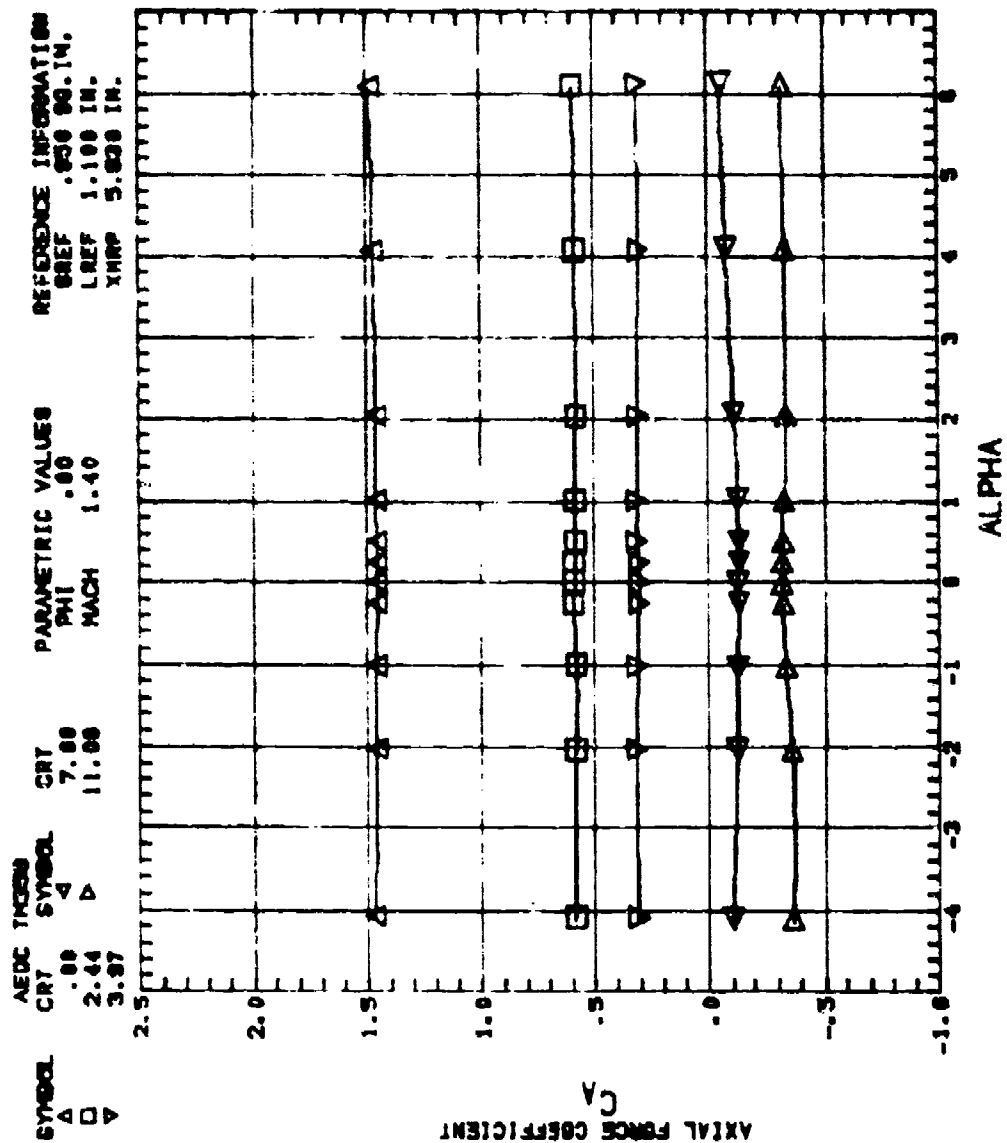


Figure 7. Continued. F12D2

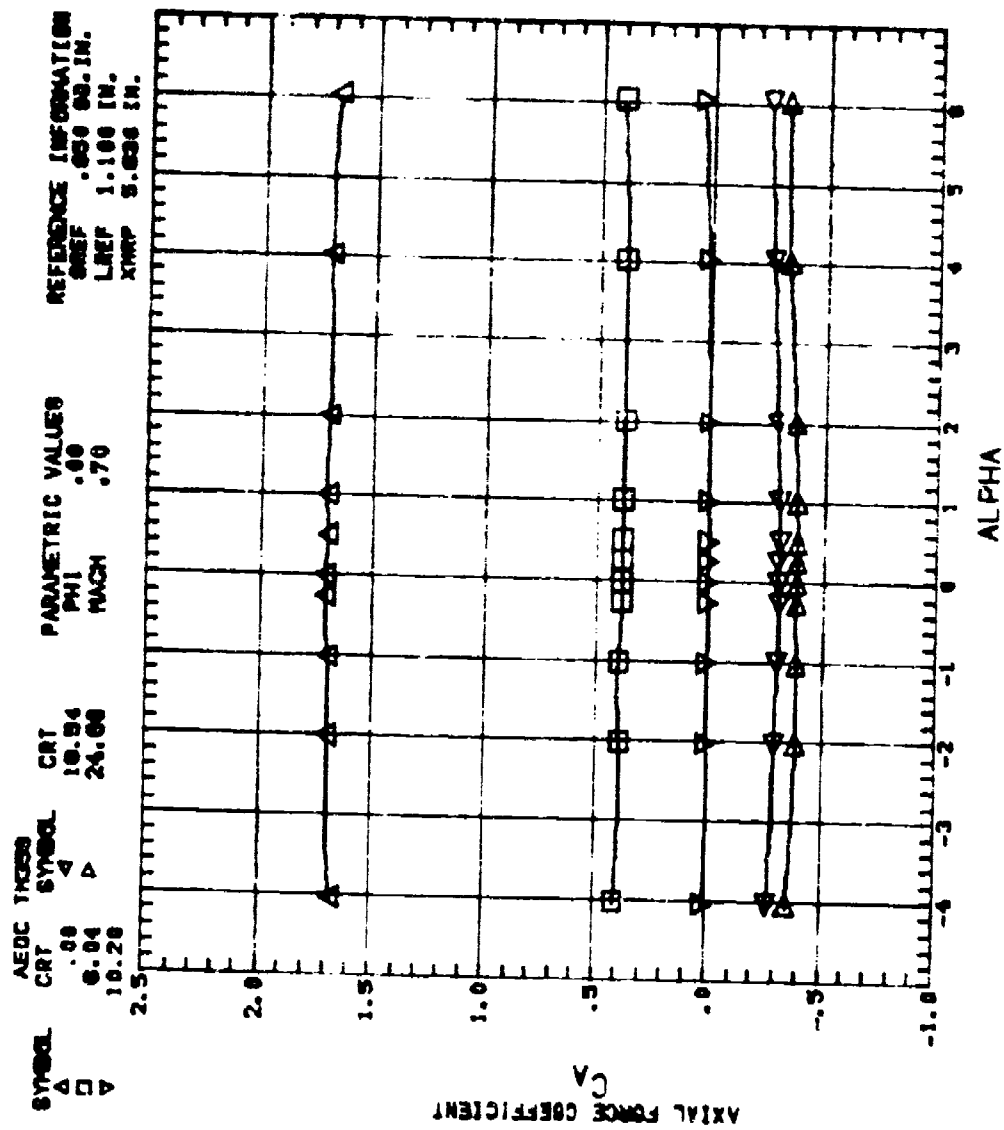


Figure 7. Continued. F6D2



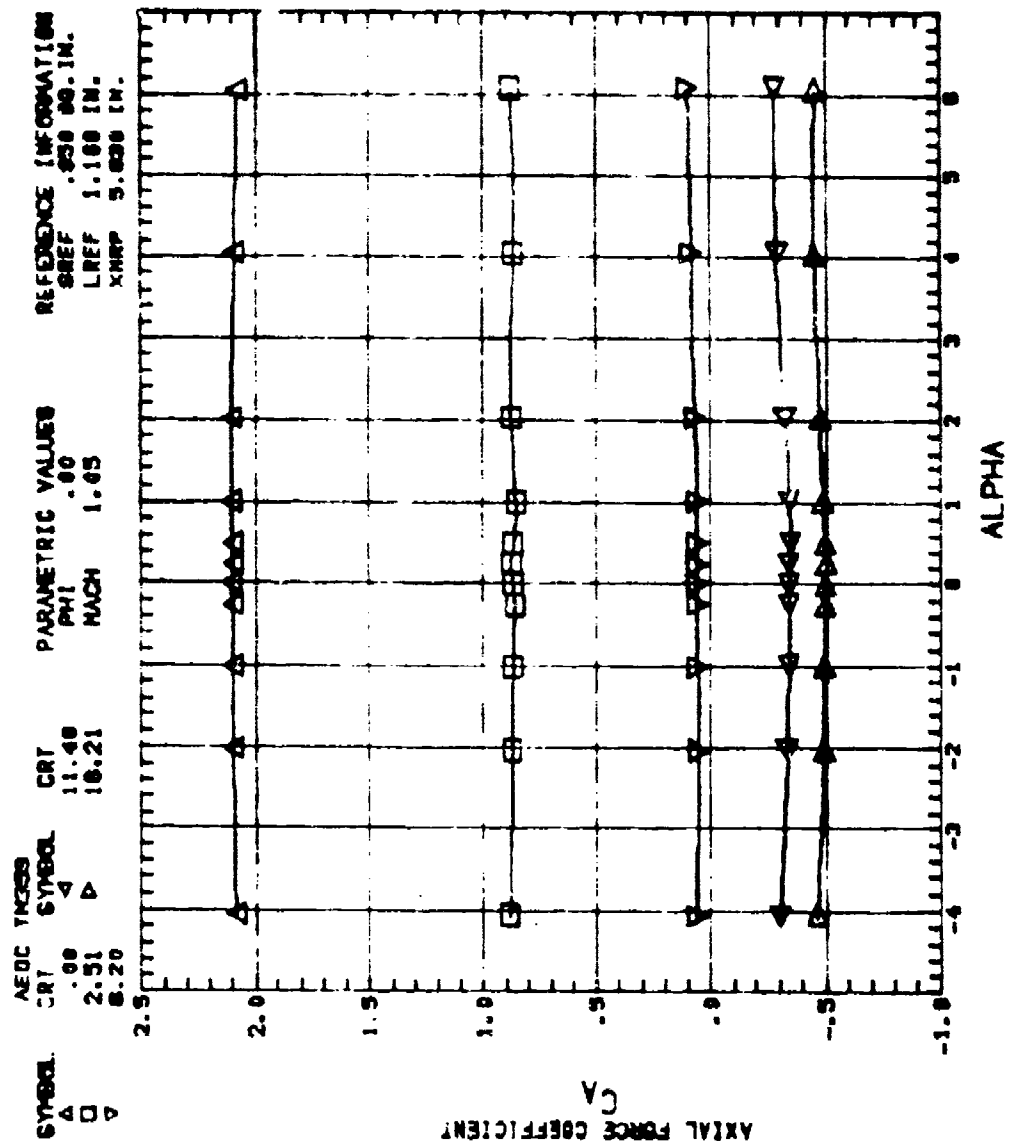


Figure 7. Continued. F6D2

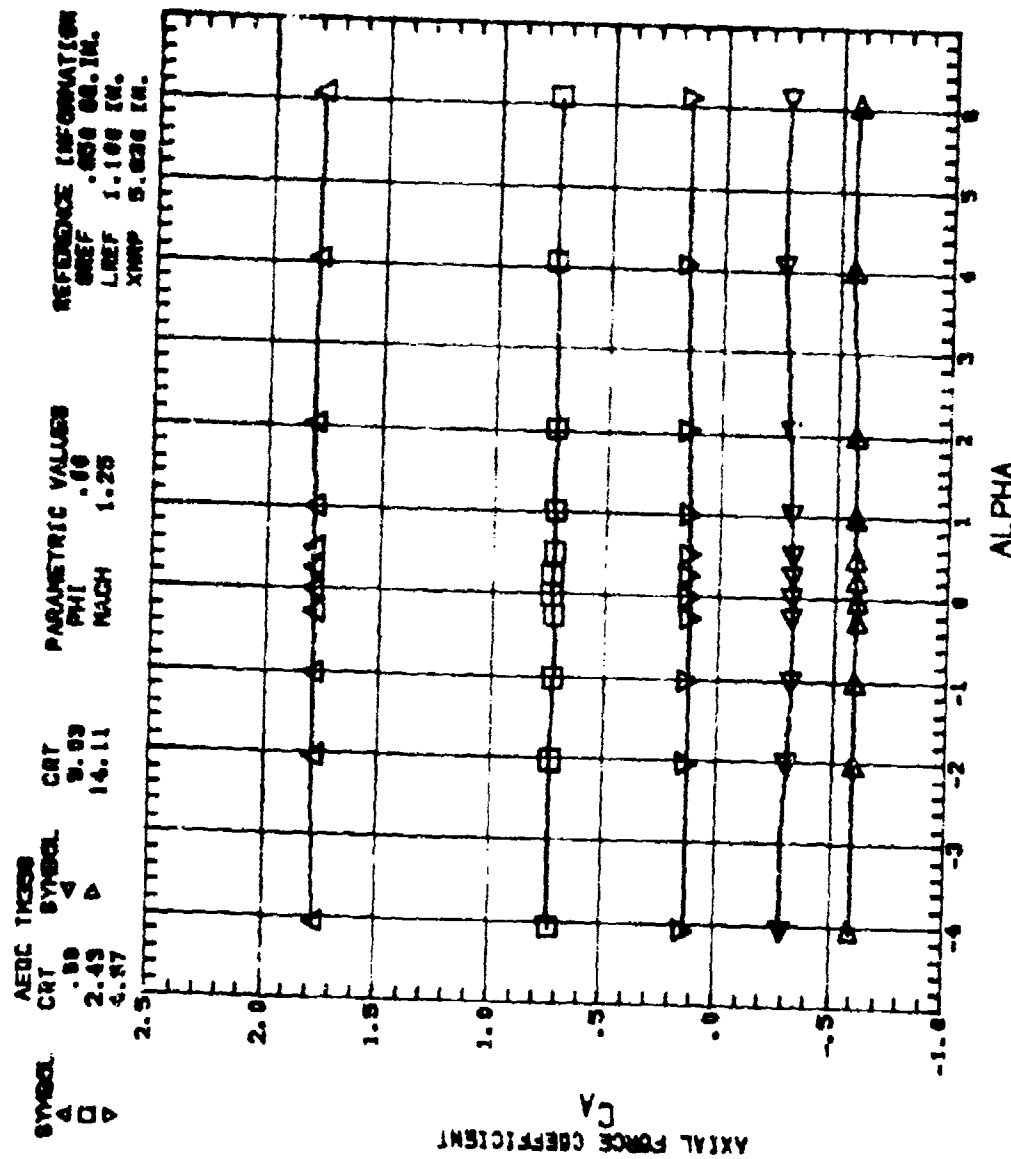


Figure 7. Continued. F6D2

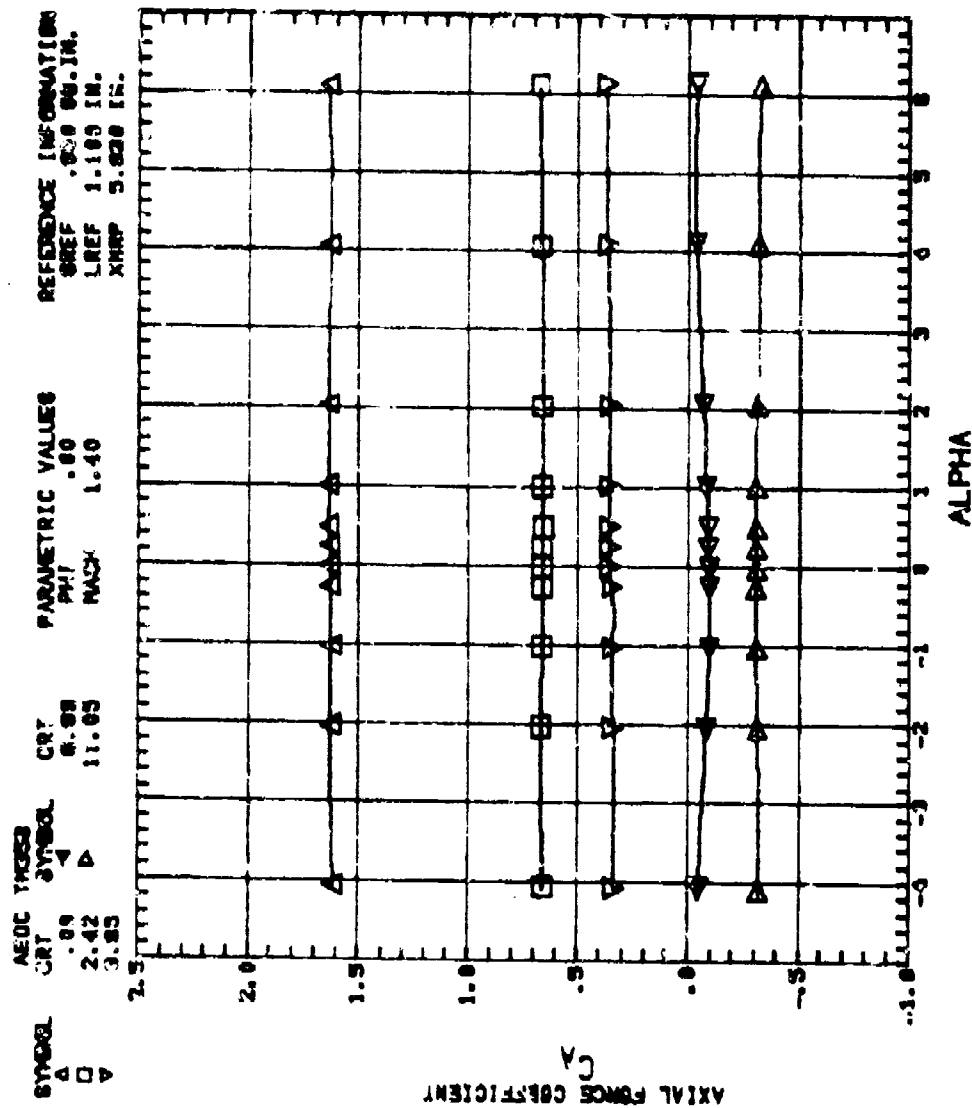


Figure 7. Continued. F6D2

# DISTRIBUTION

	Number of Copies		Number of Copies
Defense Documentation Center Cameron Station Alexandria, Virginia 22314	12	Commanding Officer Ballistic Research Laboratories ATTN: AMXRD-BEL, Mr. R. Krieger Aberdeen Proving Ground, Maryland 21005	1
Commanding General US Army Materiel Command Research & Development Directorate ATTN: DRCRD Washington, D. C. 20315	1	Commanding Officer US Naval Ordnance Laboratories ATTN: Mr. S. Hastings Mr. R. T. Hall Library	1 1 1
Commanding Officer US Army Picatinny Arsenal ATTN: SMUPA-VC3, Mr. A. Loeb Dover, New Jersey 07801	1	White Oak Silver Spring, Maryland 20910	
Director US Army Mobility Research and Development Laboratory ATTN: SAVDL-AS Ames Research Center Moffett Field, California 94035	1	NASA-Langley Research Center ATTN: Mr. Leroy Spearman Mr. Charles Jackson Technical Library Hampton, Virginia 23665	1 1 1
Commanding Officer Research Laboratories ATTN: SMUEA-RA, Mr. Abraham Flatau Edgewood Arsenal, Maryland 21010	1	Commanding Officer & Director Naval Ship Research and Development Center ATTN: Aerodynamic Laboratory Carderock, Maryland 20007	1
Commanding Officer Air Force Armament Laboratory ATTN: Mr. C. Butler Mr. F. Howard Dr. F. Findley Eglin Air Force Base, Florida 32542	1 1 1	NASA-Ames Research Center ATTN: Technical Library Moffett Field, California 94035	1
Arnold Engineering and Development Center ATTN: Dr. McKay Library Arnold Air Force Station, Tennessee 37389	1 1	NASA-Lewis Research Center ATTN: Technical Library Cleveland, Ohio 44135	1
Air Force Flight Dynamics Laboratory ATTN: FDMH, Mr. Gene Fleeman Wright-Patterson Air Force Base, Ohio 45433	1	NASA-Marshall Space Flight Center ATTN: Mr. K. Blackwell, ED32 Mr. J. Sims, ED32 Mr. H. Struck, ED31 Technical Library Marshall Space Flight Center, Alabama 35812	1 1 1 1
		US Air Force Academy ATTN: Lt. Col. W. A. Edgington DFAN USAF Academy, Colorado 80840	1

	Number of Copies		Number of Copies
Philco Corporation Aeronutronic Division ATTN: Technical Information Services-Acquisitions Mr. Lee Horowitz Ford Road Newport Beach, California 92663	1	Commander US Naval Ordnance Station Code 563 ATTN: Mr. N. Seiden Indian Head, Maryland	1
Rockwell International Columbus Aircraft Division ATTN: Mr. Fred Hessman 4300 East Fifth Avenue Columbus, Ohio 43216	1	Naval Weapons Center ATTN: Mr. R. Meeker China Lake, California 93555	1
Sandia Corporation Sandia Base Division 9322 ATTN: Mr. W. Curry Box 5800 Albuquerque, New Mexico 87115	1	University of Missouri at Columbia Dept. of Mechanical Engineering ATTN: Dr. D. E. Wollersheim Columbia, Missouri 65201	1
Purdue University ATTN: Dr. J. Hoffman, Propulsion Center Lafayette, Indiana 47907	1	University of Illinois College of Engineering ATTN: Dr. A. L. Addy Dr. H. H. Korst Dr. R. A. White Engineering Library Urbana, Illinois 61801	1 1 1 1
University of Tennessee Space Institute ATTN: Dr. J. M. Wu Tullahoma, Tennessee 37388	1	John Hopkins University Applied Physics Laboratory ATTN: Dr. L. Cronvich Mr. Gordon Dugger Mr. R. Walker Silver Spring, Maryland 20910	1 1 1
University of Alabama Department of Aerospace Engineering ATTN: Dr. Zien Dr. J. O. Doughty University, Alabama 35486	1 1	University of Notre Dame Dept. of Aerospace Engineering ATTN: Dr. T. J. Mueller Notre Dame, Indiana 46556	1
Jet Propulsion Laboratory California Institute of Technology ATTN: Mr. R. Martin, Mr. P. Jaffe 4800 Oak Grove Drive Pasadena, California 91109	1	Naval Air Systems Command ATTN: Mr. William Volz Atr 320-C, Room 778, JP-1 Washington, D. C. 20361	6
		For Transmittal to: TTCP	

	Number of Copies		Number of Copies
Boeing Company		The Martin-Marietta Corporation	
ATTN: Library Unit Chief	1	Orlando Division	
Mr. R. J. Dixon	1	ATTN: D. Tipping	1
Mr. H. L. Giles	1	L. Gilbert	1
P. O. Box 3707		Orlando, Florida 32804	
Seattle, Washington 98124			
Convair, A Division of General		McDonnell Douglas Astronautics Co.-West	
Dynamics Corporation		ATTN: Library A3-328	
ATTN: Division Library		5301 Bolsa Avenue	
Pomona, California 91776	1	Huntington Beach, California 92646	1
Nielson Engineering & Research, Inc.		McDonnell Douglas Corporation	
ATTN: Dr. Jack H. Nielson		P. O. Box 516	
850 Maude Avenue		St. Louis, Missouri 63166	1
Mountain View, California 94040	1		
Hughes Aircraft Company		Northrop Corporation	
ATTN: Documents Group Technical		Electro-Mechanical Division	
Library		ATTN: Mr. E. Clark	
Florence Avenue at Teale Street		500 East Orangethorpe Y20	
Culver City, California 90230	1	Anaheim California 92801	1
Ling-Temco-Vought Aerospace Corp.		Emerson Electric Company	
ATTN: Mr. Dick Ellison		ATTN: Mr. Robert Bauman	
P. O. Box 404		8100 Florissant Rd.	
Warren, Michigan 48090	1	St. Louis, Missouri 63136	1
Ling-Temco-Vought Aerospace Corp.		REMTECH, Inc.	
Vought Aeronautics Division		ATTN: Mr. L. M. Hair	
ATTN: C. R. James, Unit 2-53330		2603 Artie Street	
Box 5907		Huntsville, Alabama 35805	6
Dallas, Texas 75222	1		
Lockheed Missiles & Space Company		DRDMI-X	1
Huntsville R&E Center		-TX, Dr. Kobler	1
ATTN: Mr. M. M. Penny		-PD	3
4800 Bradford Boulevard, N.W.		-TDK, Mr. Deep	1
Huntsville, Alabama 35805	1	Mr. Henderson	2
Lockheed Missiles & Space Company		Mr. Burt	10
ATTN: Technical Information Center		(Record Set)	1
P. O. Box 504		(Reference Set)	1
Sunnyvale, California	1		